THICK FILAMENT REGULATION OF MYOCARDIAL CONTRACTION

A Dissertation Presented to

The Faculty of the Graduate School

University of Missouri-Columbia

In Partial Fulfillment

of the Requirements for the Degree

Doctor of Philosophy

By

F. STEVEN KORTE

Kerry S. McDonald, Ph.D., Dissertation Supervisor

AUGUST, 2006

The undersigned, appointed by the Dean of the Graduate School, have examined the dissertation entitled

THICK FILAMENT REGULATION OF MYOCARDIAL CONTRACTION

Presented by F. STEVEN KORTE

a candidate for the degree of Doctor of Philosophy

and hereby certify that in their opinion it is worthy of acceptance.

Kerry S. McDonald, Ph.D.

Mark A. Milanick, Ph.D.

Michael J. Rovetto, Ph.D.

Leona J. Rubin, Ph.D.

Ronald L. Terjung, Ph.D.

ACKNOWLEDGEMENTS

I would like to express my sincere gratitude to Dr. Kerry McDonald for his support, guidance, and friendship through the years. Kerry, your contribution to my career is immeasurable and you have made me a better scientist and a better person. I would also like to thank my committee members, Drs Mark A. Milanick, Michael J. Rovetto, Leona J. Rubin, and Ronald L. Terjung for their unique perspectives and constructive critique. You have opened my eyes to new angles. Additional thanks to Dr. Rovetto for laboratory guidance and an open door policy, and to Dr. Judith Cole for giving me the opportunity to love the laboratory. Thanks to Dr. Todd Herron, Dr. Aaron Hinken, and Dr. Laurin Hanft for their friendship, humor, and helpful advice. Thanks to Joe Schuster, Darla Tharp, Michelle Rapisardo, Patti Mierzwa and everybody else that I've had the pleasure of working with in the McDonald lab. Also, thanks to the fine faculty, departmental staff, and graduate students in the Department of Medical Pharmacology and Physiology for your helpfulness throughout the years.

Heartfelt thanks to my parents, Fred and Sharon, for your support and encouragement that has been the foundation of my achievements. Also, thank you to my mother- and father-in-law, Fred and Mary, for you faith and support, and for allowing me to marry your daughter.

Finally, I would like to thank my wife, Amanda, for her love and her ability to make me laugh under even the most extreme of conditions. Without your support and motivation, this would have been much more difficult, and I happily share my success with you.

TABLE OF CONTENTS

LIST OF TABLES

LIST OF FIGURES

THICK FILAMENT REGULATION OF MYOCARDIAL CONTRACTION

ABSTRACT

The ability of the heart to function as a pump is governed by mechanisms intrinsic to individual cardiac myocytes. These mechanisms include, but are not limited to, amount of activator Ca^{2+} released, sensitivity of the myofilaments to Ca^{2+}, and the kinetic cycling rates of motor isozymes. All of these mechanisms have the potential to be altered either on a beat-to-beat basis by factors such as sarcomere length or post-translational modification or on a long-term basis through changes in protein isoform expression. Single skinned cardiac myocytes provide an ideal platform for study of these factors because they allow precise control of the ionic milieu bathing the myocyte and protein isoform content can be determined for each myocyte following mechanical measurements. The experiments in this dissertation were designed to examine the effects of sarcomere length and thick filament protein isoform expression on the contractile properties of single skinned cardiac myocytes.

Myosin binding protein-C (MyBP-C) is a thick filament protein that is thought to have structural and regulatory effects, and mutations in the gene encoding MyBP-C are among the most commonly identified with familial hypertrophic cardiomyopathy. I examined the effect of MyBP-C ablation (MyBP-$C^{-\backslash-}$) on mechanical properties in mouse skinned cardiac myocytes. Peak normalized power output at maximal Ca^{2+} activation was significantly elevated in myocytes from MyBP-$C^{-\backslash-}$ myocardium, while isometric force and rate of force development were unchanged. At submaximal Ca^{2+} activation, however, the rate of force development was significantly elevated and peak normalized

power output was increased to an even greater extent. From these data it is concluded that MyBP-C regulates myocardial contractility by limiting crossbridge kinetics.

Sarcomere length (SL) is also an important regulator of myocardial performance, as increased SL within the physiologic-al range is known to increase isometric force production. Myocytes *in vivo*, however, are shortening against a load and the effects of SL on loaded shortening velocity have not been determined. Data presented here examined the effect of SL on force, rate of force development, loaded shortening velocity, and power output in rat skinned cardiac myocytes. Furthermore, the effects of SL on myosin heavy chain dependence (MyHC) mechanical properties were examined in myocytes containing primarily either αMyHC or β-MyHC, which are the two types of MyHC expressed in the heart. Peak absolute and normalized loaded shortening velocity and power output at short SL in both α-MyHC and β-MyHC myocytes. Matching myocyte force between long and short SL, however, sped loaded shortening -velocity and increased power output in α-MyHC myocytes to values greater than at long SL, but this did not occur in β-MyHC. Matching myocyte width between long and short SL sped loaded shortening velocity and increased power output to values greater than at long SL in both α-MyHC and β-MyHC myocytes. Effects of SL and MyHC on rate of force development and Ca^{2+} sensitivity were also determined. From the data, it is concluded that there is an increase in crossbridge kinetics at short SL as compared to long SL, which is overcome by increased lattice spacing induced decrease in actomyosin interactions. The data are presented in terms of a model whereby SL shortening induces a conformational change in MyBP-C that removes its constraint on the myosin heads, allowing them to cycle faster.

Chapter 1. INTRODUCTION

1.1 Cardiac Function and Ultrastructure

In 1628 William Harvey published "On the movement of the heart and blood in animals", wherein he was the first to describe the heart as a pump that circulates blood within a closed system [56]; a discovery that is considered the foundation for modern cardiovascular research. The heart pumps to provide oxygen and nutrients necessary to organ and organismal survival, and it does so by cyclic contraction and relaxation of cardiac muscle, a unique form of striated muscle similar to but also quite distinct from skeletal muscle. The mammalian heart has four chambers: two ventricles and two atria with a bilateral distribution such that the right side, which comprises the low pressure pulmonary circulation, and the left side, which provides high pressure systemic circulation, each have an atrium and ventricle. The two sides work against much different arterial pressures but, because the circulatory system is a closed loop, volumetric output from one side must match the other. The matching of ventricular outputs is described by the Frank-Starling mechanism, whereby increased blood flow to a ventricle results in a more forceful ejection of blood. A major focus of study in this dissertation is potential myofibrillar mechanisms that regulate this process.

The heart's function as a pump can be divided into four distinct phases, which is well illustrated using a modified Wiggers diagram that shows changes in left ventricular

pressure and volume over time (Figure 1.1). Phase 1 is filling, where the pressure in the ventricle is very low but the volume of blood in the ventricle is rising. Electrical stimulation initiates contraction, normally starting from the sino-atrial node (SA node). The SA node is a cluster of specialized pacemaker cells located in the upper right atrium near the entrance of the superior vena cava, and their electrical signal is propagated first through the atrium and then through the atrioventricular node (AV node) and then to the ventricles. The fact that the atria are stimulated slightly before the ventricles is significant because it results in an "atrial kick", which can be seen on the left ventricular pressure-volume relationship as the increase in both volume and pressure near the end of the filling phase. The atrial kick accounts for up to as much as 1/3 more blood volume filling the ventricle [6], which, in accordance with Starling's Law, accounts for 15-30% of ventricular stroke volume. Electrical excitation of the ventricles initiates phase 2 of the cardiac cycle, isovolumic contraction. Pressure rapidly rises in the ventricles, which causes the atrioventricular valve to close, but ventricular pressure remains below aortic pressure so the aortic semilunar valve remains closed. Since blood cannot enter or leave, the volume of blood in the ventricle, also known as end-diastolic volume (EDV), remains constant during phase 2. Pressure will continue to rise in the ventricle until it exceeds aortic pressure at which point the aortic semilunar valve will open and phase 3, or ejection, will commence. During ejection, the heart is contracting against the load imposed, in part, by the arterial resistance. As the myocardium shortens and the volume of blood in the ventricles is decreased, the ventricular pressure starts to decline. When ventricular pressure falls below the pressure in the aorta, the aortic valve closes and the

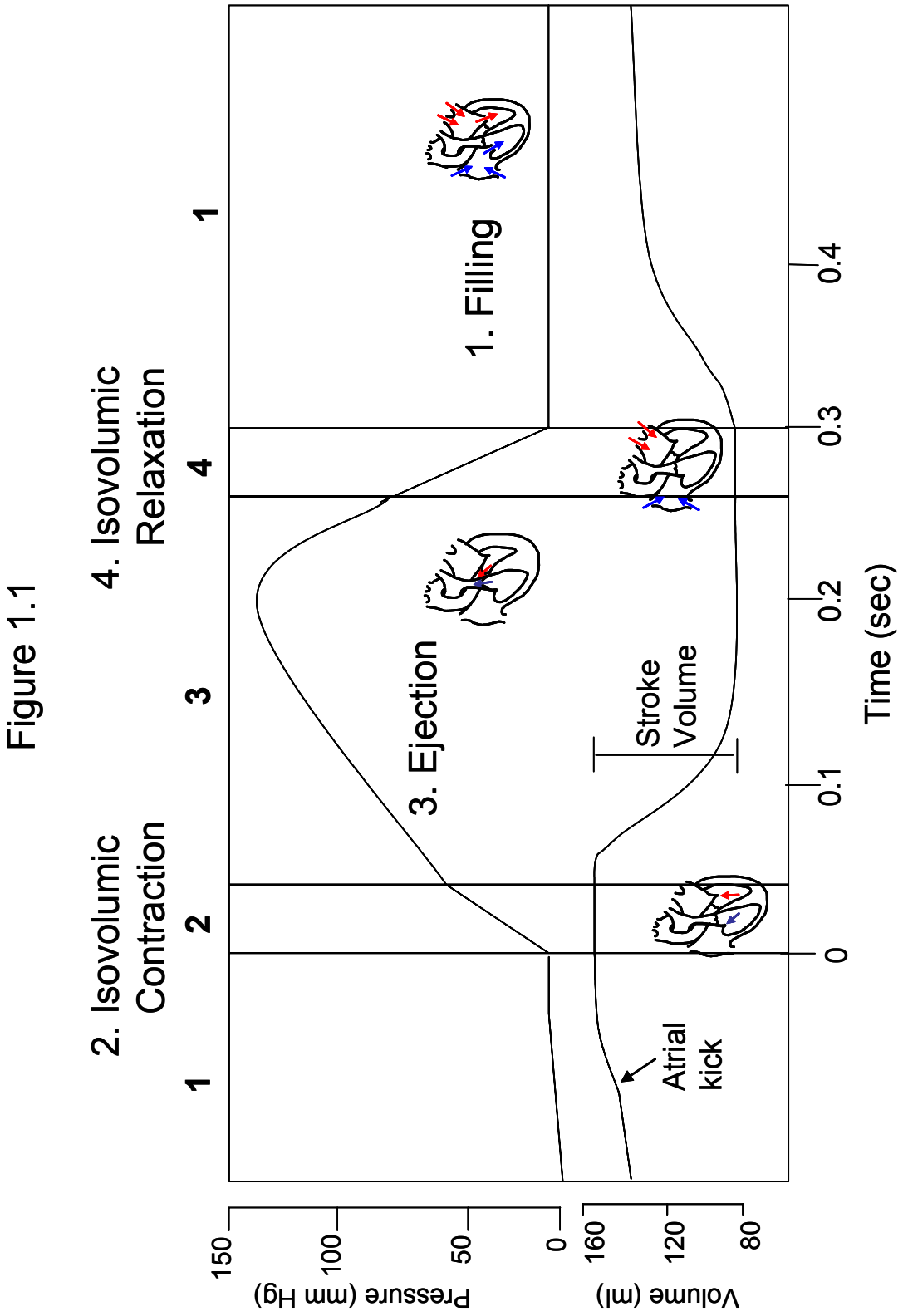

Figure 1.1: Wiggers Diagram of the Cardiac Cycle in Human Left Ventricle.

left ventricle now undergoes isovolumic relaxation, the fourth phase of the cardiac cycle. The volume of blood in the ventricle at this point is called end-systolic volume (ESV). The volumetric difference between EDV and ESV is known as stroke volume (SV) (i.e., the amount of blood ejected during systole). The product of stroke volume and heart rate (HR) is termed cardiac output (CO), and is a major index of ventricular function.

In 1895 Otto Frank showed that a frog ventricle developed more pressure as end-diastolic pressure increased (a phenomenon that may have been observed as early as 1866 [190]), while in 1914 Ernest Starling demonstrated, in an isolated heart-lung preparation from a dog, that cardiac output (SV x HR) increases coincident with venous filling pressure . These observations have since become known as the Frank-Starling relationship (Figure 1.2), whereby increased end-diastolic volume leads to an increased stroke volume, and it is recognized as essential in beat-to-beat regulation of heart contractility and ventricular function. To understand how an increase in end-diastolic volume can lead to an increase in the forcefulness of contraction first requires an understanding of the functional anatomy of the heart.

Figure 1.2

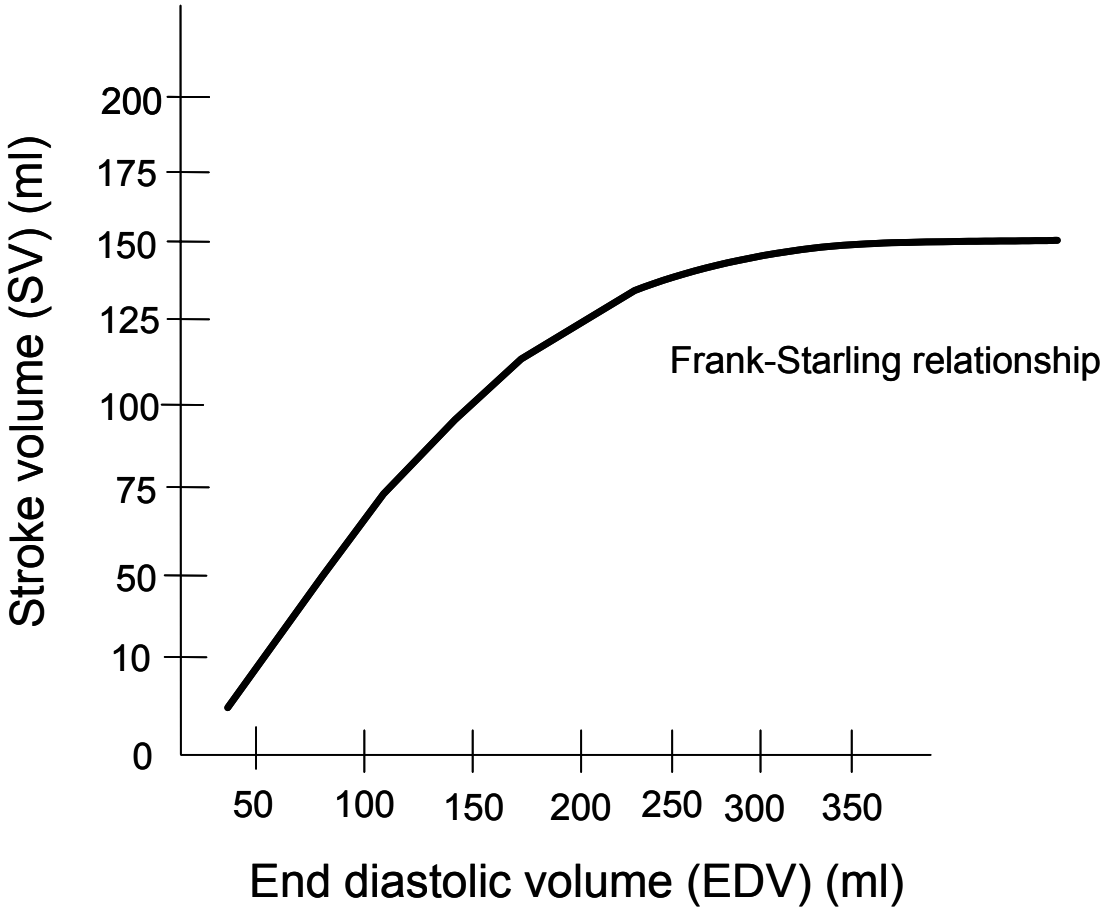

Figure 1.2: Ventricular Function Curve

A ventricular function curve illustrates the Frank-Starling relationship. At constant heart rate and ejection pressure, stroke volume increases with rising end-diastolic volume. Impairment of this relationship (i.e., a shallower curve) is associated with heart failure.

1.2 Structure of the Myocardium

The working myocardium is primarily composed of individual cardiac myocytes. Myocytes are typically mononucleated cells approximately 120 μm in length and 30 μm in width, and are arranged in overlapping sheets of muscle that spiral from the base of the heart to the apex in such a manner that the endocardial surface spirals in a counter right-handed helix and myocytes tend to be circumferentially oriented while the epicardium forms a left-handed helix from the apex to the base and the myocytes are perpendicularly oriented to the base-apex axis at the epicardial surface (Figure 1.3). This orientation of myocardial fibers lends a torsional aspect to contraction that effectively adds a wringing motion that results in more efficient chamber squeezing and propulsion of blood and is thought to equalize stress and strain throughout the heart [167], and likely has consequences for regulation through stretch-activation [16] (see discussion). Neighboring myocytes are connected mechanically by intercalated discs and electrically by gap junctions that allow rapid propagation of ions and action potentials. Thus, the heart acts as a functional syncytium with all working myocytes contracting in near synchrony. Because of this, myocardial function is not altered by recruitment of more or fewer muscle cells as occurs in skeletal muscle, but rather by factors intrinsic to the individual myocytes. Myocytes have a characteristic striation pattern, which arises from the orderly longitudinal arrangement of cylindrical bundles of thick and thin filaments called myofibrils (Figure 1.3). The functional unit of the myofibril is the sarcomere, which extends from one Z-line to another. The Z-line anchors the thin filament, which interdigitates with the thick filament that extends in each direction from the

Figure 1.3

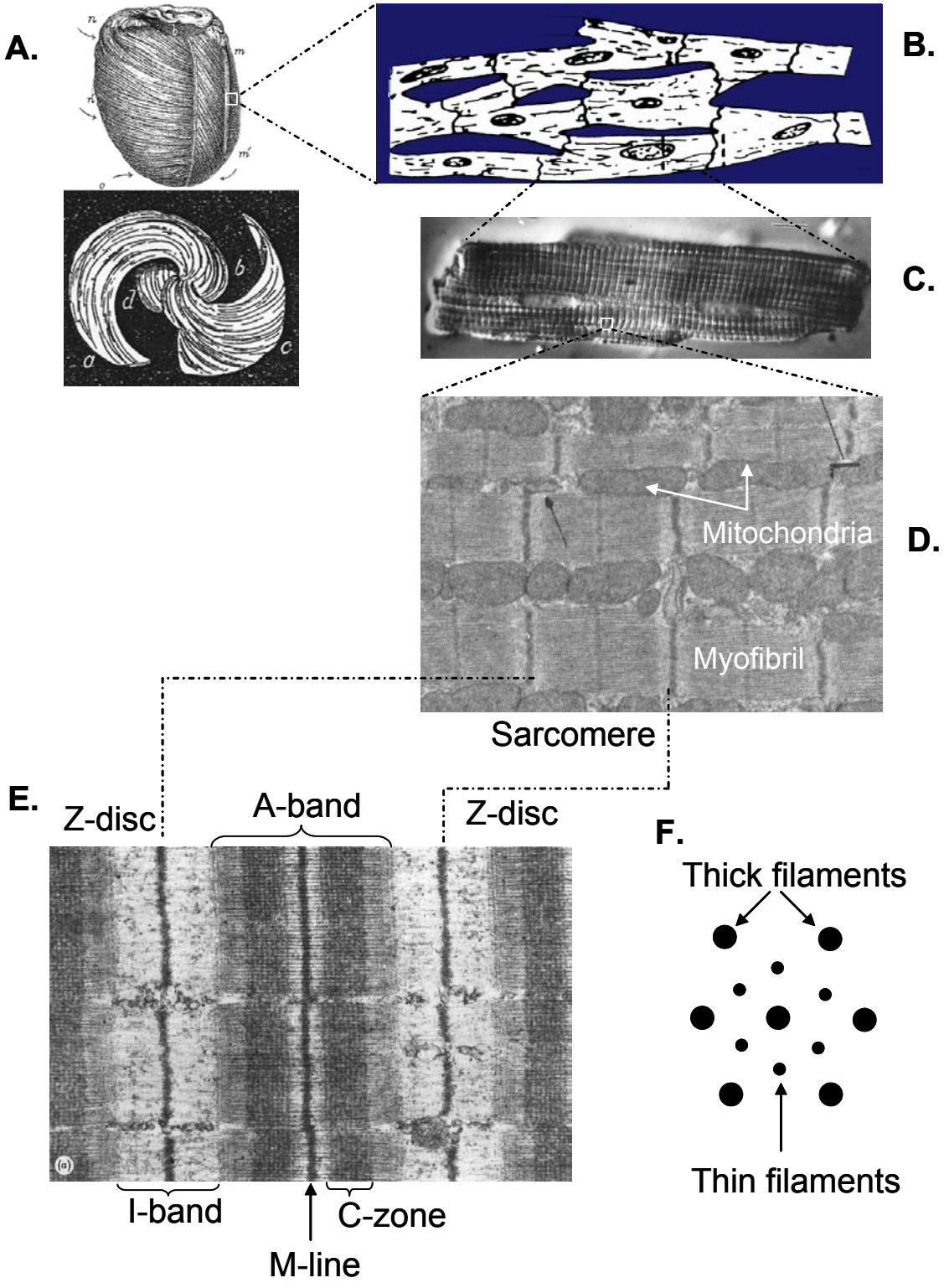
A.
B.
C.
D.
Mitochondria
Myofibril
Sarcomere
E.
Z-disc
A-band
Z-disc
I-band
C-zone
M-line
F.
Thick filaments
Thin filaments

Figure 1.3: Cardiac Structure (previous page)

A. The myocardial fibers align angularly throughout the ventricular wall (top) and also show a spiral arrangement from epicardium to endocardium as they sweep from the apex of the left ventricle (taken from Pettigrew, 1908 [138]. **B.** Illustration of myocyte arrangement within the myocardium. **C.** Photomicrograph of a single cardiac myocyte. **D.** Electron micrograph of the internal structure of a myocyte detailing the individual myofibrils and mitochondria that comprise the bulk of a myocyte. **E.** Electron micrograph of a single sarcomere, the functional unit of muscle (taken from Winegrad, 1999 [183]. The sarcomere runs from Z-disk to Z-disk. **F.** Illustration of the hexagonal arrangement of thick and thin filaments when viewed in cross-section.

middle of the sarcomere called the M-line. A cross section of this assembly shows that each thick filament is surrounded by six thin filaments that lie at trigonal points between neighboring thick filaments. The region where the thin filament does not overlap with the thick filament is called the I-band because it is isotropic and does not polarize light, whereas the region where the thick and thin filaments do overlap is strongly birefringent and is called the A-band (anisotropic). There is also a distinct region with the A-band called the C-zone, where the thick filament protein myosin binding protein-C (MyBP-C) aggregates. The thick filament is approximately 1.65 um in length, while the thin filament extends 1.0 um from the Z-disc. Increasing the sarcomere length over the working range of the myocardium leads to more optimal overlap of thick and thin filaments [43]. Returning to the Frank-Starling relationship, the anatomical result of an increase in EDV is a stretching of the ventricular myocardium, which lengthens individual myocytes and the sarcomeres contained within the myocytes. In maximally Ca^{2+}-activated skinned cardiac cells, more optimal overlap leads to greater force generating capacity [28]. However, the steepness of the SL-force relationship in cardiac muscle is too great to be solely due to extent of thick and thin filament overlap. In fact, the steepness of this relationship increases as Ca^{2+} activation level decreases [3, 88, 173]. This is important because, unlike skeletal muscle which typically sees maximal Ca^{2+} activation, the myocardium *in vivo* operates at approximately half-maximal Ca^{2+} activation [2, 5, 27]. At increasing SL, there is both increased calcium release from the sarcoplasmic reticulum [5] and increased myofilament calcium sensitivity [5, 66, 79, 101]. Thus, there are intrinsic myofibrillar mechanisms that detect and respond to changes in SL on a beat-to-beat basis.

1.3 Thin Filament Structure and Function

The thin filament is primarily composed of actin monomers (G-actin) that polymerize to form F-actin filaments. Two actin filaments intertwine in a macromolecular helical arrangement to form the thin filament backbone, and each half-turn of the thin filament helix contains 7 actin monomers. This is noteworthy because the dimeric filamentous molecule tropomyosin (Tm) spans 7 actin monomers as it binds to the actin filament and lies in the groove between the two strands of actin. This provides additional structural integrity to the thin filament and positions Tm for regulation of contraction, which it does in conjunction with the troponin complex. The troponin (Tn) complex is comprised of three subunits; TnI, TnT, and TnC. TnC contains a Ca^{2+} binding site that, when bound with Ca^{2+}, causes a conformational change that relieves the crossbridge inhibitory property of TnI. TnT binds the troponin complex to tropomyosin. This complex of proteins (7 actin monomers, Tm dimer, Tn complex) forms the structural regulatory unit of muscle, which can undergo further regulation by post-translational modification. For example, the cardiac isoform of TnI contains a NH_2-terminal extension (which is absent in skeletal TnI) that contains two phosphorylation sites (Ser 23/24) for cAMP-dependent protein kinase (PKA) associated with a decrease in Ca^{2+} sensitivity of the myofilaments [147]. cTnI also contains PKC phosphorylation sites (Ser 43/45, Thr 144) that are associated with decreased myosin ATPase rate [94, 126], as is PKC phosphorylation of cTnT [127, 128, 170]. The thick filament is discussed in more detail below, but is primarily composed of myosin and myosin binding protein-C and is

attached to the Z-disk by the giant filamentous protein titin (also known as connectin). The sarcomeric proteins are illustrated in Figure 1.4.

A key aspect of cardiac muscle function is the relationship between isometric force and the concentration of activator Ca^{2+}. A current model of contractile regulation proposes that the regulatory unit of the thin filament exists in three distinct states, each depending on the relative position of the regulatory protein tropomyosin [42]. In the absence of Ca^{2+}, and thus absence of contraction, the thin filaments are thought to be in a "blocked" state where tropomyosin sterically prevents myosin from interacting strongly with actin. Upon the addition of Ca^{2+} and its subsequent binding to the regulatory protein troponin C, there is a conformational change in troponin I (TnI) that causes tropomyosin to reduce its steric inhibition, allowing a weakly-bound actomyosin interaction in what is known as the "closed state". Populations of weakly interacting actomyosin cross-bridges then undergo a transition to strongly bound but non-force generating cross-bridges that force tropomyosin into the groove of the actin filament initiating an "open" state that allows the strongly-bound cross-bridges to isomerize to force-generating states. In fact, this displacement of Tm by strong crossbridges has been shown to spread to adjacent regulatory units [146], illustrating the highly cooperative behavior of the thin filament.

Figure 1.4

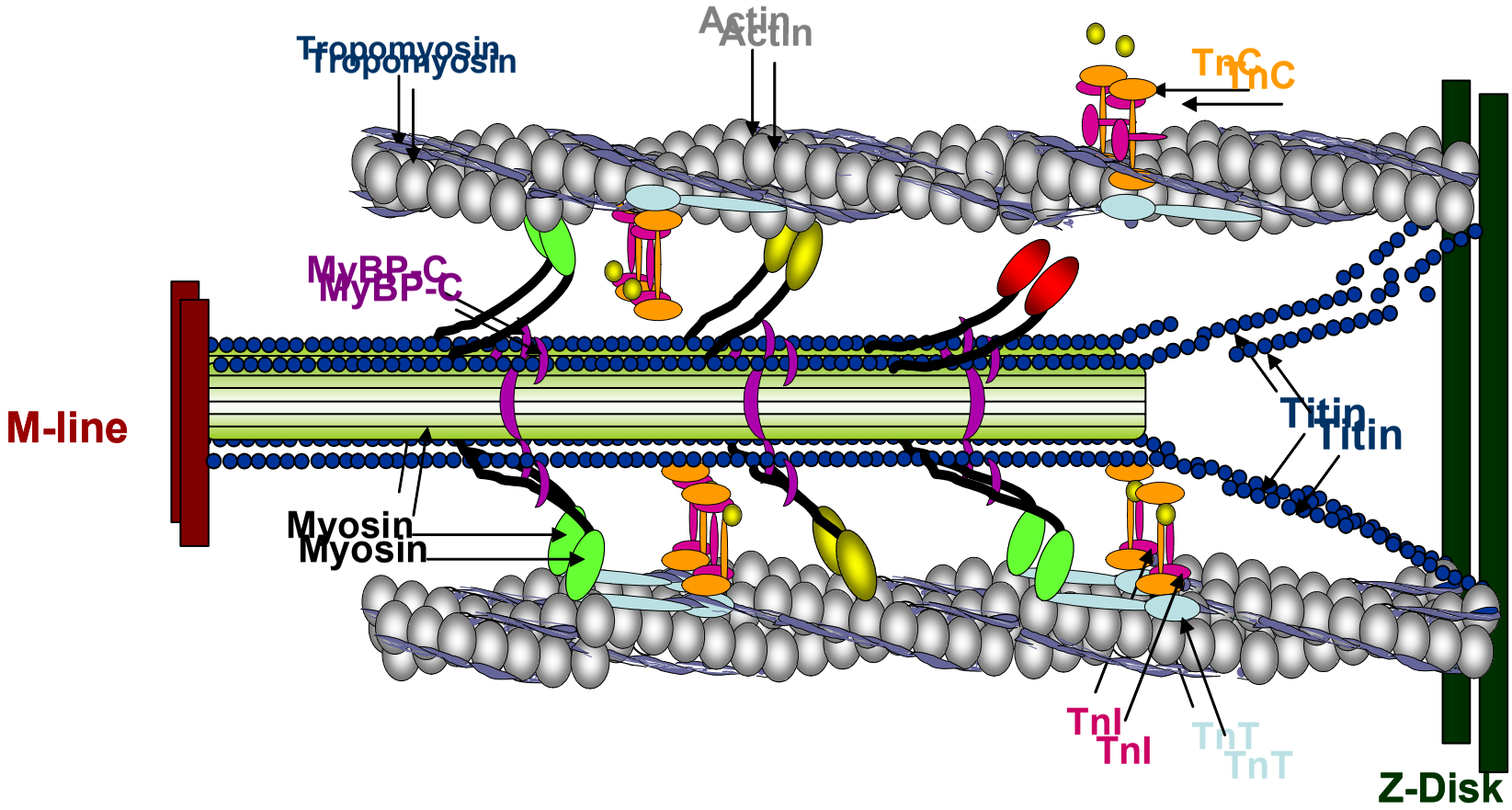
Tropomyosin
Actin
TnC
MyBP-C
M-line
Titin
Myosin
TnI
TnT
Z-Disk

As noted previously, increases in SL result in increased Ca^{2+} sensitivity. Specifically, this increased Ca^{2+} sensitivity is associated with an increase in Ca^{2+} affinity for the Ca^{2+} binding site on cardiac TnC (cTnC) [66, 67], which led to speculation that cTnC is the length sensor in cardiac muscle [8]. However, neither substitution of cTnC into skeletal muscle [119] nor expression of skeletal TnC in cardiac myocytes [101] altered the length dependence of Ca^{2+} sensitivity of tension. It is important to note that full activation of thin filaments requires both Ca^{2+} and strongly-bound myosin cross-bridges. For this reason, length dependence likely involves regulation, at least in part, by the thick filament.

1.4 Thick Filament Structure and Function

The major component of the thick filament is myosin, a highly asymmetrical hexameric protein consisting of two myosin heavy chains (MyHCs) and two pairs of myosin light chains (MLCs) for a total molecular weight of approximately 520 kDa. Each heavy chain is between 200-240 kDa, with a globular "head" at the N-terminus of the protein and an α-helical C-terminal "tail" that interacts with another MyHC in a coiled-coil motif. This coiled-coil intertwines to form a left-handed superhelix that makes up the rod portion of myosin, which interacts with other rod portions of myosin to make up the backbone of the thick filament. Myosin can be proteolytically cleaved to yield two subfragments termed heavy meromyosin (HMM) and light meromyosin (LMM) (Figure 1.5).

Figure 1.5

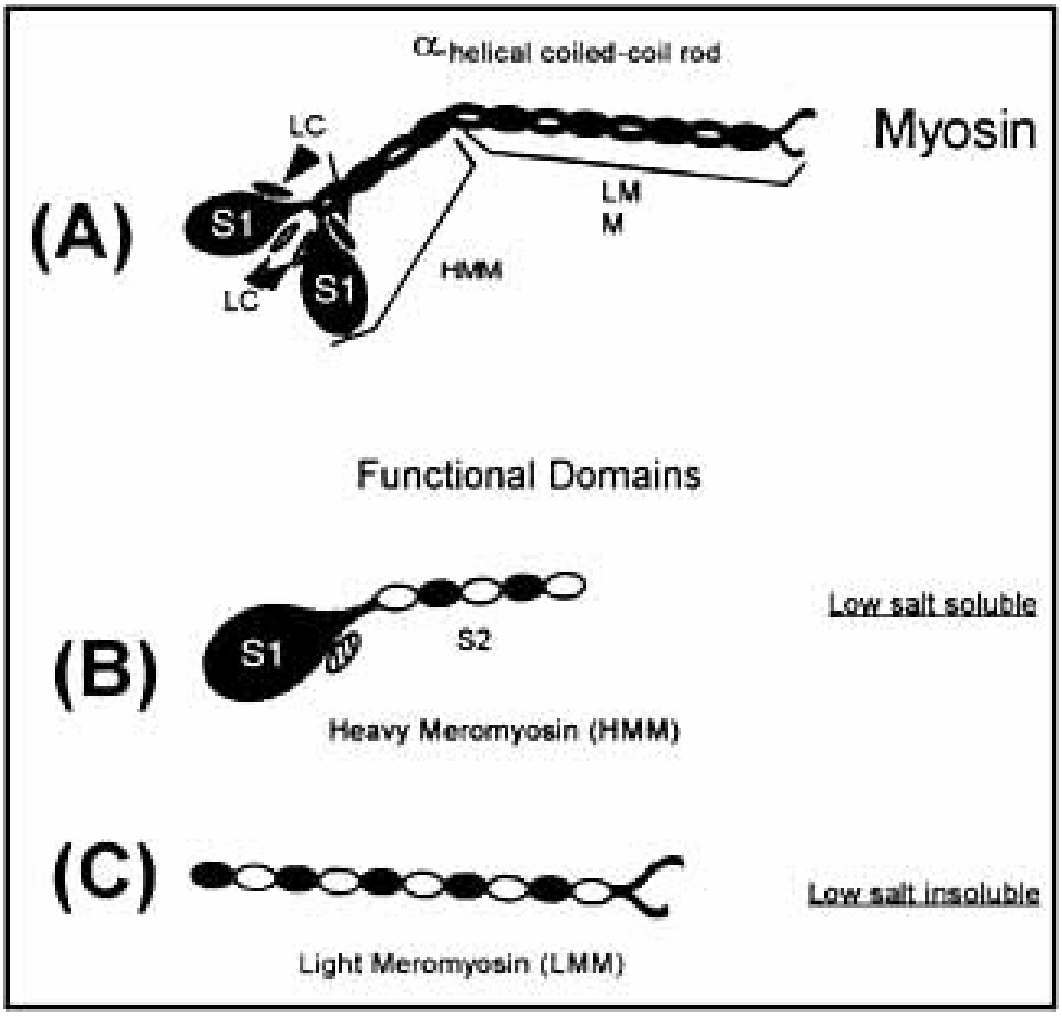

Figure 1.5: Illustration of Myosin and Myosin Fragments and Subunits

A. Illustration of the myosin molecule consisting of four light chains and two heavy chains with globular heads and an α-helical coiled-coil tail. Enzymatic cleavage with trypsin yields the low salt soluble heavy meromyosin **(B)** and the low salt insoluble light meromyosin **(C)**. (Taken from Wick [182])

HMM is composed of the two globular head and neck regions of MyHC termed subfragment-1 (S-1) that contain both the actin binding site and the ATP binding and catalyzing site, and a short part of the double stranded α-helical tail called subfragment 2 (S-2). LMM is the remaining two-thirds of the α-helical tail region. The two pairs of light chains consist of one pair of regulatory light chains (RLC) and one pair of essential light chains (ELC). ELC is thought to be required for normal actin-activated ATPase activity. Evidence suggests that it does so by providing stability to MHC by binding at the head-rod junction, also called the neck region that is thought to function as a "lever arm" for force generation. RLC also is thought to provide stability to the neck region of myosin, but can also regulate ATPase activity via phosphorylation by myosin light chain kinase (MLCK).

There are two types of myosin heavy chains expressed in the myocardium of mammals; α-MyHC and β-MyHC. Hoh et al., [70] were the first to discover three isozymes of cardiac myosin termed V_1, V_2, and V_3 based on decreasing electrophoretic mobility. It was later determined that V_1 and V_3 are homodimers of α- and β-MyHC respectively, while V_2 is a heterodimer of α- and β-MyHC. The expression of the MyHC isoforms is closely regulated in mammals, with β-MyHC being the dominant isoform expressed during early development of all mammals. β-MyHC remains high throughout life in humans, with α-MyHC comprising only ~10% of total MyHC protein [109, 154] despite α-MyHC mRNA representing ~35% of total ventricular MyHC mRNA [93, 121].

Rodents, on the other hand, experience a shift to α-MyHC around birth that remains high throughout life with some reversion to β-MyHC with age.

Increases in β-MyHC also are seen in pathophysiological conditions such as pressure overload [90, 92, 95], diabetes [25, 38], and hypothyroidism [22, 40, 115] in rodents. There is strong evidence that this is also the case in human myocardium where the small amount of α-MyHC (~10%) is replaced with β-MyHC in heart failure [109]. This appears to be functionally significant as it has been shown that a loss of as little as ~12% α-MyHC reduced power output by ~50% in rat single cardiac myocytes [62], although it has been postulated that this switch to β-MyHC is energetically favorable as it increases economy (i.e., force per ATP hydrolyzed) [50, 71, 91, 151, 168]. More recent evidence, however, suggests that α-MyHC may be as much as 70% of total MyHC in neonatal and young adult human myocardium, which diminishes with age [58].

These isozymes are highly homologous with 93% amino acid sequence homology [106]. Structurally, the amino acid changes most likely to account for mechanical differences are known to occur in the actin binding pocket, the ATP binding pocket, the neck region near ELC, the neck region near RLC, and in the rod segment of myosin [7] (illustrated as arrows in Figure 1.6). These few amino acid changes yield vast differences in the enzymatic and mechanical properties they convey on muscle. Myocytes containing 100% α-MyHC were shown to generate ~170% greater peak normalized power output than myocytes containing 100% β-MyHC [60, 85]. Similarly, α-MyHC has been shown to exhibit ~3 times higher actin activated ATPase activity and actin filament sliding

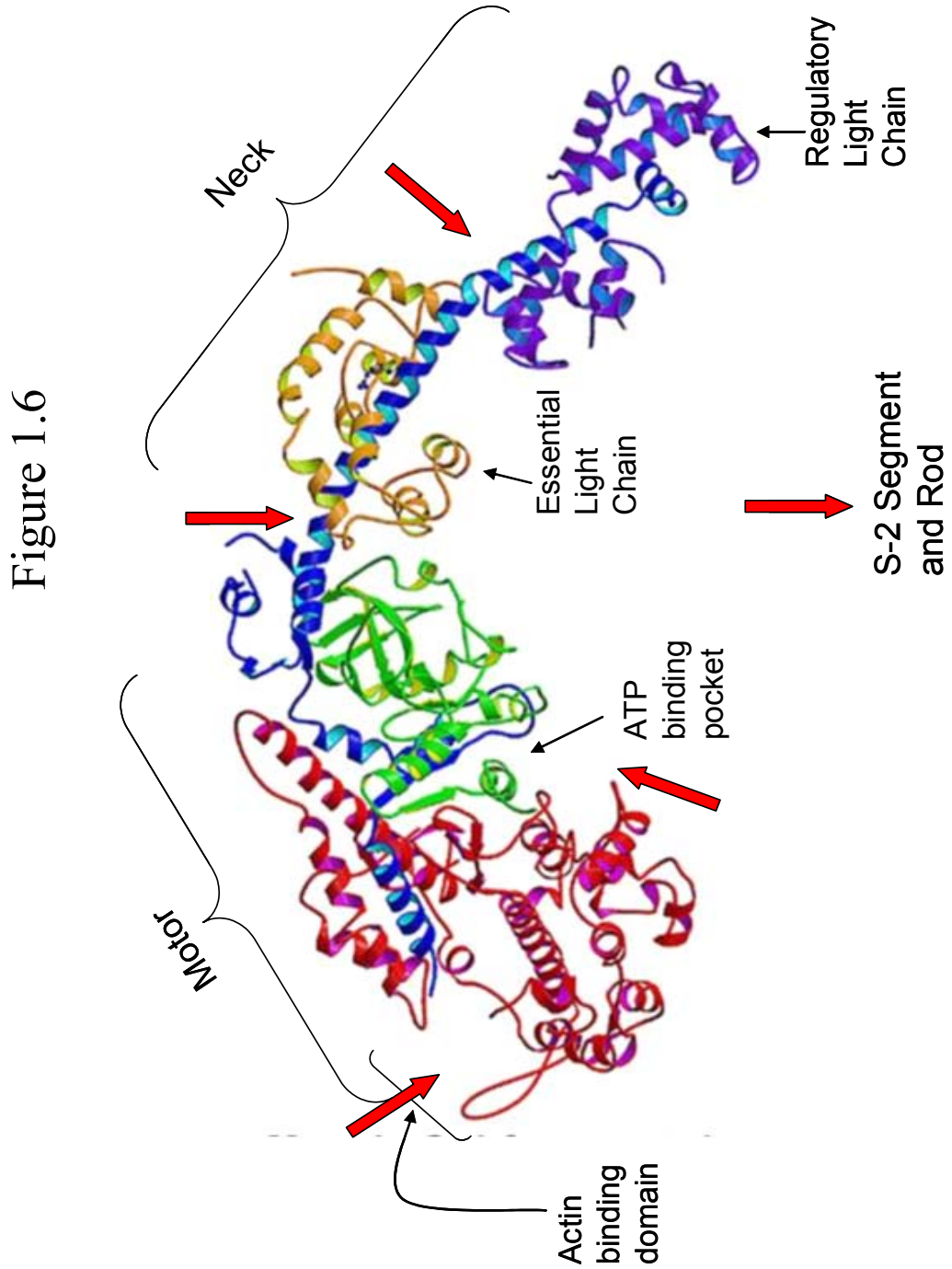

Figure 1.6: Crystal Structure of Chicken Myosin

Crystal structure of chicken myosin heavy chain, taken from Rayment et al., [143] illustrating the major domains of myosin heavy chain with points of amino acid differences between α-MyHC and β-MyHC indicated with arrows.

velocity than β-MyHC [141, 176, 184], and 2 to 6 times faster maximum shortening velocities in myocardial preparations [24, 30, 131]. β-MyHC, however, has been reported to produce twice the crossbridge force per ATPase cycle as α-MyHC, meaning it requires less energy consumption to maintain a given force (i.e., a lower tension cost) as noted above [50, 71, 91, 151, 168]. Expression of β-MyHC may therefore be energetically favorable for failing myocardium, but may compromise cardiac output due to slower rates of the rise of force [31, 32, 151], which would slow pressure development. β-MyHC also has slower myocardial shortening velocities [31, 32, 59, 60, 85, 131, 156], which would lessen ejection volume. Increased β-MyHC content also appears to be tightly correlated with slower heart rate across species, which may further compromise cardiac output (HR x SV). However, a slower heart rate also increases the time for ventricular filling, which would increase end-diastolic volume and lead to a more forceful ejection in accordance with the Frank-Starling relationship. Due to loss of sympathetic activation associated with heart failure [172], a failing heart must rely primarily on Starling's law to achieve more forceful contractions. Teleologically, it may be possible that β-MyHC is more responsive to changes in sarcomere length than α-MyHC as a compensatory mechanism to rely on changes in SL to tune power under more economical conditions. Experiments in this study were designed to test this novel hypothesis.

Different chemomechanical states in the cross-bridge cycle appear to differentially affect thin filament activation. Cycling cross-bridges have been reported to increase Ca^{2+} binding affinity to a greater degree than rigor cross bridges[13, 48]. As α-MyHC and β-MyHC exhibit different cross-bridge cycling rates, there is the possibility

that isometric tension-[Ca^{2+}] relationships are dependent on MyHC isoform content. Studies of this possibility have produced conflicting results. For example, a study that compared saponin-treated bundles of rabbit myocardium expressing either α-MyHC or β-MyHC showed no difference in the force-pCa relationships [132], whereas ventricular bundles from hypothyroid rats containing primarily β-MyHC were left-shifted (i.e., more sensitive to Ca^{2+}) compared to bundles from euthyroid α-MyHC rats containing primarily α-MyHC [40]. Single myocyte experiments have yielded no shift [30] or a rightward shift (less sensitivity to Ca^{2+}) in myocytes from hypothyroid rats [107]. The reasons for these discordant results are not known but may be due to undetected variations in the degree of protein kinase A (PKA) and/or protein kinase C (PKC) induced phosphorylation of myofibrillar proteins between the groups. PKA phosphorylation of serines 23 and 24 on TnI is known to decrease Ca^{2+} sensitivity of force in myocardial preparations [77, 166, 179], while PKC apparently increases Ca^{2+} sensitivity by phosphorylating TnI at serines 43 and 45 and threonine 144 [139].

Another confounding factor may be phosphorylation of troponin T (TnT), which binds to tropomyosin and acts as a molecular interface between tropomyosin and TnI/TnC. The functionally critical phosphorylation site on TnT may be Thr^{206}, which was preferentially phosphorylated by PKCα and resulted in decreased Ca^{2+} sensitivity [169]. PKA and PKC both phosphorylate the thick filament regulatory protein myosin binding protein-C (MyBP-C) but at the same sites [178]. The role of MyBP-C in Ca^{2+} sensitivity is not known but mice lacking MyBP-C showed decreased Ca^{2+} sensitivity [51]. Furthermore, myosin light chain 2 (RLC) is phosphorylated by PKC, which results

in increased Ca^{2+} sensitivity[78]. An inverse correlation also was found between the percentage of phosphorylated MLC_2 and pCa_{50} in donor and failing human hearts[175], whereas other studies show only modest changes in MLC_2 phosphorylation with changes in Ca^{2+} sensitivity arising from TnI phosphorylation[139]. Clearly, regulation of Ca^{2+} sensitivity is a complex interaction between a number of myofibrillar proteins that need to be controlled for as carefully as possible when assessing Ca^{2+} sensitivity of force in cardiac muscle. The experiments performed in this dissertation attempted to determine if myocytes containing α-MyHC or β-MyHC have different Ca^{2+} sensitivity of force, working under the hypothesis that previously seen differences in Ca^{2+} sensitivity of force were due to undetected differences in myofibrillar protein phosphorylation levels. Tension-pCa relationships were compared between skinned myocytes expressing either 100% α-MyHC or 100% β-MyHC in which the level of myofibrillar phosphorylation was at least partly controlled by incubating the myocytes with the catalytic subunit of PKA.

Another major component of the thick filament is myosin binding protein-C (MyBP-C). MyBP-C is a "C" shaped protein found at 43 nm repeats in a segment of the A band called the C zone (see Figure 1.3E) in both skeletal and cardiac muscle [9]. It consists of 10 distinct domains (termed C1 through C10), 7 fibronectin and 3 immunoglobin, but the cardiac isoform contains an additional immunoglobin segment at the N terminus (termed C0) and a 105 amino acid residue linker between C1 and C2 called the MyBP-C motif [130]. The MyBP-C motif carries 3 phosphorylation sites

unique to the cardiac isoform that can be phosphorylated by PKA and PKC, and has also been shown to interact with the S2 segment of myosin [39]. MyBP-C was long thought to be a structural element as its carboxy terminus binds and interacts with the rod portion of myosin [41] and titin [33]. Synthetic myosin filaments show increased uniformity and decreased diameter in the presence of MyBP-C [84], while cardiac muscle cells expressing truncated MyBP-C have increased disorder and myofibrillar disarray [188]. Interestingly, x-ray diffraction patterns suggest that there are changes in MyBP-C structure and myosin backbone arrangement during contraction [69, 73, 162], underlining the intimate interaction between MyBP-C and myosin. More recent evidence suggests that the C5 and C8 domains, and to a lesser extent the C7 and C10 domains, of neighboring MyBP-Cs preferentially interact with each other, leading to the hypothesis that MyBP-C forms a trimeric "collar' that wraps around the thick filament [110] (Figure 1.7). In this arrangement, it is well positioned to provide structural integrity to the backbone of the thick filament, as well as to provide potential regulatory action on titin, actin, and the myosin heads. Functionally, addition of MyBP-C to cardiac myosin increases the ATPase activity at all ionic strengths [155]. Importantly, the entire myosin molecule must be present for this change in ATPase activity to occur [55, 96, 112], suggesting that ATPase activity is influenced by the rod portion of myosin. Removal of RLC abolishes the MyBP-C induced increase in ATPase activity, while restoration of RLC also restores this effect [96]. Thus, MyBP-C may be interacting with RLC to affect the ATPase rate of myosin, which makes sense considering that MyBP-C is thought to bind at the hinge region of myosin very near RLC [114, 162]. In terms of contractile function, it has been suggested that MyBP-C contributes to an internal load because

Figure 1.7

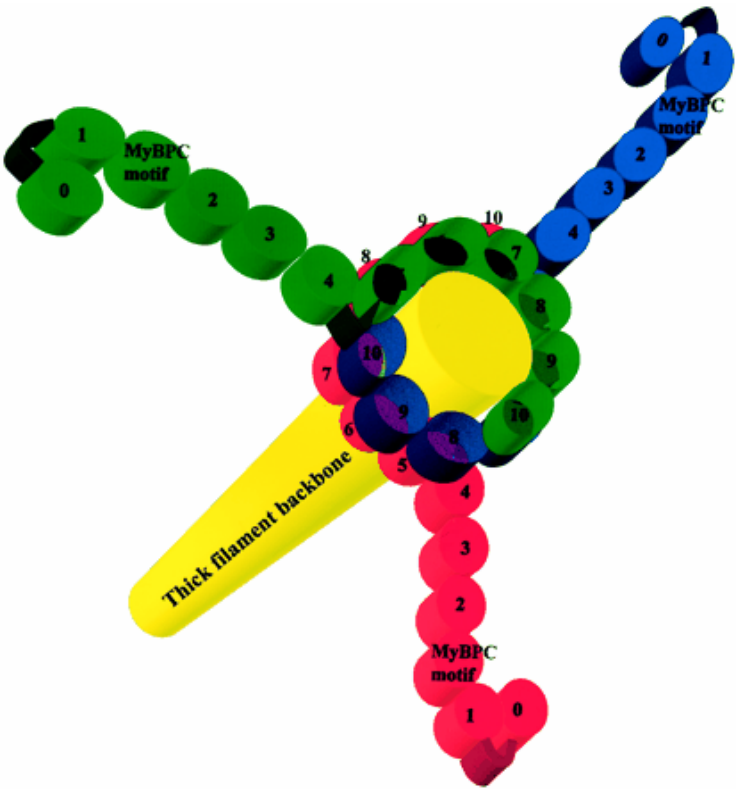

Figure 1.7: Proposed Trimeric Collar for MyBP-C

MyBP-C forms a collar around the rod portion of the thick filament backbone, providing structural support and potential crossbridge regulation (taken from Moolman-Smook et al., 2002) [110].

partial extraction resulted in an increase in maximal shortening velocity (V_{max}) at submaximal Ca^{2+} concentrations [68, 69]. Partial extraction of MyBP-C also resulted in an increase in submaximal force with no change in maximal force, which was reversible when MyBP-C was restored [68, 118]. Phosphorylation of MyBP-C by PKA is thought to reduce the interaction between MyBP-C and the S2 segment of myosin, and PKA is known to increase loaded shortening velocity and power output in skinned cardiac myocytes [61]. Furthermore, disruption of the interaction between MyBP-C and S2 enhanced myocyte shortening [15] and increased Ca^{2+} sensitivity of force in skinned myocardium [87, 185]. Together, these results imply that MyBP-C acts as a "brake" to limit contractility. However, PKA also phosphorylates TnI, necessitating a separation of the effects of TnI phosphorylation from MyBP-C phosphorylation. Experiments performed here utilized a transgenic mouse model of MyBP-C to test the hypothesis that myocytes lacking MyBP-C would have increased loaded shortening velocity, power output, and rates of force development due to lack of restraint normally imposed by MyBP-C on crossbridge kinetics.

1.5 Sarcomere Length Dependence of Myocardial Function

The Frank-Starling mechanism is an important determinant of cardiac output, and failure of this mechanism will inevitably lead to fluid buildup such as pulmonary edema or inadequately supply peripheral tissue leading to organ failure. Furthermore, there is significant evidence demonstrating that the Frank-Starling mechanism is compromised in human [72, 80, 157] and other animal models of heart failure [76, 81, 123, 150]. As

discussed above, the cellular basis for the Frank-Starling mechanism involves an enhancement of force and Ca^{2+} sensitivity of force [4, 5, 43, 66, 79, 101]. Interestingly, a recent study showed that the rate of force development was actually faster at short SL when the difference in isometric force was normalized in rat skinned cardiac trabeculae [1]. The experiments presented in this dissertation measured the rate of force development at long and short SL with and without matched isometric forces. While many studies involving the Frank-Starling relationship have focused on the steady-state measurement of force, there have been few studies that addressed myocardial shortening, most of which measured unloaded shortening velocity. Early studies indicated that unloaded shortening velocity in frog skeletal fibers was independent of SL, but these experiments were performed at maximal Ca^{2+} activation [26]. A more recent study using ferret papillary muscle showed SL dependence of muscle segment shortening under very lightly loaded contractions [97]. This also was seen in rat cardiac trabeculae activated at submaximal Ca^{2+} levels where unloaded shortening velocity correlated with SL; the authors speculated the unloaded shortening velocity is limited by an internal passive viscoelastic element, such as titin [24]. Myocytes in vivo, however, undergo shortening against an afterload and there is a dearth of literature regarding the effects of sarcomere length on the dynamic measurement of shortening against a load. Thus, we examined SL dependence of loaded shortening velocity and power output. Additionally, SL was monitored and recorded during these measurements to provide as thorough a characterization of sarcomeric shortening velocity as possible. Potential subcellular mechanisms that regulate SL responsiveness also were examined. As a myocyte shortens, the distance between the thick and thin filament, known as the interfilament

lattice space, increases [74, 98, 149]. Similar changes have also been observed in myocardium *in situ* [137]. The result of an increase in lattice spacing is that the distance between actin and the myosin heads is increased, thereby decreasing the likelihood of crossbridge interaction. Conversely, decreasing the interfilament distance by increasing SL enhances the probability of crossbridge interaction. Similarly, decreasing the interfilament spacing independent of SL by osmotic compression has been shown to increase force, enhance Ca^{2+} sensitivity, and speed loaded shortening velocity [54, 82, 101]. Shortening velocity is likely increased due to elevated levels of thin filament activation arising from increased numbers of strongly bound myosin crossbridges [99, 103]. Thus, we also examined SL dependence of sarcomeric shortening velocity and rate of force development at matched thin filament activation levels indexed by isometric force or matched lattice spacing indexed by myocyte width.

Chapter 2: LOADED SHORTENING, POWER OUTPUT, AND RATE OF FORCE REDEVELOPMENT ARE INCREASED WITH KNOCKOUT OF CARDIAC MYOSIN BINDING PROTEIN-C

ABSTRACT

Myosin binding protein-C (MyBP-C) is localized to the thick filaments of striated muscle where it appears to have both structural and regulatory functions. Importantly, mutations in the cardiac MyBP-C gene are associated with familial hypertrophic cardiomyopathy. The purpose of this study was to examine the role that MyBP-C plays in regulating force, power output, and force development rates in cardiac myocytes. Skinned cardiac myocytes from wild type (WT) and MyBP-C knock-out (MyBP-$C^{-/-}$) mice were attached between a force transducer and position motor. Force, loaded shortening velocities, and rates of force redevelopment were measured during both maximal and half-maximal Ca^{2+} activations. Isometric force was not different between the two groups with force being 17.0 ± 7.2 kN/m^2 and 20.5 ± 3.1 kN/m^2 in wild type and MyBP-$C^{-/-}$ myocytes, respectively. Peak normalized power output was significantly increased by 26% in MyBP-$C^{-/-}$ myocytes (0.15 ± 0.01 versus 0.19 ± 0.03 P/P_o*ML/sec) during maximal Ca^{2+} activations. Interestingly, peak power output in MyBP-$C^{-/-}$ myocytes was increased to an even greater extent (46%, 0.09 ± 0.03 versus 0.14 ± 0.02 P/P_o*ML/sec) during half-maximal Ca^{2+} activations. There was also an effect on the rate constant of force redevelopment (k_{tr}) during half-maximal Ca^{2+} activations, with k_{tr} being significantly greater in MyB-$C^{-/-}$ myocytes (WT = 5.8 ± 0.9 s^{-1} vs. MyBP-$C^{-/-}$ = 7.7 ± 1.7 s^{-1}). These results suggest that cMyBP-C is an important regulator of myocardial work capacity whereby MyBP-C acts to limit power output.

INTRODUCTION

Myosin binding protein-C (MyBP-C) is a thick filament associated protein [129] that is present in vertebrate striated muscle, and mutations in the cardiac MyBP-C gene have been implicated in the development of some familial hypertrophic cardiomyopathies (FHC) [171]. Although the exact role of MyBP-C in muscle development and function is unclear, it has been postulated that MyBP-C plays both structural and regulatory roles [183]. The role of MyBP-C as a structural element involves its carboxy terminus binding to the thick filament where it interacts with both the rod portion of myosin [41] and titin [33]. These C-terminal interactions are thought to stabilize the structure of the thick filament and produce a more ordered arrangement of myosin heads. Moolman-Smook et al., have provided evidence that the immunoglobulin-like domains C5 and C8 of MyBP-C preferentially interact with each other, which taken together with previous structural and biochemical data led them to propose that MyBP-C molecules form a collar around the backbone of the thick filament [110]. They speculated that the collar packs the backbone more tightly and restricts actin-myosin interactions, whereas release of the collar would result in a looser backbone and perhaps enhance cross-bridge formation. Additionally, mutations in the MyBP-C gene that produce C-terminal truncated proteins have been found to result in acute changes in structure not only at the myofilament, but also in the structure of the heart that ultimately leads to impaired myocardial performance [19]. Cardiac MyBP-C (cMyBP-C) also contains a unique immunoglobulin-like domain at the N-terminal portion of the protein termed C0 [19] and a distinct region between two Ig-like domains (C1 and C2), which is termed the MyBP-C motif [39]. This motif has

been shown to bind to the S2 segment of myosin near the lever arm domain of the myosin head, and this interaction is modified in response to phosphorylation of the MyBP-C motif by cAMP-dependent protein kinase (PKA) [39, 46]. Mutations in the cardiac MyBP-C gene that lead to changes near the N-terminus have also been linked to familial hypertrophic cardiomyopathy [125].

Recently, targeted ablation of the cMyBP-C gene was used to produce mice lacking MyBP-C in the heart [51]. Mice lacking cMyBP-C (MyBP-$C^{-/-}$) were viable and displayed well-developed sarcomeres indicating MyBP-C is not essential for myofibrillogenesis. However, MyBP-$C^{-/-}$ mice exhibited profound concentric cardiac hypertrophy and impaired diastolic and systolic function *in vivo* [51]. The impaired heart function was somewhat surprising in light of several studies showing enhanced myocyte contractility following manipulations of MyBP-C. For instance, disrupting the interactions between MyBP-C and S2 enhanced myocyte shortening [15] and increased Ca^{2+} sensitivity of force in skinned myocardial preparations [87, 185]. Consistent with these results, partial extraction of MyBP-C also increased Ca^{2+} sensitivity of force in skinned myocytes [69] and sped shortening velocity in skinned skeletal muscle fibers [68]. These results are all consistent with a model in which MyBP-C affects myosin head flexibility and position perhaps by serving as collar or a tether. Removal of this collar/tether would increase myosin head flexibility and bring the head in closer proximity to actin, thereby enhancing the probability of cross-bridge formation.

The purpose of this study was to examine the effects of targeted deletion of cMyBP-C on contractile function in single skinned myocytes, working under the hypothesis that myocytes lacking MyBP-C would have faster loaded shortening velocities, greater power output, and increased force redevelopment rates all due to elevated cross-bridge interaction kinetics resulting from removal of myosin head constraints normally imposed by MyBP-C.

METHODS

Experimental Animals

Homozygous cardiac MyBP-C knockout mice (cMyBP-C$^{-/-}$) were generated as previously described in detail [51]. Briefly, exons 3 through 10 of the murine cMyBP-C gene were deleted from mouse genomic DNA by homologous recombination. Properly targeted embryonic stem cells were injected into C57/B6 blastocysts and implanted into C57/B6 pseudopregnant mice. Appropriate breeding resulted in homozygous MyBP-C null mice. Animals were housed in groups of two to three and provided food and water ad libitum. All procedures involving animal use were performed according to the Animal Care and Use Committees of the University of Wisconsin and University of Missouri. The animals were anesthetized by intraperitoneal injection of sodium pentobarbital and euthanasia by excision of the heart.

Cardiac Myocyte Preparation

Skinned cardiac myocyte preparations were obtained from mouse hearts using methods similar to those described previously for rats [60]. The compositions of relaxing

and activating solutions were as follows (in mmol/L, obtained from Sigma at highest possible purity): free Mg^{2+} 1, EGTA 7, MgATP 4, imidazole 20, and creatine phosphate 14.5 (pH 7.0); various [Ca^{2+}] between $10^{-4.5}$ (maximal Ca^{2+} activating solution) and 10^{-9} (relaxing solution); and sufficient KCl to adjust ionic strength to 180 mmol/L [116]. A portion of cardiac myocytes were aliquoted and stored in ATP free relaxing solution containing phosphatase inhibitors (20 mmol/L NaF and 50 μg/ml microcystin LR) at –70°C for autoradiographic analysis. The experimental apparatus used for physiological measurements of single skinned myocytes has been described [60]. The dimensions of the myocyte preparations are included in Table 2.1.

Table 2.1: Summary of myocyte dimensions

	Length, μm	Width, μm	SL at pCa 4.5, μm
Wildtype	132.8 ± 28.4	20.1 ± 2.3	2.31 ± 0.097
MyBP-$C^{-/-}$	123.8 ± 31.4	24.3 ± 4.3	2.28 ± 0.089

Values are means ± S.D., SL = sarcomere length

Force-velocity and power-load measurements

The protocol for obtaining force-velocity and power-load measurements has been described in detail [99] and all measurements were done at 13±1°C. The attached myocyte was first transferred in maximal Ca^{2+} activating solution and allowed to obtain a steady state force, after which a series of sub-steady state force clamps were applied to

determine isotonic shortening velocities. The isotonic force was maintained using a servo system for 150-250 ms while the length change during this time was monitored. Following the force clamp, the myocyte was slackened to near zero force to estimate the relative load sustained during the isotonic shortening, after which the myocyte was re-extended to its starting length. Due to the short lengths of single myocyte preparations, the rapid slackening following isotonic shortening did not always yield a baseline force value, the result of which is an underestimation of peak force and, thus, of the relative force during loaded contractions. In these cases, more accurate estimates of the relative force during isotonic shortening were obtained by interpolating between the peak forces in isometric contractions that were performed before and after every series of loaded contractions. The myocytes were kept in maximal Ca^{2+} activating solution for 2-3 minutes during which 10-20 force clamps were performed without significant loss of force. If maximal force fell below 80% of the initial value while performing the force clamps, the myocyte was discarded and the data not included. Force-velocity measurements also were obtained during half-maximal Ca^{2+} activations following the protocol above. Hyperbolic force-velocity curves were fitted to the relative force-velocity data using the Hill equation:

$$(P + a)\,(V + b) = (P_0 + a)b,$$

where P is force during shortening at velocity V; P_o is the isometric force; and a and b are constants with dimensions of force and velocity, respectively. Power load curves were obtained by multiplying force by velocity at each load on the force-velocity curve.

Rate of force redevelopment

The kinetics of force development were obtained using a procedure similar to that previously described [104]. While in activating solution (either maximal or half-maximal Ca^{2+}), the myocytes were slackened by ~15% of myocyte length to produce zero force and subsequently underwent a brief period of unloaded shortening. The myocyte was then rapidly restretched to its initial pre-slack length. The slack-restretch maneuver caused nearly complete dissociation of cross-bridges, and the subsequent tension redevelopment was due to reattachment of cross-bridges and their transition into force-generating states. Force redevelopment traces were fit by a single exponential function:

$$F = F_{max}(1 - \exp(-k_{tr}t)) + F_{res},$$

where F is tension at time t, F_{max} is maximal tension, and k_{tr} is the rate constant of tension redevelopment. F_{res} represents any residual tension present immediately after the slack-restretch maneuver.

SDS-PAGE and Autoradiography

To determine the effects that deletion of MyBP-C had on baseline phosphorylation of cardiac troponin I, myofibrillar samples were incubated 30 minutes with the catalytic subunit of PKA (3-5 μg/mL, Sigma) in the presence of (γ-^{32}P)-ATP (50 μCi, NEN). The reaction was terminated by addition of electrophoresis sample buffer and heating at 95°C for 3 minutes. Equivalent protein loads were then separated by SDS-PAGE, silver stained, dried overnight, and exposed to a Kodak phosphoimaging screen for visualization on a phosphoimager. Individual radiolabeled protein bands were then excised from the gel and quantified using a scintillation counter (Packard 1900 TR).

Stoichiometric cTnI phosphate incorporation was calculated using the following equation:

$$\text{cpm cTnI/[TnI]} * [P_i]/\text{cpm total} = [P_i]/[\text{cTnI}],$$

where all concentrations are in moles and cpm is counts per minute. Figure 2.1 shows that MyBP-C and cTnI were phosphorylated by PKA in wild-types, while only cTnI was phosphorylated in myofibrils from MyBP-$C^{-/-}$ mice. Additionally, stoichiometric analysis indicated that PKA-induced phosphorylation of cTnI was similar between WT (0.96 ± 0.14 mol P_i/mol cTnI) and MyBP-$C^{-/-}$ (0.97 ± 0.17 mol P_i/mol cTnI) cardiac myofibrils.

Data and Statistical Analysis

Skinned myocyte preparation length traces, force-velocity curves, power-load curves, and rate constants of force redevelopment were analyzed as previously described [104, 105]. Student *t* tests were performed to determine significant differences between WT and MyBP-$C^{-/-}$ as well as between maximal Ca^{2+} and half-maximal Ca^{2+} measurements. $P<0.05$ was chosen as signifying significance. All values are expressed as means ± SD.

Figure 2.1

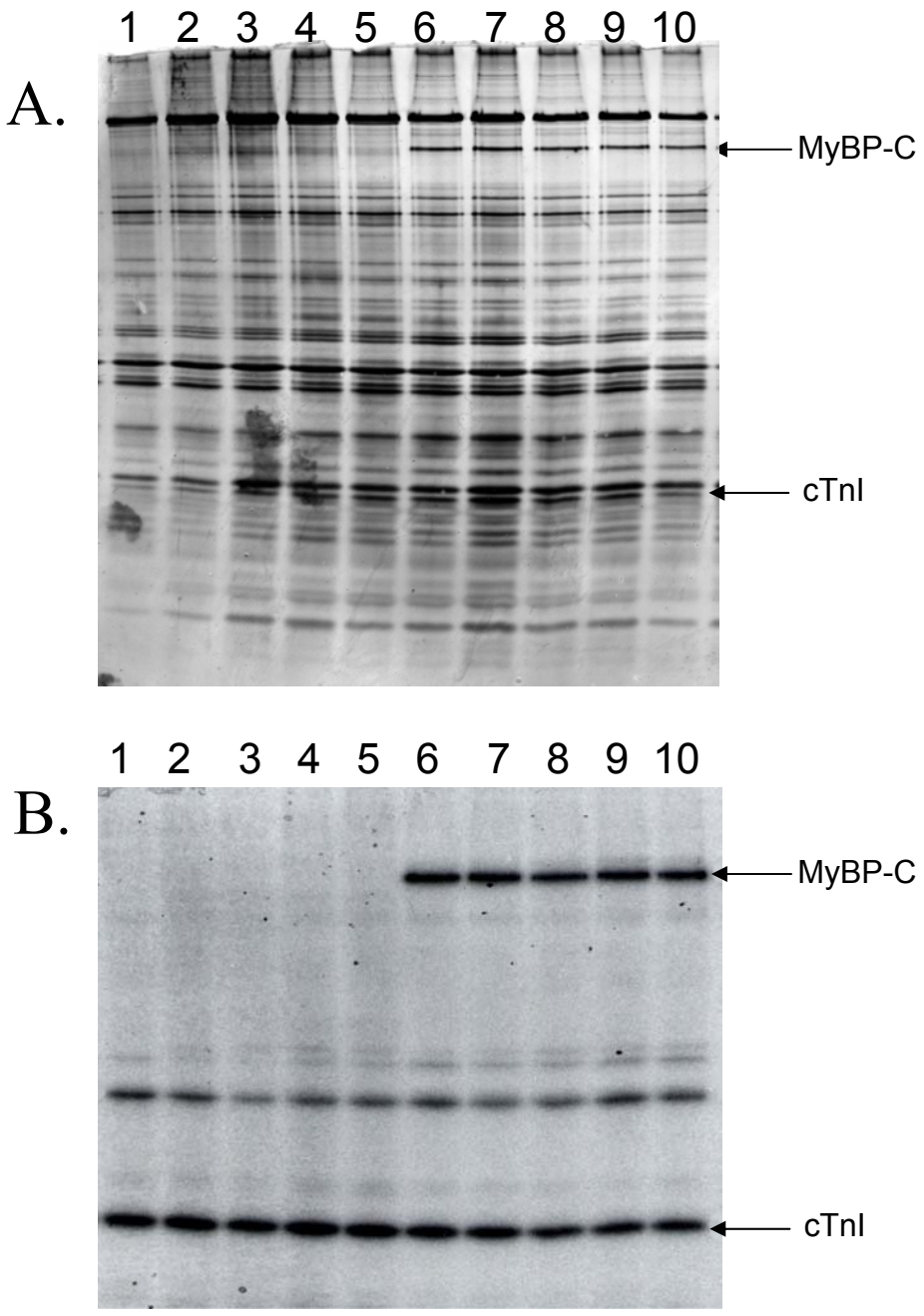

Figure 2.1: Effect of MyBP-C ablation on PKA-induced phosphate incorporation.

Silver stain **(A)** and autoradiogram **(B)** of cardiac myofibrils from MyBP-C$^{-/-}$ (lanes 1-5) and WT (lanes 6-10) mice. Note the lack of phosphorylation of MyBP-C in MyBP-C$^{-/-}$ myofibrils. Also, the absence of MyBP-C did not appear to alter cTnI phosphorylation levels. PKA-induced phosphorylation of cTnI was similar between MyBP-C$^{-/-}$ (0.97 ± 0.17 mol P_i/mol cTnI) and WT (0.96 ± 0.14 mol P_i/mol cTnI) cardiac myofibrils.

RESULTS

Force-velocity and power-load curves were measured in MyBP-C$^{-/-}$ myocytes to assess the role of MyBP-C on work capacity of cardiac myocytes. Maximal Ca^{2+} activated force was unaffected by the absence of MyBP-C (WT = 17.0 ± 7.2 kN m^{-2} vs. MyBP-C$^{-/-}$ = 20.5 ±4.5 kN m^{-2}). On the other hand, force-velocity relationships were markedly altered in myocytes lacking MyBP-C. Deletion of MyBP-C shifted the force-velocity relationship upwards such that shortening velocity was faster at nearly all relative loads (Figure 2.2). The bottom panel of Figure 2.2 shows that power output (normalized to isometric force, i.e., normalized power output) was also greater at nearly all relative loads in MyBP-C$^{-/-}$ myocytes, with peak normalized power output significantly increased by 26% (WT = 0.15 ± 0.01 versus MyBP-C$^{-/-}$ = 0.19 ± 0.03 P/P_o*ML/sec ($p<0.05$)) (Table 2.2). The mean shortening velocity at loads optimal for power output (V_{opt}) was 25% faster in MyBP-C$^{-/-}$ myocytes (WT = 0.45 ± 0.03 ML/s versus MyBP-C$^{-/-}$ = 0.56 ± 0.10 ML/s ($p<0.05$)) (Table 2.2).

Figure 2.2

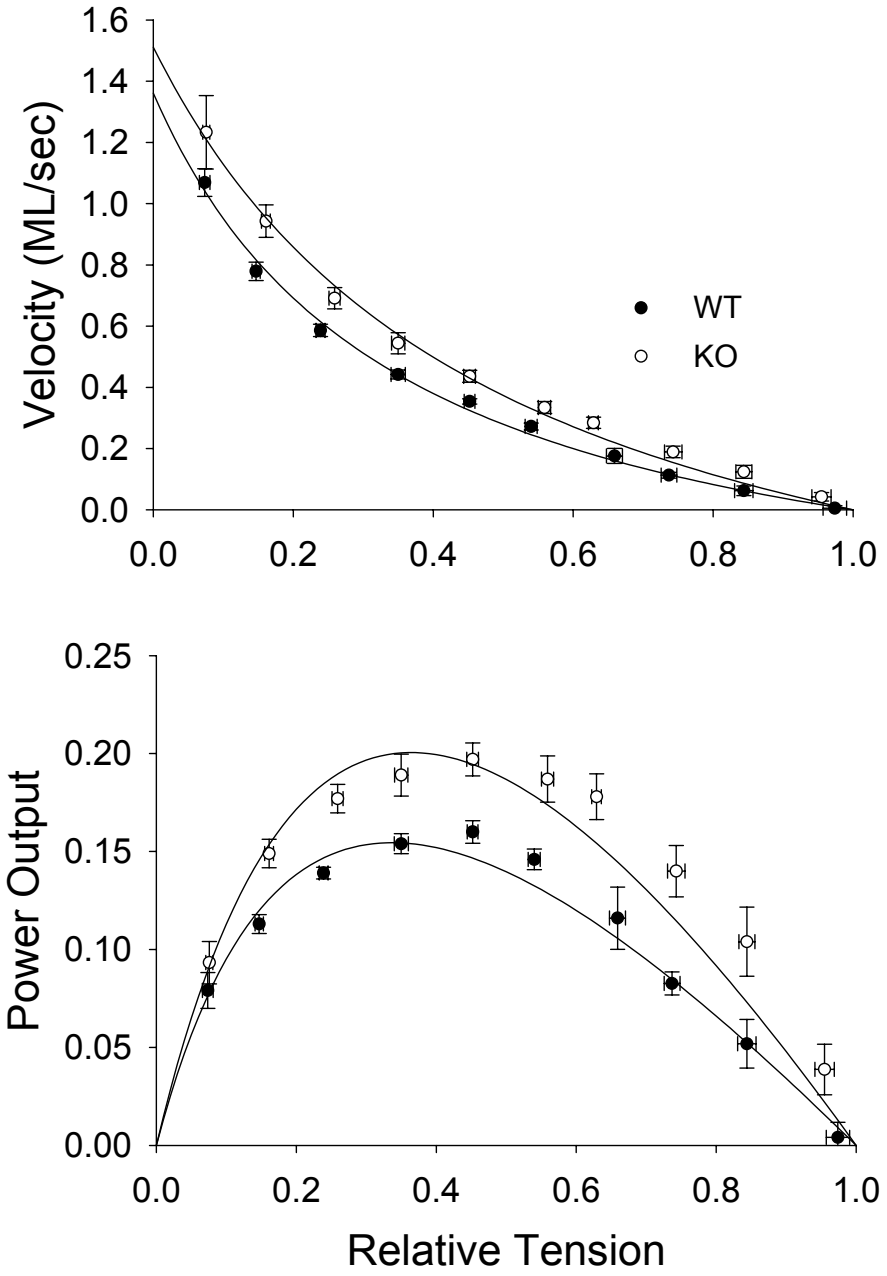

Figure 2.2: Effect of MyBP-C ablation on loaded shortening during maximal Ca^{2+} activation.

Force-velocity (top) and power-load (bottom) curves from WT and MyBP-$C^{-/-}$ skinned cardiac myocytes during maximal Ca^{2+} activations. Loaded shortening and power output significantly increased at intermediate loads in MyBP-$C^{-/-}$ myocytes during maximal Ca^{2+} activation. Data points are means ± S.D.

Overall, these results suggest that the absence of MyBP-C increased power output of single myocytes solely by increasing loaded shortening rates (rather than an increase in force generating capacity), which likely resulted from faster crossbridge cycling rates at each given load.

Table 2.2: Maximal calcium activated force, velocity and peak power output in wildtype and MyBP-C$^{-/-}$ mouse skinned cardiac myocytes.

	Wildtype	MyBP-C$^{-/-}$
Maximum Force, kN*m^{-2}	17.03 ± 7.22	20.48 ± 4.45
V_{max}, ML * s^{-1}	1.29 ± 0.19	1.60 ± 0.36
F_{opt}	0.348 ± 0.028	0.351 ± 0.026
V_{opt}, ML * s^{-1}	0.446 ± 0.033	0.559 ±0.103*
Peak normalized power output, P/P_0 * ML * s^{-1}	0.154 ± 0.011	0.194 ± 0.032*

Values are means ± S.D., n = 6 for each. F_{opt} indicates relative force at which power was optimal. *Significant difference from wildtype; $P<0.05$

Because Ca^{2+} activation of cardiac myofilaments does not likely reach a maximum *in vivo*, we also examined the effects of MyBP-C ablation on force, velocity, and power output during half-maximal Ca^{2+} activations. These results are shown in Figure 2.3 and summarized in Table 2.3. The pCa solution that yielded half-maximal force was 5.77 ± 0.08 in wild type and 5.67 ± 0.08 in MyBP-C$^{-/-}$, indicating a slight reduction in Ca^{2+} sensitivity to force in MyBP-C$^{-/-}$ myocytes, although this shift was not

statistically significant (p=0.06). Half-maximal Ca^{2+} activation also yielded force-velocity and power-load curves that were shifted to higher velocities and loads in MyBP-$C^{-/-}$ myocytes as compared to WT myocytes. Interestingly, this upward shift was greater than that seen during maximal Ca^{2+} activation. Deletion of MyBP-C increased loaded shortening and power output at all relative loads, and increased peak normalized power output 46% (WT = 0.09 ± 0.03 wildtype versus MyBP-$C^{-/-}$ = 0.14 ± 0.02 P/P_o*ML/sec) compared to 26% during maximal Ca^{2+} activation. Likewise, V_{opt} was 42% faster (WT = 0.25 ± 0.05 versus MyBP-$C^{-/-}$ = 0.36 ±0.10) at half-maximal Ca^{2+} activation, compared to 25% during maximal Ca^{2+} activation. Overall, these results indicate that removal of MyBP-C results in faster loaded crossbridge cycling, and that this effect is relatively greater at half-maximal Ca^{2+} activation than at maximal Ca^{2+} activation.

Figure 2.3

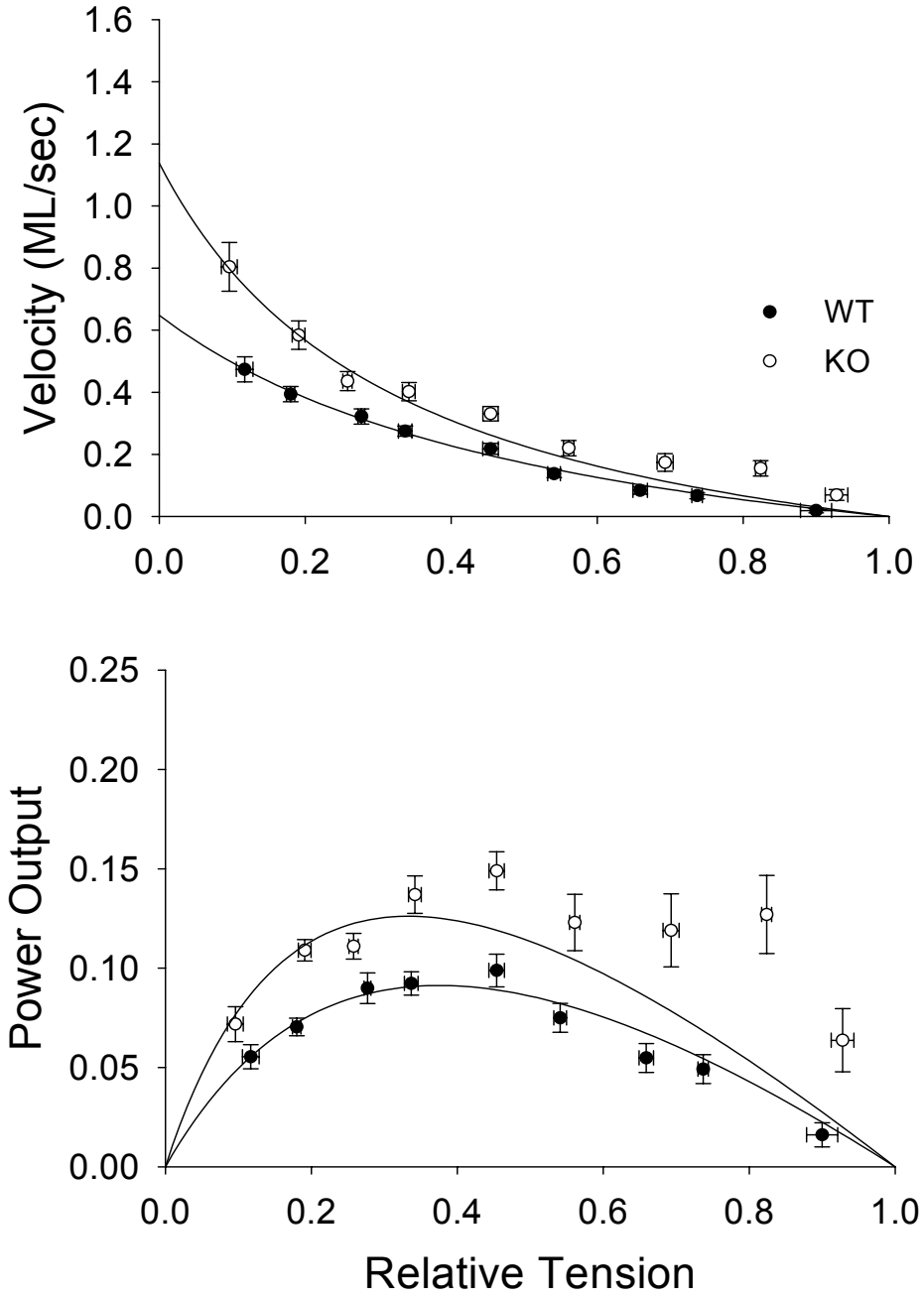

Figure 2.3: Effect of MyBP-C ablation on loaded shortening during half-maximal Ca^{2+} activation.

Force-velocity (top) and power-load (bottom) curves from WT and MyBP-$C^{-/-}$ skinned cardiac myocytes during half-maximal Ca^{2+} activations. Loaded shortening velocity and power output were significantly increased in MyBP-$C^{-/-}$ myocytes at all loads. Data points are mean ± S.D.

Table 2.3: Half-Maximal calcium activated force, velocity and peak power output in wildtype and MyBP-C$^{-/-}$ mouse skinned cardiac myocytes

	Wildtype	MyBP-C$^{-/-}$
Maximum Force, kN*m^{-2}	10.82 ± 6.32	10.51 ± 1.53
Vmax, ML * s^{-1}	0.687 ± 0.224	0.833 ± 0.252
Fopt	0.377 ± 0.059	0.388 ± 0.057
Vopt, ML * s^{-1}	0.251 ± 0.049	0.356 ±0.098*
Peak normalized power output, P/P_0 * ML * s^{-1}	0.093 ± 0.017	0.135 ± 0.031*

Values are means ± S.D. n = 6 for each. *Significant difference from wildtype; $P<0.05$

To further examine the effects of MyBP-C ablation on crossbridge turnover kinetics, the rate of force redevelopment was measured during maximal and half-maximal Ca^{2+} activations. Results are summarized in Figure 2.4. Deletion of MyBP-C did not alter the rate constant of force redevelopment (k_{tr}) during maximal Ca^{2+} activations. However, k_{tr} at half-maximal Ca^{2+} activation was significantly greater in MyB-C$^{-/-}$ myocytes compared to WT (see inset in Figure 2.4).

Figure 2.4

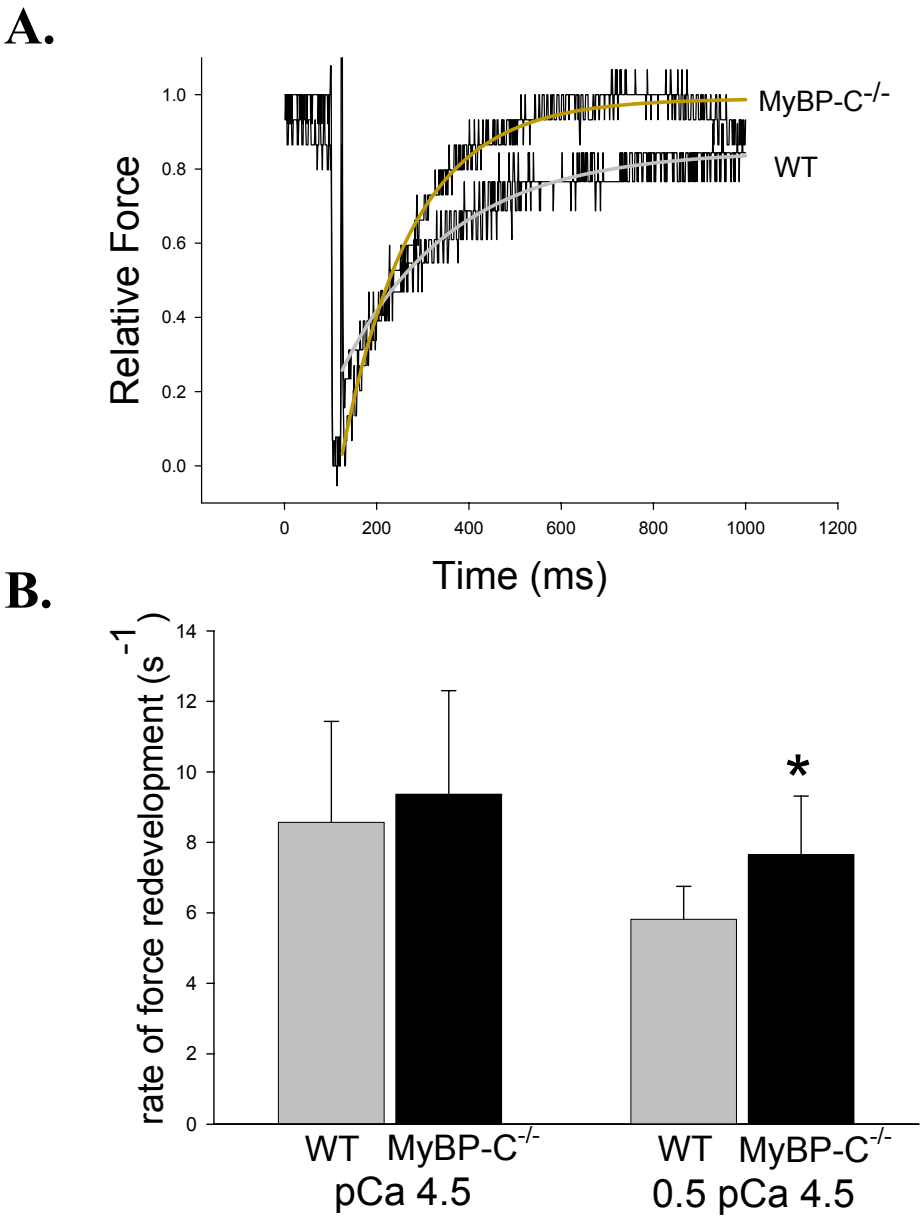

Figure 2.4: Effect of MyBP-C ablation on rates of force development.

A. Force traces following a slack-restretch maneuver in WT and MyBP-C$^{-/-}$ myocytes. The rate of force redevelopment was significantly increased in MyBP-C$^{-/-}$ myocytes at half-maximal Ca^{2+} activations as compared to WT. *P<0.05 for MyBP-C$^{-/-}$ half maximal Ca^{2+} activation vs. WT half-maximal Ca^{2+} activation. **B.** Summary of rates of force redevelopment in WT and MyBP-C$^{-/-}$ skinned cardiac myocytes during maximal (left) and half-maximal (right) Ca^{2+} activations.

DISCUSSION

We examined the effects of targeted MyBP-C ablation on the functional properties of mouse skinned cardiac myocytes. Deletion of MyBP-C significantly increased loaded shortening and power output during both maximal and half-maximal Ca^{2+} activation, as well as yielded faster rates of force redevelopment at half-maximal Ca^{2+} activation. These increases in contractile function imply faster cross-bridge cycling rates under load in myocytes lacking MyBP-C.

Function of MyBP-C on myocyte contraction

Various functions have been suggested for MyBP-C, including a role in the assembly and structural support of the thick filament, and serving as a regulator of crossbridge movement. Studies of the binding of MyBP-C to myosin have revealed MyBP-C binding sites on both light meromyosin (LMM) and the S2 subfragment of myosin, but not on the S1 subfragment [113, 114, 162]. The strong affinity of MyBP-C for LMM suggests a structural role for MyBP-C in the assembly and stabilization of the thick filament; however, MyBP-C does not appear to be necessary *in vivo* for assembly of highly organized myofibrils, which were observed in MyBP-$C^{-/-}$ mice [51]. MyBP-C also binds actin and regulated thin filaments (actin plus troponin-tropomyosin complex) in solution, and the latter is Ca^{2+} dependent [111, 113]. As the length of the MyBP-C molecule is sufficient to simultaneously contact both the thick and thin filaments in the intact filament lattice, an interaction between MyBP-C and actin in myofibrils is possible. In fact, MyBP-C has been observed to alter actin-activated myosin ATPase in solution

[112], an effect that varies depending on the ionic strength and molar ratio of actin and myosin, suggesting MyBP-C may facilitate positioning myosin and actin for interaction.

The binding of MyBP-C to S-2 and actin suggests that MyBP-C is involved in regulating the contractile process and hypotheses regarding its possible regulatory function have been investigated using both cardiac myocytes and skeletal muscle fibers. Along these lines, the incorporation of soluble S2 myosin into intact cardiac myocytes [15], the addition of the N-terminal MyBP-C motif into skinned skeletal muscle fibers [87], and knock-in expression of a shortened N-terminal domain of cMyBP-C [185] have all been shown to increase Ca^{2+} sensitivity of force. These results are consistent with the idea that the N-terminal domain of endogenous cMyBP-C constrains the flexibility and position of the myosin head via its interaction with S2. Also consistent with this idea is the finding that extraction of 60-70% of endogenous MyBP-C in skinned cardiac myocytes and skeletal muscle fibers resulted in reversible increases in isometric tension at submaximal Ca^{2+} concentrations and a decrease in the apparent cooperativity of Ca^{2+}-dependent force development [69]. Based on these results, a model was proposed in which MyBP-C modulates the range of movement of myosin crossbridges, perhaps by tethering the crossbridges to the thick filament backbone, so that following MyBP-C extraction crossbridges are less constrained and the probability of myosin binding to actin is increased [69]. This model is consistent with a more recently proposed model in which three MyBP-C molecules interact to form a collar around the backbone of the thick filament, with projections from this collar able to interact with S2 [110].

MyBP-C also was shown to modify the apparent kinetics of cross-bridge interaction during muscle shortening [68], in that partial extraction of MyBP-C sped maximum shortening velocity (V_o) of fast skeletal muscle fibers at low levels of Ca^{2+} activation. In control fibers at low levels of activation, the time course of unloaded shortening is normally biphasic, i.e., an initial phase of high velocity shortening is followed by low-velocity shortening. The slowing of V_o as shortening proceeds is thought to result from an activation-dependent internal load that arises once there is a given amount of active shortening [117]. Partial extraction of MyBP-C reversibly increased V_o in the low velocity phase of unloaded shortening but had no effect on the high velocity phase. One interpretation of this result is that at low levels of activation, MyBP-C gives rise to an internal load by simultaneously binding actin and myosin. An alternative hypothesis is consistent with the model mentioned above (as proposed by Hofmann, et al. [68, 69]), whereby MyBP-C tethers the myosin head to the thick filament backbone, such that at low levels of Ca^{2+} when the rate of cross-bridge detachment is slow, cross-bridges give rise to an internal load once their useful working stroke is completed. A similar hypothesis could arise from the trimeric collar model proposed by Moolman-Smook, et al. [110] in which the MyBP-C C-terminal collar restricts cross-bridge formation while the N-terminal end is free to interact with S-2 and/or actin. A prediction from these models is that both loaded shortening velocity and force redevelopment rates will be increased if extraction of MyBP-C is complete and thus the tether point or collar is removed. This idea was addressed in this study using cardiac myocytes from MyBP-C-null mice and, indeed, both loaded shortening and force development rates were increased in MyBP-$C^{-/-}$ myocytes and these effects were greater

during half-maximal Ca^{2+} activation. These results are consistent with the idea that MyBP-C constrains interactions of myosin heads with actin, as well as contributes an internal load that tends to reduce shortening velocity. These results also agree with the idea that phosphorylation of cMyBP-C relieves constraint of the myosin head [181] as phosphorylation of cMyBP-C by cAMP dependent protein kinase A has been correlated with both faster force redevelopment in mouse skinned myocardium [135] and faster loaded shortening in rat skinned cardiac myocytes [61]. Interestingly, we saw significantly increased power output in single myocytes lacking MyBP-C despite MyBP-$C^{-/-}$ myocardium containing increased amount of β-MyHC as seen by Harris et al. [51]. β-MyHC is known to result in decreased power output in rat skinned cardiac myocytes [60] even if its quantity is small [59]. Because the upregulation of β-MyHC would likely depress the work capacity of single myocytes, the observed increase in power output may actually be an underestimation of what would be observed if MyBP-C ablation could be studied in myocytes containing 100% α-MyHC.

There are, however, two predictions based on the above models that have not been borne out experimentally. First, Ca^{2+} sensitivity of force was predicted to increase because both competitive inhibition of S2 binding by MyBP-C [87] and partial MyBP-C extraction [69] increased Ca^{2+} sensitivity. It is reasonable to predict that if removal of MyBP-C reduces S1 constraints, more cross-bridges would be able to interact with the thin filaments, which in turn would cooperatively activate additional regulatory units and result in more force at a given $[Ca^{2+}]$. However, ablation of MyBP-C was found to *decrease* Ca^{2+} sensitivity [51] and our current results are in agreement with this finding

because MyBP-C$^{-/-}$ myocytes required a slightly higher Ca^{2+} concentration to reach a force value that was half-maximal, although this difference was not considered significant (see results). This unexpected finding may be accounted for by the fact that previous experiments in which MyBP-C was chemically extracted resulted in only partial relief of the constraint of myosin heads by MyBP-C. As mentioned, previous studies that utilized N-terminal truncations [185], C-terminal truncations [188, 189], MyBP-C extraction [68, 69], and addition of phosphorylatable MyBP-C motif to skeletal muscle [87], all maintained at least some intact portions of MyBP-C, which may be involved in mediating mechanical interactions between myosin and actin. For example, Witt et al., [185] produced an N-terminally shortened MyBP-C, which led to increased Ca^{2+} sensitivity. In that instance, the carboxy terminal end was unaffected and thus able to normally interact with the rod portion of myosin. Also, the increased Ca^{2+} sensitivity seen following MyBP-C extraction [69] occurred with many MyBP-C molecules still bound to S2, the myosin rod, and titin. Interestingly, Yang et al., [188, 189] developed two different mouse models with a C-terminal truncation that also exhibited increased Ca^{2+} sensitivity of force. Thus, it appears that both the N-terminal and C-terminal ends of MyBP-C exert separate regulatory effects and that complete deletion of MyBP-C yields an effect opposite to C-terminal or N-terminal deletions at least with regard to Ca^{2+} sensitivity of force. A second possibility to explain the discrepancy between the expected and actual results is that some studies involved acute modifications of MyBP-C content while others, including this one, involved chronic changes. For instance, our knockout model completely lacks MyBP-C from the onset of myocardial development. Thus, some type of chronic compensatory changes in the myofilaments may account for the

unexpected decrease in Ca^{2+} sensitivity. However, the decreased Ca^{2+} sensitivity does not appear to be due to increased baseline phosphorylation of cardiac troponin I because stoichiometric analysis indicated no significant difference in PKA-dependent phosphate incorporation between MyBP-$C^{-/-}$ and wildtype myofibrils (Figure 2.1). Another possible explanation for reduced Ca^{2+} sensitivity is that Ca^{2+} affinity of TnC is reduced in MyBP-$C^{-/-}$ myocardium due to changes in the normal feedback by which strongly bound cross-bridges increase the binding affinity of TnC for Ca^{2+}. [66] For instance, the loss of the normal constraint of S1 by MyBP-C [110] would perhaps yield more flexible and compliant myosin cross-bridges, which could result in less developed force per cross-bridge. Reducing the force per cross-bridge may adversely affect the normal allosteric changes induced by cross-bridges on the thin filament that tend to enhance Ca^{2+} and/or cross-bridge binding.

Another apparent contradiction between the present results and literature reports is the finding that loaded shortening, power output, and force development rates were increased in MyBP-$C^{-/-}$ myocytes whereas MyBP-$C^{-/-}$ hearts demonstrate decreased contractile function *in vivo*. This does not appear to be due to intercellular connections in some myocytes as control experiments yielded qualitatively similar differences between multi-cellular preparations from WT and MyBP$^{-/-}$ mice (data not shown). It is possible that temperature differences between in vitro and in vivo measurements or some type of compensatory changes in myofibrillar proteins may contribute to these differences. An alternative mechanism is compensated hemodynamic loads in MyBP-$C^{-/-}$ mice. For

instance, when Calaghan et al., [15] introduced exogenous S2 into rat ventricular myocytes to compete with endogenous MyBP-C, skinned myocytes exhibited a 30% increase in contractility, but also an increase in the time to half-relaxation. This is consistent with the finding that isovolumic relaxation is prolonged in MyBP-$C^{-/-}$ mouse hearts [51]. Slowed relaxation rates would lead to reduced filling time and decrease the end diastolic volume, which would depress systolic performance in accordance with the Frank-Starling relationship. Prolonged relaxation is consistent with a model in which ablation of MyBP-C reduces structural constraint on myosin heads, allowing myosin heads to move closer on average to actin binding sites, and thereby increasing the probability of cross-bridge binding, delaying inactivation of thin filaments and prolonging relaxation. Another possible explanation for prolonged relaxation in MyBP-$C^{-/-}$ hearts *in vivo* is that there are compensatory alterations in $[Ca^{2+}]_i$ handling, but this remains to be investigated.

Overall, we found that complete removal of cMyBP-C led to faster loaded shortening and force development rates in mouse skinned cardiac myocytes. Our results are consistent with a model whereby MyBP-C acts to constrain actin-myosin interaction, which limits loaded shortening velocity and ultimately power output.

Chapter 3: SARCOMERE LENGTH DEPENDENCE OF RAT SKINNED CARDIAC MYOCYTE MECHANICAL PROPERTIES: DEPENDENCE ON MYOSIN HEAVY CHAIN ISOFORM

ABSTRACT

We investigated the effects of sarcomere length (SL) on Ca^{2+}-sensitivity of force, rate of force development, and sarcomeric loaded shortening velocity and power output in rat skinned cardiac myocytes containing either α-myosin heavy chain (α-MyHC) or β-MyHC at 12 ± 1°C. Decreasing SL from 2.3 μm to 2.0 μm decreased submaximal isometric force ~40% in both α-MyHC and β-MyHC myocytes. Peak absolute power output, however, decreased 55% in α-MyHC myocytes during submaximal Ca^{2+} activation, whereas β-MyHC myocytes exhibited a more pronounced decrease of ~70% between long and short SL. Furthermore, peak power output was decreased about twice as much in β-MyHC as in α-MyHC myocytes (41% vs. 20%) after normalizing for the fall in isometric force from long to short SL. To determine whether the fall in normalized power with decreased SL was due to the lower force levels (and presumably reduced thin filament activation levels) we increased Ca^{2+} at short SL to match force at long SL. Surprisingly, this led to a 32% greater peak normalized power output at short SL compared to long SL in α-MyHC myocytes. However, in β-MyHC myocytes peak normalized power output remained depressed at short SL as compared to long SL when force levels were matched. This implies that lower thin filament activation levels are important in governing the fall in power with reduced SL as it appears that loaded crossbridge cycling is actually faster at short SL, at least in α-MyHC myocytes.

The role that interfilament spacing plays in determining SL dependence of power was tested by adding the osmotic polymer dextran to compress myocytes at short SL. Addition of 2% dextran at short SL decreased myocyte width, likely decreased the lateral spacing between the thick and thin filaments, and increased force to levels obtained at long SL. Peak normalized power output at short SL with dextran was increased to values greater than at long SL in both α- MyHC and β-MyHC myocytes. This suggests that the greater lattice spacing at short SL tends to mitigate optimal crossbridge binding and reduce power. The effect of α-MyHC and β-MyHC content on Ca^{2+} sensitivity of force was determined following incubation with PKA to normalize for potential differences in basal myofibrillar protein phosphorylation. There was no difference in maximal isometric force between α-MyHC and β-MyHC myocytes but Ca^{2+} sensitivity of force was slightly greater in β-MyHC myocytes at both long and short SL. A decrease in SL from 2.3 μm to 2.0 μm decreased Ca^{2+} sensitivity of force similarly in both α-MyHC and β-MyHC myocytes. The rate constant of force development (k_{tr}) also was measured and was not different between long and short SL in α-MyHC myocytes but was increased at short SL in β-MyHC myocytes. At short SL with matched levels of activation with either dextran or [Ca^{2+}], k_{tr} was increased versus long SL in both α-MyHC and β-MyHC myocytes. These results are consistent with the idea that an intrinsic length component increases crossbridge kinetics at short SL.

INTRODUCTION

Increased end-diastolic volume has been shown to increase stroke volume in isolated heart preparations [136] and in intact animals [11], a relationship commonly referred to as the Frank-Starling relationship. The underlying cellular mechanism of this relationship is thought to involve, at least in part, an increase in the tension generating capacity of individual myocytes with increased sarcomere length (SL) in accordance with the length-tension relationship of striated muscle [29, 43, 160]. This is especially steep in cardiac muscle at submaximal Ca^{2+} activations [79], which myocytes are thought to encounter *in vivo*. During ejection, however, the ventricles are contracting against an afterload and are therefore undergoing loaded shortening (i.e., performing work). Despite the physiological and pathophysiological importance of the Frank-Starling relationship, few experiments have attempted to determine the effects of SL on loaded shortening in cardiac myocytes. We tested the hypothesis that cardiac myocyte power output is tightly regulated by initial SL, which was examined by measuring load dependence of shortening velocity and power output at two initial sarcomere lengths (i.e., 2.3 μm and 2.0 μm).

Numerous studies suggest a primary cause of length dependence of myocardial function arises from a change in myofilament Ca^{2+} sensitivity of force [4, 64], brought about, in part, by a change in interfilament lattice spacing (for review see [34]). As a myocyte is shortened, the lateral spacing between the thick and thin filament is increased [74, 137, 148, 187], which likely decreases the probability of myosin binding to actin and

yields fewer force-generating crossbridges that activate the thin filament. This study additionally tested the hypothesis that SL dependence of power output results from changes in thin filament activation levels and/or lattice spacing We measured loaded shortening velocity and power output at short SL at the same force (by addition of activating Ca^{2+}) or the same force and myocyte width (by addition of 2% dextran) to those at long SL.

Myosin heavy chain (MyHC) isoform content also has been shown to be a key regulator of loaded shortening and power output [60, 85]. No studies, however, have addressed how MyHC affects SL dependence of power output in spite of the observation that several disease states in rodents and humans have been shown to up-regulate β-MyHC and down-regulate α-MyHC [25, 109]. Increased β-MyHC has negative consequences for power [62, 85] but seems to increase the economy of contraction [152]. Additionally, it has been shown that heart rate is inversely related to β-MyHC content [49]. Since a slower heart rate allows more filling time it may be that ventricles containing β-MyHC rely more on SL changes to modulate stroke volume than do ventricles with α-MyHC. This is consistent with the finding that rat left ventricles that contained >70% β-MyHC exhibited steeper ventricular function curves than left ventricle that contained predominantly α-MyHC [31]. Therefore, we also tested the hypothesis that β-MyHC myocytes have increased SL dependence of power output compared to α-MyHC myocytes.

Additionally, we examined whether there are inherent differences between α-MyHC and β-MyHC myocytes in the sarcomere length dependence of Ca^{2+} sensitivity of force and the rates of force development. Experiments were designed to determine if changes in these parameters could explain potential variations in left ventricular function curves between α-MyHC and β-MyHC hearts.

MATERIALS AND METHODS

Experimental animals

Male Sprague-Dawley rats (6 weeks old) were obtained from Harlan (Madison, WI), housed in groups of 2 or 3 and provided access to food and water *ad libitum*. Rats were made hypothyroid by adding 6-propylthiouracil (PTU, 0.8 mg/mL) to the drinking water. PTU treatment shifted cardiac MyHC isoform content from 100% α-MyHC to 100% β-MyHC over a three week period. Thyroidectomy, PTU (intraperitoneally or orally) administration, or the combination of thyroidectomy and PTU have been shown to alter MyHC isoform expression without altering the expression of other key myofilament proteins [32, 60, 107]. All procedures involving animal use were performed according to the Animal Care and Use Committee of the University of Missouri.

Solutions

The compositions of relaxing and activating solutions were as follows (in mmol/L, obtained from Sigma at highest possible purity): free Mg^{2+} 1, EGTA 7, MgATP 4, imidazole 20, and creatine phosphate 14.5 (pH 7.0); specific $[Ca^{2+}]$ between $10^{-4.5}$

(maximal Ca^{2+} activating solution) and 10^{-9} (relaxing solution); and sufficient KCl to adjust ionic strength to 180 mmol/L. Relaxing solution also contained 2 mM Pefabloc (Roche) and 0.25 mM leupeptin (Sigma) to inhibit proteases and preserve the integrity of the myocytes.

Myocardial preparations

Skinned cardiac myocytes were obtained by mechanical disruption of hearts from Sprague-Dawley rats as described previously [99]. Briefly, rats were anaesthetized by inhalation of isoflurane (20% v/v in olive oil), and their hearts were excised and rapidly placed in ice cold relaxing solution. The left ventricle was separated from the right ventricle and dissected from the atria, cut into 2-3 mm pieces and further disrupted for 5 seconds in a Waring blender. The resulting suspension of cells was centrifuged for 105 sec at 165 x *g*, after which the supernatant fluid was discarded. The myocytes were skinned by suspending the cell pellet for 5 min in 0.3 % ultrapure Triton X-100 (Pierce Chemical Co.) in cold relaxing solution. The skinned cells were washed twice with cold relaxing solution, suspended in 10 ml of relaxing solution and kept on ice. One myocyte per heart was used.

Experimental Apparatus

The experimental apparatus for physiological measurements of myocyte preparations was similar to one previously described in detail [116] and modified specifically for cardiac myocyte preparations [99]. Briefly, a myocyte was attached between a force transducer and high speed motor by gently placing the ends of the

myocyte into stainless steel troughs (25 gauge). The ends of the myocyte were secured by overlaying a 0.5 mm long piece of 3-0 monofilament nylon suture (Ethicon, Inc.) onto each end of the myocyte, and then tying the suture into the troughs with two loops of 10-0 monofilament suture (Ethicon, Inc.). The attachment procedure was performed under a stereomicroscope (~100x magnification) using very fine tipped forceps.

Prior to mechanical measurements the experimental apparatus was mounted on the stage of an inverted microscope (model IX-70, Olympus Instrument Co., Japan), which rested on a pneumatic anti-vibration table with a cut-off frequency of ~1 Hz. Force measurements were made using a capacitance-gauge transducer (Model 403-sensitivity of 20 mV/mg plus a x10 amplifier and resonant frequency of 600 Hz; Aurora Scientific, Inc., Aurora, ON, Canada). Length changes during mechanical measurements were introduced at one end of the preparation using a DC torque motor (model 308, Aurora Scientific, Inc.) driven by voltage commands from a personal computer via a 12-bit D/A converter (AT-MIO-16E-1, National Instruments Corp., Austin, TX, USA). Force and length signals were digitized at 1 kHz using a 12-bit A/D converter and each was displayed and stored on a personal computer using custom software based on LabView for Windows (National Instruments Corp.). Sarcomere length was monitored and recorded using IonOptix SarcLen system (IonOptix, Milton, MA), which used a fast fourier transform algorithm of the video image of the myocyte (Figure 3.1). Figure 3.1A illustrates muscle length (top) and sarcomere length (middle) traces during a load clamp (bottom) at both long and short SL. Figure 3.1B illustrates that muscle length and sarcomere length traces are closely matched over the entire range of relative loads.

Videomicroscopy was completed using a 40x objective (Olympus UWD 40) and 25x intermediate lenses.

Force-velocity and power-load measurements

The protocol to obtain force-velocity and power-load measurements has been described in detail [100] and all measurements were done at 12 ± 1°C. An attached myocyte was first transferred into maximal Ca^{2+} activating solution (pCa 4.5) and allowed to obtain maximal steady-state isometric force. It was then transferred to a submaximal Ca^{2+} activating solution and a series of sub-isometric force clamps were applied to determine isotonic shortening velocities. The isotonic force was maintained using a servo system for 150-250 ms while muscle length and sarcomere length changes during this time were monitored. Figure 3.1A illustrates a force clamp and corresponding muscle length and sarcomere length changes. Following the force clamp, the myocyte was slackened to near zero force to estimate the relative load sustained during the isotonic shortening, after which the myocyte was re-extended to its starting length. Due to the short lengths of the myocytes the rapid slackening following isotonic shortening did not always result in an accurate baseline force value and consequently resulted in an underestimation of peak force and, thus, of the relative force during loaded contractions. In these cases, more accurate estimates of the relative forces during isotonic shortening were obtained by interpolating between the peak forces in isometric contractions that were performed before and after every series of loaded contractions. The myocytes were kept in submaximal Ca^{2+} activating solution 2-4 minutes during which 10-20 force clamps were performed without significant loss of force. If force fell below 80% of initial force, data

Figure 3.1

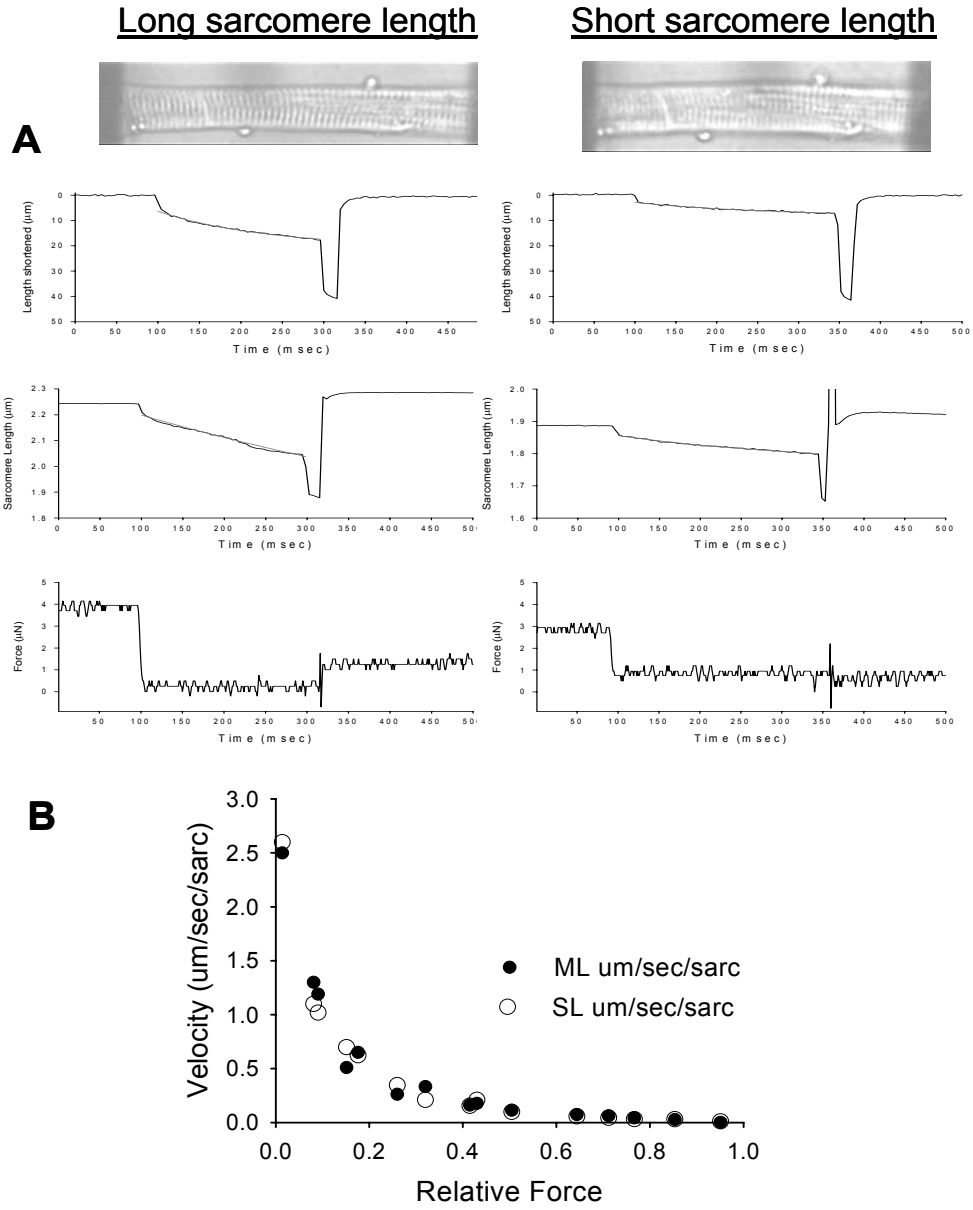

Figure 3.1: Muscle length, sarcomere length, and force traces of a submaximally Ca^{2+} activated cardiac myocyte.

A. Examples of myocyte shortening (top) and sarcomere shortening (middle) at clamped force (bottom) at long and short sarcomere length during submaximal Ca2+ activations. Photomicrographs of Ca^{2+} activated myocyte at long and short sarcomere length are inset. **B.** Force-velocity points generated from muscle length (ML) traces (closed circles) and sarcomere length traces (open circles) demonstrate that SL and ML are closely matched in our system.

from that myocyte were discarded. Force-velocity measurements were obtained in this manner for all experimental conditions.

Measurement of rate constant of force development

Measurement of tension development kinetics was accomplished by using a modification of [14] as previously described [104] and adjusted for cardiac myocytes. Briefly, a myocyte in activating solution was allowed to develop tension to plateau after which it was rapidly slacked by 15-20% of original myocyte length (L_0) and held for 20 msec and then was rapidly restretched to a value slightly greater than L_0 for 2 ms before it was returned to L_0. This slack-restretch maneuver caused dissociation of crossbridges, and thus tension redevelopment was due to reattachment of crossbridges to the thin filament and subsequent transition to force generating states.

SDS-PAGE and silver staining

Following power output measurements the relative expression of MyHC was determined for each myocyte. The myocyte was removed from the experimental apparatus and stored in 10 μl of SDS sample buffer at -80°C for subsequent SDS-PAGE analysis. The gel electrophoresis procedure was similar to one previously described [60, 62]. The gels were prepared with 3.5% acrylamide in the stacking gel and 12% acrylamide in the resolving gel. Myocyte proteins were separated at constant current (12 mA) for 8.5 hours. The separated proteins were fixed in an acid-alcohol solution followed by glutaraldehyde. MyHC isoforms were visualized by ultrasensitive silver staining and then gels were dried and stored between Mylar sheets (Figure 3.2). The relative expression of each MyHC isoform was

Figure 3.2: MyHC separation using SDS-PAGE.

Silver stained gel image of single cardiac myocytes using SDS-PAGE to specifically separate myosin heavy chains.

determined by using QuantiScan (Biosoft) software and an Epson scanner to measure the relative intensities and areas of each MyHC band. MyHC content expressed as relative β-MyHC content is summarized in Table 3.1.

Data analyses

Myocyte length traces, force-velocity curves, and power-load curves were analyzed as previously described [99]. Myocyte length and sarcomere length traces during loaded shortening were fit to a single decaying exponential equation:

(1) $$L = Ae^{-kt} + C$$

where L is cell length at time *t*, A and C are constants with dimensions of length, and *k* is the rate constant of shortening ($k_{shortening}$). Velocity of shortening at any given time, *t*, was determined as the slope of the tangent to the fitted curve at that time point. In this study velocities of shortening were calculated by extrapolation of the fitted curve to the onset of the force clamp (i.e., $t = 0$).

Hyperbolic force-velocity curves were fit to the relative force-velocity data using the Hill equation.[65]

(2) $$(P + a)(V + b) = (P_o + a)b$$

where P is force during shortening at velocity V; P_o is the peak isometric force; and *a* and *b* are constants with dimensions of force and velocity, respectively. Power-load curves were obtained by multiplying force *x* velocity at each load on the force-velocity curve

Table 3.1

Table 3.1: Myocyte properties

	% β-MyHC		SL, μm	Length	Width	μN	P/P_0	pCa_{50}
α-MyHC myocytes	0.8 ± 2.8	Long SL	2.31 ± 0.04	132 ± 20	18 ± 2.5	5.9 ± 1.8	0.53 ± 0.11	5.58 ± 0.03
		Short SL	2.00 ± 0.04*	106 ± 25*	20 ± 2.8*	3.6 ± 1.7*	0.32 ± 0.10*	5.49 ± 0.02*
β-MyHC myocytes	93.6 ± 8.1	Long SL	2.31 ± 0.06	138 ± 22	20 ± 3.2	5.9 ± 1.6	0.54 ± 0.13	5.48 ± 0.03†
		Short SL	2.01 ± 0.04*	114 ± 17*	22 ± 3.6*	3.5 ± 1.3*	0.32 ± 0.09*	5.39 ± 0.03*†

Values are means ± S.D. SL, sarcomere length at submaximal Ca^{2+} activation; P/P_0, fraction of isometric force (P_0)
*Significant difference from long SL; P<0.05, †Significant difference from corresponding α-MyHC value; p<0.05

.The optimum force for mechanical power output (F_{opt}) was calculated using the equation [186]

(3) $$F_{opt} = (a^2 + a \cdot P_o)^{1/2} - a$$

Curve fitting was performed using a customized program written in Qbasic, as well as commercial software (Sigmaplot).

The shape and mid-point (pCa_{50}) of the tension-pCa relationship were calculated by Hill plot analyses of the data as previously described [158]. Linear fits to the tension data above and below 0.5 P_0 were obtained by least-squares analysis using the equation:

$$Log[P_r/(1-P_r)] - n(\log[Ca^{2+}] = pCa_{50},$$

where P_r is tension expressed as a fraction of P_0 and pCa_{50} is the Ca^{2+} concentration for half-maximal activation. Mean tension-pCa data were displayed (Figure 3.6) using the equation:

$$P_r = [Ca^{2+}]^n/(([Ca^{2+}]_{50})^n + [Ca^{2+}]^n),$$

where P_r is tension expressed as a fraction of P_0, $[Ca^{2+}]_{50}$ is the Ca^{2+} concentration for half-maximal activation, and n is the Hill coefficient.

Tension redevelopment following slack-restretch maneuver was well fit by a single exponential equation:

$$F = F_{max}(1 - e^{-ktr t}),$$

where F is tension at time *t*, F_{max} is maximal tension, and k_{tr} is the rate constant of force development.

Paired *t* tests were used to determine if SL significantly affected loaded shortening velocity, power, k_{tr} or pCa_{50}. Student's *t* test was used to test for differences in velocity, power, k_{tr} or pCa_{50} between α-MyHC and β-MyHC myocytes. One-way ANOVA was used to determine differences between long SL, short SL + matched force, and short SL + matched width groups, and a Student-Neuman-Keuls was performed as a post-hoc test to assess differences between group means. In all cases, $P < 0.05$ was accepted as a significant difference. Data are presented as means ± S.D. n = the number of myocyte preparations.

RESULTS

Sarcomere length dependence of absolute and normalized power output in α-MyHC myocytes.

The sarcomere length dependence of loaded shortening was examined by characterizing force-velocity and power-load curves during submaximal Ca^{2+} activation at long (~2.3 μm) and short SL (~2.0 μm) in α-MyHC myocytes (n = 12). Figure 3.3A illustrates the sarcomere length dependence of loaded shortening and absolute power output from skinned cardiac myocytes containing α-MyHC. At short SL as compared to long SL, isometric force was decreased 40% while peak absolute power fell 55%, indicating power fell by mechanisms other than just decreased isometric force. This can be more clearly seen in force-velocity and power-load curves after normalization to isometric force (Figure 3.3B.) The normalized force-velocity curve shows that loaded shortening velocity was decreased at short versus long SL for given relative loads less

Figure 3.3

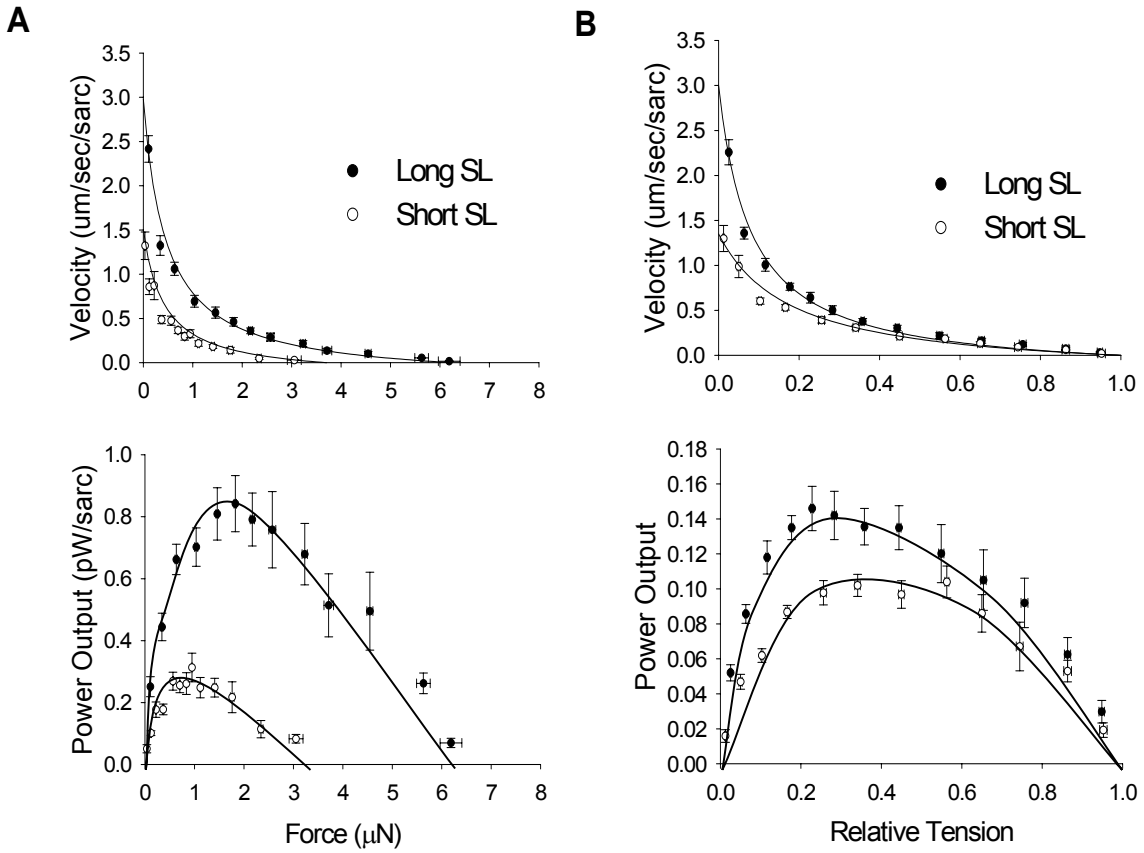

Figure 3.3: Sarcomere length dependence of isotonic shortening velocity and power output in α-MyHC cardiac myocytes.

A. Absolute force-velocity (top) and power output (bottom) curves from myocytes expressing α-MyHC at long (closed circles) and short (open circles) sarcomere length. **B.** Normalized force-velocity (top) and power output (bottom) curves from myocytes expressing α-MyHC at long (closed circles) and short (open circles) sarcomere length as labeled. At short SL isometric force was decreased, which caused a fall in absolute power output. However, the decrease in absolute power output was greater than the decrease in force, which indicates slower shortening velocities for a given relative load as seen in the normalized force-velocity and power load curves. Data points are means ± S.D., force-velocity curves fit by Hill equation as described in Methods, power-load curves fit by eye.

than ~40% of isometric force, which resulted in a 20% decrease in peak normalized power output. Interestingly, shortening velocity did not appear to be slower at short SL at loads greater than 40% of isometric force. The mechanical properties of α-MyHC myocytes are presented in Table 3.2.

Sarcomere length dependence of absolute and normalized power output in β-MyHC myocytes.

The sarcomere length dependence of loaded shortening and power output were also examined at long and short SL in β-MyHC myocytes (n = 11). Figure 3.4A illustrates the sarcomere length dependence of absolute loaded shortening and power output in β-MyHC myocytes. As with α-MyHC myocytes, isometric force was decreased at short SL, which led to a decrease in absolute power. However, the fall in absolute power was even more pronounced in β-MyHC myocytes. Isometric force was decreased 41% while peak absolute power fell nearly 70%. After normalization of the curves to isometric force (Figure 3.4B), loaded shortening velocity was clearly decreased at short versus long SL for a given relative load less than ~50% of isometric force; this resulted in a 41% decrease in peak normalized power output in β-MyHC myocytes. Thus β-MyHC myocytes are more sensitive to changes in SL at a given [Ca^{2+}] than are α-MyHC myocytes.

Table 3.2

Table 3.2: β-MyHC mechanical properties (n = 11)

SL, μm	k_{tr}	F_{opt}	V_{opt}, um • $sarc^{-1}$ • s^{-1}	a/P_0	Peak Absolute power output, μW/mg	Peak normalized power output, P/P_0 • um • $sarc^{-1}$ • s^{-1}
2.31 ± 0.04	2.38 ± 0.56	0.21 ± 0.05	0.66 ± 0.15	0.10 ± 0.06	1.49 ± 0.67	0.14 ± 0.03
2.00 ± 0.04*	2.52 ± 0.69	0.29 ± 0.07*	0.40 ± 0.14*	0.23 ± 0.20*	0.66 ± 0.31*	0.11 ± 0.03*

Values are means ± S.D. SL, sarcomere length at submaximal Ca^{2+} activation; k_{tr}, rate constant of force development; F_{opt}, relative force at which power was optimal; V_{opt}, velocity at F_{opt}; a/P_0, curvature of force-velocity relationship; P/P_0, fraction of isometric force (P_0). *Significant difference from long SL; $P<0.05$

Figure 3.4

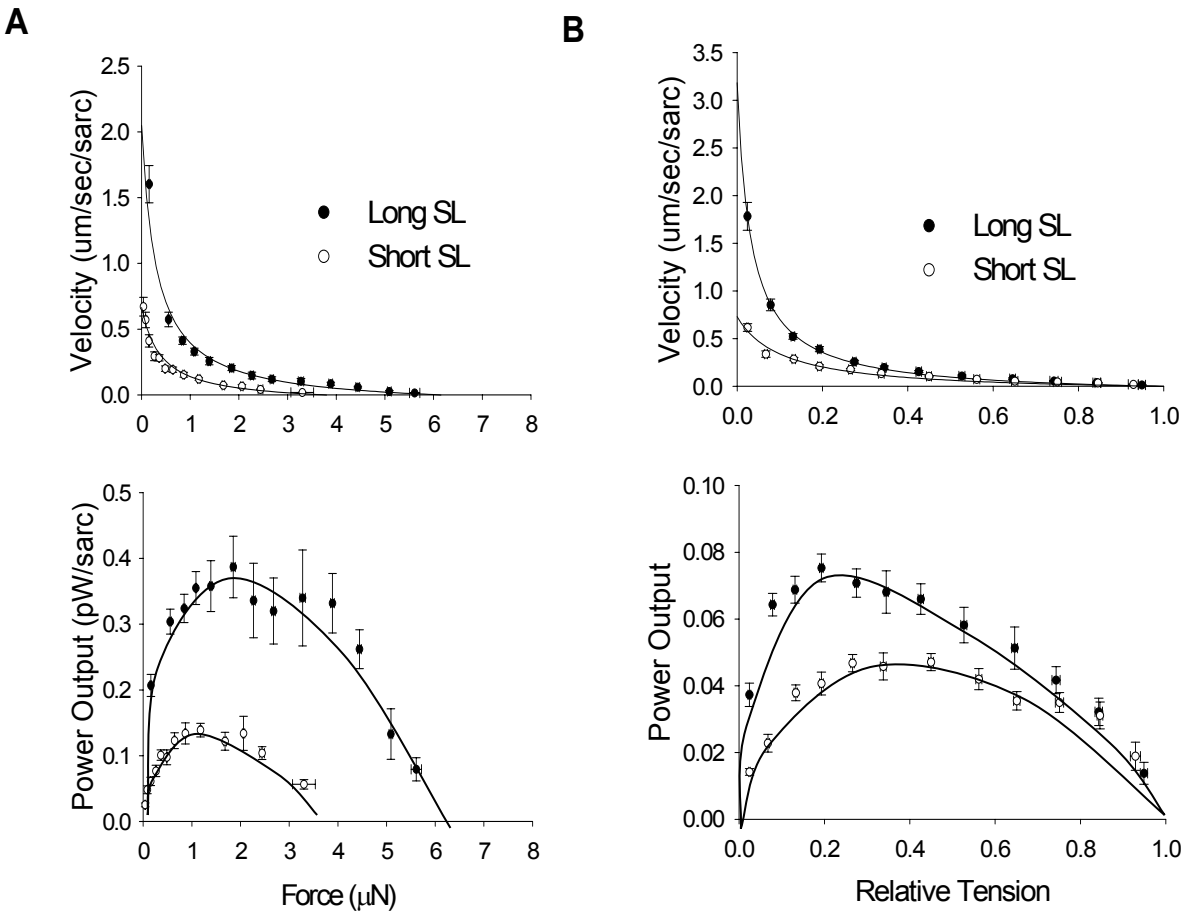

Figure 3.4: Sarcomere length dependence of isotonic shortening velocity and power output in β-MyHC cardiac myocytes.

A. Absolute force-velocity (top) and power output (bottom) curves from myocytes expressing β-MyHC at long (closed circles) and short (open circles) sarcomere length. **B.** Normalized force-velocity (top) and power output (bottom) curves from myocytes expressing β-MyHC at long (closed circles) and short (open circles) sarcomere length as labeled. As in α-MyHC myocytes, isometric force and absolute power output were decreased at short SL, but the decrease in shortening velocity and power was even more pronounced in β-MyHC myocytes as indicated by the greater fall in peak normalized power output. Data points are means ± S.D., force-velocity curves fit by Hill equation as described in Methods, power-load curves fit by eye.

However, similar to α-MyHC, shortening velocities at short SL did not appear to be slower at loads greater than 50% of isometric force. The mechanical properties of β-MyHC myocytes are presented in Table 3.3.

Effects of Ca^{2+} activation on normalized loaded shortening and power output

It was previously shown that shortening SL decreases Ca^{2+} sensitivity of force [64, 79] and loaded shortening velocity is tightly regulated by force and thin filament activation levels [75, 99, 103]. Thus, a possible mechanism underlying the decreases in loaded shortening velocity and power output at short SL could be the associated decrease in force and thin filament activation levels. To probe this mechanism, force and, presumably the thin filament activation levels, at short SL were matched to those seen at long SL by increasing the Ca^{2+} concentration. Figure 3.5A illustrates that matching force at long and short SL actually led to faster loaded shortening velocities and 32% greater peak normalized power output at short SL (0.18 ± 0.02 $P/P_0 \bullet um \bullet sarc^{-1} \bullet s^{-1}$) than observed at long SL (0.14 ± 0.03 $P/P_0 \bullet um \bullet sarc^{-1} \bullet s^{-1}$) in α-MyHC myocytes. This implies that there is a myofibrillar mechanism that leads to faster loaded crossbridge kinetics at shorter SL in α-MyHC myocytes. In β-MyHC myocytes normalization of force at short SL slightly sped loaded shortening and increased power output as would be expected with the increase in force but, in contrast to α-MyHC myocytes, peak normalized power output was decreased 28% at short SL (0.07 ± 0.02 $P/P_0 \bullet um \bullet sarc^{-1} \bullet s^{-1}$) compared to long SL ($0.09 \pm 0.02$ $P/P_0 \bullet um \bullet sarc^{-1} \bullet s^{-1}$) (Figure 3.5B).

Table 3.3

Table 3.3: β-MyHC mechanical properties (n = 11)

SL, μm	k_{tr}	F_{opt}	V_{opt}, um • $sarc^{-1}$ • s^{-1}	a/P_0	Peak Absolute power output, μW/mg	Peak normalized power output, P/P_0 • um • $sarc^{-1}$ • s^{-1}
2.31 ± 0.06	1.18 ± 0.35	0.16 ± 0.04	0.43 ± 0.08	0.05 ± 0.03	0.63 ± 0.16	0.075 ± 0.018
2.01 ± 0.04*	1.79 ± 0.40*	0.27 ± 0.08*	0.17 ± 0.05*	0.18 ± 0.15*	0.20 ± 0.04*	0.044 ± 0.009*

Values are means ± S.D. SL, sarcomere length at submaximal Ca^{2+} activation; k_{tr}, rate constant of force development; F_{opt}, relative force at which power was optimal; V_{opt}, velocity at F_{opt}; a/P_0, curvature of force-velocity relationship; P/P_0, fraction of isometric force (P_0) *Significant difference from long SL; $P<0.05$

Effects of osmotic compression on normalized loaded shortening and power output

The effects of changes in lattice spacing that occur with changes in sarcomere length were examined by adding the osmotic polymer dextran to activating solution at short SL. Dextran osmotically decreased myocyte width by decreasing cell volume. In this study, 2% dextran at short SL was sufficient to decrease the width of the myocyte and to increase force to match both the width and force seen at long SL in α-MyHC and β-MyHC myocytes. In α-MyHC myocytes at short SL, 2% dextran increased loaded shortening velocity at nearly all relative loads and increased peak normalized power output 59% (0.22 ± 0.05 $P/P_0 \bullet um \bullet sarc^{-1} \bullet s^{-1}$) compared to long SL (Figure 3.5A), This was 21% greater than at short SL with matched force. This further implicates a myofibrillar mechanism that leads to faster loaded crossbridge kinetics at short SL in α-MyHC myocytes. Interestingly, addition of 2% dextran to β-MyHC myocytes increased loaded shortening velocity at nearly all relative loads, and peak normalized power output was increased 52% (0.14 ± 0.06 $P/P_0 \bullet um \bullet sarc^{-1} \bullet s^{-1}$) above that at long SL (Figure 3.5B); this was more than double that seen at short SL with matched force. Therefore, β-MyHC myocytes also appeared to have a myofibrillar mechanism that led to faster loaded crossbridge kinetics at shorter SL but, in contrast to α-MyHC myocytes where power increased at short SL with both matched force via increased calcium and matched width via dextran, power output in β-MyHC myocytes only increased with matched width via dextran.

Figure 3.5

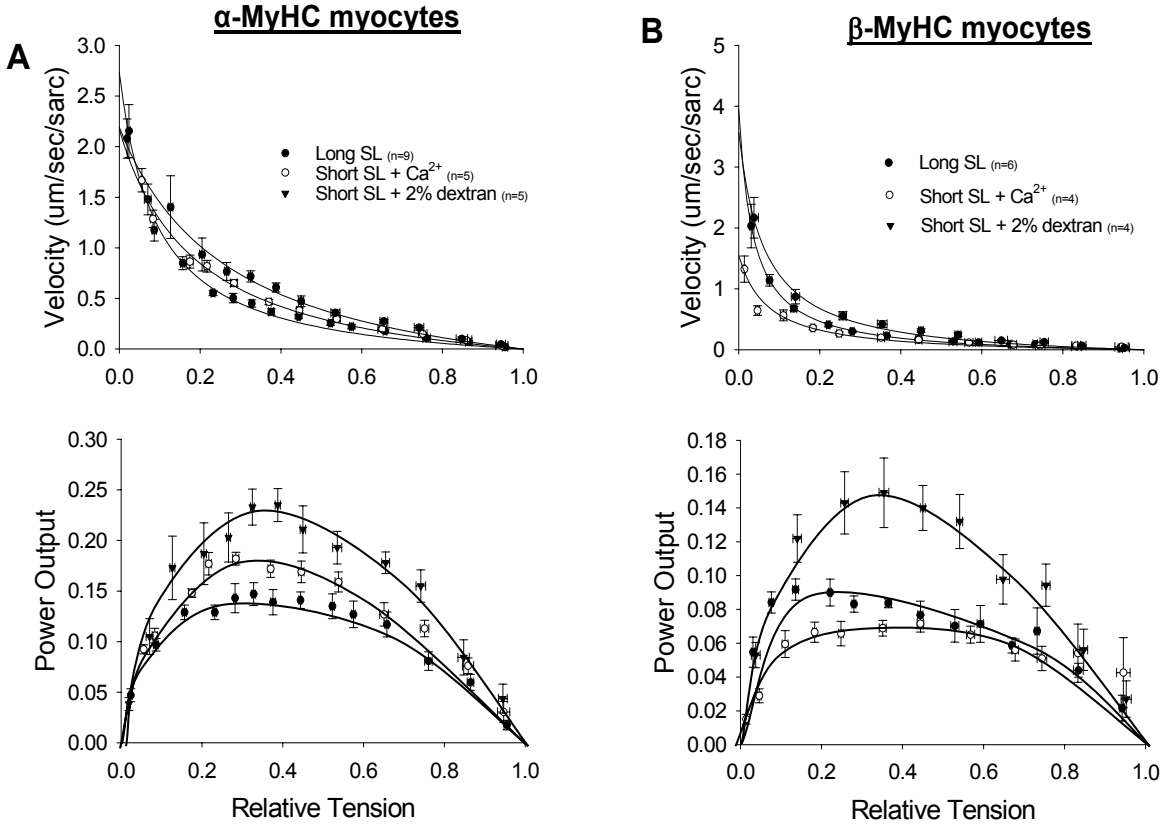

Figure 3.5: Sarcomere length dependence of isotonic shortening velocity and power output in α-MyHC and β-MyHC cardiac myocytes with matched activation levels.

A. Normalized force-velocity (top) and power output (bottom) curves from myocytes expressing α-MyHC at long SL (closed circles), short SL with increased Ca^{2+} to match force (closed triangles), and short SL + Dextran (open triangles). Loaded shortening velocity and peak normalized power output are elevated at short SL to levels greater than at long SL when activation levels are matched by either increased [Ca^{2+}] or by osmotic compression in α-MyHC myocytes. **B.** Normalized force-velocity (top) and power output (bottom) curves from myocytes expressing β-MyHC at long SL (closed circles), short SL with increased Ca^{2+} to match force (closed triangles), and short SL + Dextran (open triangles). In β-MyHC myocytes, matched activation by osmotic compression sped loaded shortening and increased normalized power output to levels greater than at long SL while matched activation through increased [Ca^{2+}] only sped loaded shortening to levels equivalent to that seen at long SL. Data points are means ± S.D., force-velocity curves fit by Hill equation as described in Methods, power-load curves fit by eye.

Thus, β-MyHC myocytes appeared to be more responsive to changes in interfilament spacing and, as a result, the increase in lattice spacing associated with short SL was, in part, responsible for the decrease in loaded shortening velocity and power even at matched Ca^{2+} activation levels. This also is consistent with the observed increased SL dependence of loaded shortening in β-MyHC myocytes.

Role of myosin heavy chain in determining sarcomere length dependence of Ca^{2+} sensitivity to force

MyHC dependence of Ca^{2+} sensitivity to force was determined with tension-pCa curves generated using skinned cardiac myocytes containing either α-MyHC or β-MyHC that had been exposed to the catalytic subunit of PKA. PKA was used to normalize PKA-induced phosphorylation levels in myofibrillar proteins myosin binding protein-C (MyBP-C) and troponin I (TnI). Figure 3.6 illustrates the tension-pCa relationships of α-MyHC and β-MyHC myocytes at long (2.3 μm) and short (2.0 μm) SL. There was a statistical difference in pCa_{50} of ~0.1 pCa units at both long SL and short SL between α-MyHC and β-MyHC myocytes (Table 3.1). The shifts in pCa_{50} (ΔpCa_{50}) from long SL to short SL were not different between α-MyHC and β-MyHC myocytes and were 0.09 ± .02 and 0.08 ± 0.01, respectively.

Figure 3.6

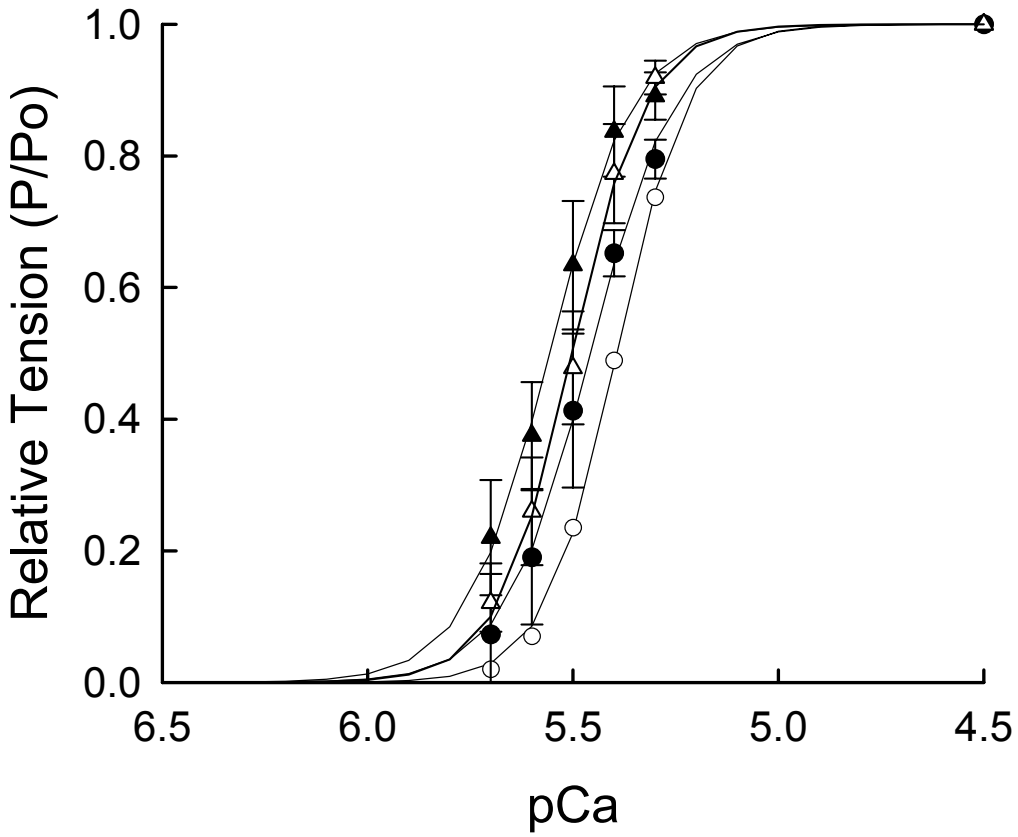

Figure 3.6: Tension-pCa relationship following PKA treatment in α-MyHC and β-MyHC myocytes.

Myocytes containing α-MyHC were more sensitive to Ca^{2+} at long SL (closed circles) than at short SL (closed triangles) following PKA treatment. Myocytes containing β-MyHC also were more sensitive to Ca^{2+} at long (open circles) than at short SL (open triangles). There was a statistical difference in Ca^{2+} sensitivity at both long and short SL between α-MyHC and β-MyHC. Data points are means ± S.D.

Effects of sarcomere length, osmotic compression, and Ca^{2+} activation on force development

In α-MyHC myocytes, there was no difference in the rate constants of force development (k_{tr}) between long SL (k_{tr} = 2.38 ± 0.56 s^{-1}) and short SL (k_{tr} = 2.52 ± 0.69 s^{-1}) (Figure 3.7A). At short SL, however, increasing [Ca^{2+}] to match force activation levels at long SL (k_{tr} = 4.63 ± 0.26 s^{-1}) or adding 2% dextran to match myocyte width (k_{tr} = 4.76 ± 0.18 s^{-1}) led to significantly greater rates of force redevelopment compared to long or short SL alone (Figure 3.7C). This strengthens the implication that crossbridge kinetics increased at short SL in α-MyHC myocytes. Interestingly, β-MyHC myocytes exhibited faster rates of force development at short SL (k_{tr} = 1.18 ± 0.35 s^{-1}), short SL with matched force (k_{tr} = 2.15 ± 0.30 s^{-1}), and short SL with matched width (k_{tr} = 2.39 ± 0.74 s^{-1}), compared to long SL (k_{tr} = 1.79 ± 0.40 s^{-1}) (Figures 3.7B and 3.7D). Moreover, force development rates were not significantly faster at short SL with matched force versus short SL alone, but were faster at short SL with matched width in β-MyHC myocytes. Again, this implies increased crossbridge kinetics at short SL but β-MyHC myocytes appear to be more affected by lattice spacing than α-MyHC myocytes, vis-à-vis the change in myocyte width.

Figure 3.7

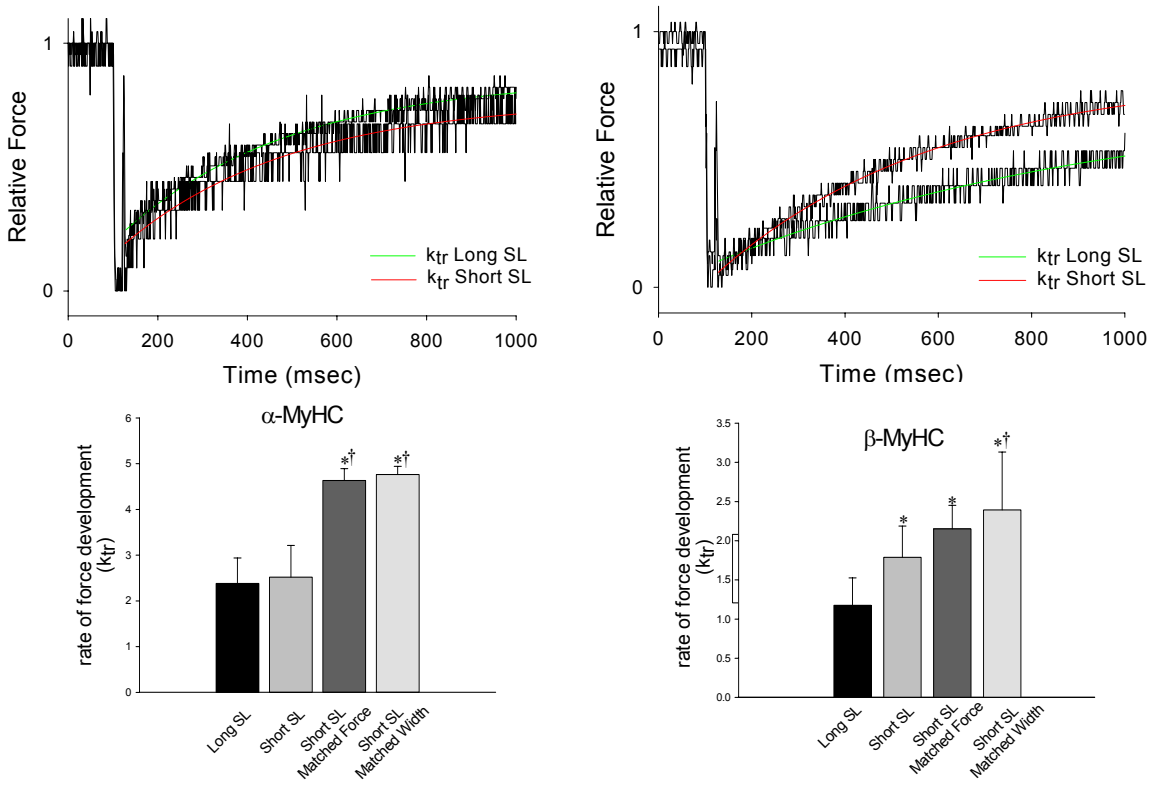

Figure 3.7: Sarcomere length dependence of rate constant of force development in α-MyHC and β-MyHC cardiac myocytes.

A. Normalized force traces fit with a rising exponential to calculate the rate constant of force development from an α-MyHC myocyte at long (upper solid line) and short SL (lower dashed line). **B.** Normalized force traces fit with a rising exponential from a β-MyHC myocyte at long (lower solid line) and short SL (upper dashed line). **C.** Rate constants of force development for α-MyHC myocytes at long SL, short SL, short SL with matched force, and short SL with matched width. **D.** Rate constants of force development for β-MyHC myocytes at long SL, short SL, short SL with matched force, and short SL with matched width. * Significantly different from long SL ($p<0.05$). † Significantly different from short SL ($p<0.05$). Data are means ± S.D.

DISCUSSION

The results of these experiments show that decreasing sarcomere length in rat skinned cardiac myocyte preparations significantly decreased both absolute and normalized loaded shortening velocity and power output, and that this SL dependent decrease is more pronounced in myocytes containing β-MyHC. Additionally, when force was matched at short SL to that seen at long SL by increased calcium, loaded shortening velocity and power were increased above that seen at long SL in α-MyHC myocytes but not β-MyHC myocytes. When myocyte width was matched at short SL to that seen at long SL loaded shortening velocity and power were increased above that seen at long SL in both α-MyHC and β-MyHC myocytes. There was no difference in maximal force generating capacity between α-MyHC and β-MyHC but β-MyHC myocyte force was more sensitive to calcium than α-MyHC myocytes at both long and short SL following incubation with PKA. Also, faster rates of force development were observed at short SL than at long SL in β-MyHC myocytes, whereas α-MyHC myocytes rate constants of force development between long and short SL were not different. The results of these experiments indicate that crossbridge kinetics are increased at short SL in both α-MyHC and β-MyHC myocytes and that there are MyHC specific differences in responsiveness to SL changes.

The cellular basis for the Frank-Starling relationship arises from beat-to-beat changes in diastolic myocyte length, and thus changes in myocyte sarcomere length. Increasing sarcomere length within the working range of the myocardium (~1.9 μm to 2.3

μm) [45, 47, 140] increases force generating capacity due , in part, to more optimal overlap of the thick and thin filaments [43], increased activator Ca^{2+} released from the sarcoplasmic reticulum [5], and enhanced myofibrillar sensitivity to Ca^{2+} [5, 66, 79, 101]. A study by Sonnenblick found that increasing initial muscle length increased force without an apparent change in the maximal velocity of shortening (V_{max}), as extrapolated from force-velocity curves [160]. However, a study utilizing lightly loaded ferret papillary muscle showed that shortening velocity of a well-defined central muscle segment declined with decreased muscle segment lengths [97]. Also, a more recent study showed that V_0 of sarcomere shortening was increased in proportion to SL between 1.9 μm and 2.3 μm at submaximal Ca^{2+} activation in rat cardiac trabeculae [24]. These studies imply a SL-dependent effect of cardiac muscle shortening. We sought to directly address this hypothesis by measuring sarcomere shortening velocity in skinned cardiac myocytes that allow control of Ca^{2+} activation levels and that lack extracellular viscoelastic elements that may affect shortening. The use of rats also allowed manipulation of MyHC content via administration of propylthiouracil, which binds circulating thyroid hormone and induces a shift in the heart from α-MyHC to β-MyHC. It is important to determine the difference in SL responsiveness between α-MyHC and β-MyHC because there are changes in MyHC expression in response to a number of physiological and pathophysiological conditions, including up-regulation of β-MyHC in rodents in response to diabetes [25, 38] and pressure overload [90, 92, 95] and in failing human myocardium [109]. The latter carries clinical relevance, as there are a number of studies that have demonstrated the Frank-Starling mechanism is compromised in animal models of heart failure [81, 150] and in human failing myocardium [72, 157].

Sarcomere length dependence of loaded shortening and power output

This study found a sarcomere length dependence of absolute loaded shortening velocity and power output in both α-MyHC and β-MyHC skinned cardiac myocytes, but the effect of sarcomere length was more pronounced in β-MyHC myocytes. Much of the sarcomere length dependence arose from changes in isometric force, but relative force curves between long and short SL still showed SL dependence of loaded shortening velocity and power output, especially at loads around 30% of isometric force where the heart is thought to work *in vivo*. A plausible reason for slower shortening velocity at short SL is increased cooperative inactivation of the thin filament during myocyte shortening [75, 99]. For instance, at shorter sarcomere length there is decreased Ca^{2+} sensitivity of force arising at least in part from fewer crossbridges. The reduction in shortening velocity could then arise from more cooperative inactivation of the thin filament at the onset of and throughout the force clamp, leaving fewer crossbridges to bear a fixed relative load at short SL. This is supported by our previous work [99] that showed decreasing activator Ca^{2+} to yield force changes similar to those seen in the present study between long SL and short SL resulted in significantly slower loaded shortening velocity and a quantitatively similar decrease in peak normalized power output as seen in the present study. However, changes in Ca^{2+} activation alone resulted in lower power output at all relative loads, whereas decreased SL seemed to only alter loaded shortening and power at loads less than ~40% of isometric force. This implies that a sarcomere length component alters loaded shortening velocity independent of changes in thin filament activation.

Sarcomere length dependence of loaded shortening and power output at matched levels of thin filament activation.

We determined if decreased power between long and short SL was due to decreased thin filament activation by normalizing thin filament activation levels with increased calcium concentration at short SL to match force seen at long SL. Interestingly, α-MyHC myocytes exhibited significantly faster loaded shortening velocities and increased power output at short SL with matched force when compared to long SL, implying increased crossbridge cycling kinetics at short SL. These increased crossbridge kinetics were observed at matched force despite the increased myocyte width and lattice spacing that occurs with shorter SL . This result may arise because α-MyHC crossbridges either become more flexible in the azimuthal direction or extend away from the thick filament in the radial direction at short SL in addition to, or perhaps resulting in, faster kinetics. In contrast, peak normalized power output in β-MyHC myocytes remained significantly depressed at short SL compared to long SL even with matched force levels. This suggests that β-MyHC crossbridges do not undergo as much of an increase in azimuthal flexibility or radial extension from the thick filament, at least as compared to α-MyHC, and this may explain, in part, why β-MyHC myocytes exhibit a greater SL dependent decrease in loaded shortening velocity and power than α-MyHC myocytes.

Changes in sarcomere length are known to cause changes in the lateral spacing between the thick and thin filament [74, 98], and decreased interfilament spacing induced by osmotic compression has been shown to increase force at a given sarcomere length in

single skinned cardiac myocytes [102]. Lattice spacing, then, is thought to influence the probability of crossbridge formation and thin filament activation by moving toward or away from the optimal binding range for myosin. Thus, another potential mechanism for decreased loaded shortening velocity at short SL is the resultant increase in lattice spacing, which would lead to less than optimal crossbridge interaction and greater cooperative inactivation at the onset of and throughout shortening. Reduced myocyte width and, thus, lattice spacing in our myocytes caused a striking increase in loaded shortening velocity and power output in both α-MyHC and β-MyHC. This certainly implies that lattice spacing plays a major role in the reduced loaded shortening velocity and power output from long SL to short SL, and further implies faster crossbridge kinetics at short SL. Again, this may be due in part to increased radial crossbridge extension from the thick filament at short SL, especially in α-MyHC myocytes. Evidence for such a conformational change in cardiac muscle is lacking, but changes in radial and azimuthal flexibility have been seen as a consequence of lattice spacing and temperature in activated skeletal muscles [21, 89].

Interestingly, it has been shown that phosphorylation of myosin binding protein-C by PKA results in extension of crossbridges from the thick filament backbone [180]. MyBP-C is thought to form a collar around the thick filament, with extensions that bind the myosin head in an inhibitory manner [110]. Phosphorylation of MyBP-C has been shown to relieve this inhibition and increase force [87] and myocytes from MyBP-C null mice have been shown to have increased rates of force development, loaded shortening velocity, and power output generating capacity [86, 164]. The thick filament anchoring

protein titin is responsible for nearly all of the passive force encountered at physiological sarcomere lengths [33, 44], and is known to bind to MyBP-C [33]. It may be possible that as the sarcomere length is increased and titin becomes taut, it exerts a force on MyBP-C that in turn affects myosin head radial or azimuthal mobility. Conversely, as SL is shortened titin becomes more slack and exerts less force on MyBP-C that in turn reduces MyBP-C constraint on myosin head mobility. Force and power still decrease at short SL because interfilament distance is increased and there are fewer myosin crossbridges to cooperatively activate the thin filament as there is likely cooperative inactivation at the onset of shortening [75, 99]. However, in α-MyHC myocytes, the decrease in normalized power output was not as large as might be expected with a decrease in SL and, in fact, there was virtually no effect on loaded shortening velocity at loads greater than 50% isometric force. We observed a similar phenomenon in MyBP-C null myocytes in which loaded shortening velocities were greatly elevated at high loads. This was not observed in wild-type myocytes [86]. Additionally, when thin filament calcium activation is increased or the interfilament distance decreased (by osmotic compression) at short SL an increase in crossbridge kinetics becomes apparent. This is schematically illustrated in Figure 3.8, where a decrease in SL causes titin to slack, which induces a conformational change in MyBP-C that results in release of myosin constraint (similar to MyBP-C phosphorylation) and radial extension of myosin heads from the thick filament backbone (in α-MyHC). Interestingly, Weisberg and Winegrad did not see a change in β-MyHC crossbridge extension with PKA-phosphorylation of MyBP-C, indicating that MyBP-C may have less of an effect on radial extensibility with β-MyHC thick filaments [180]. Consistent with this, we observed a much larger decrease in

Figure 3.8

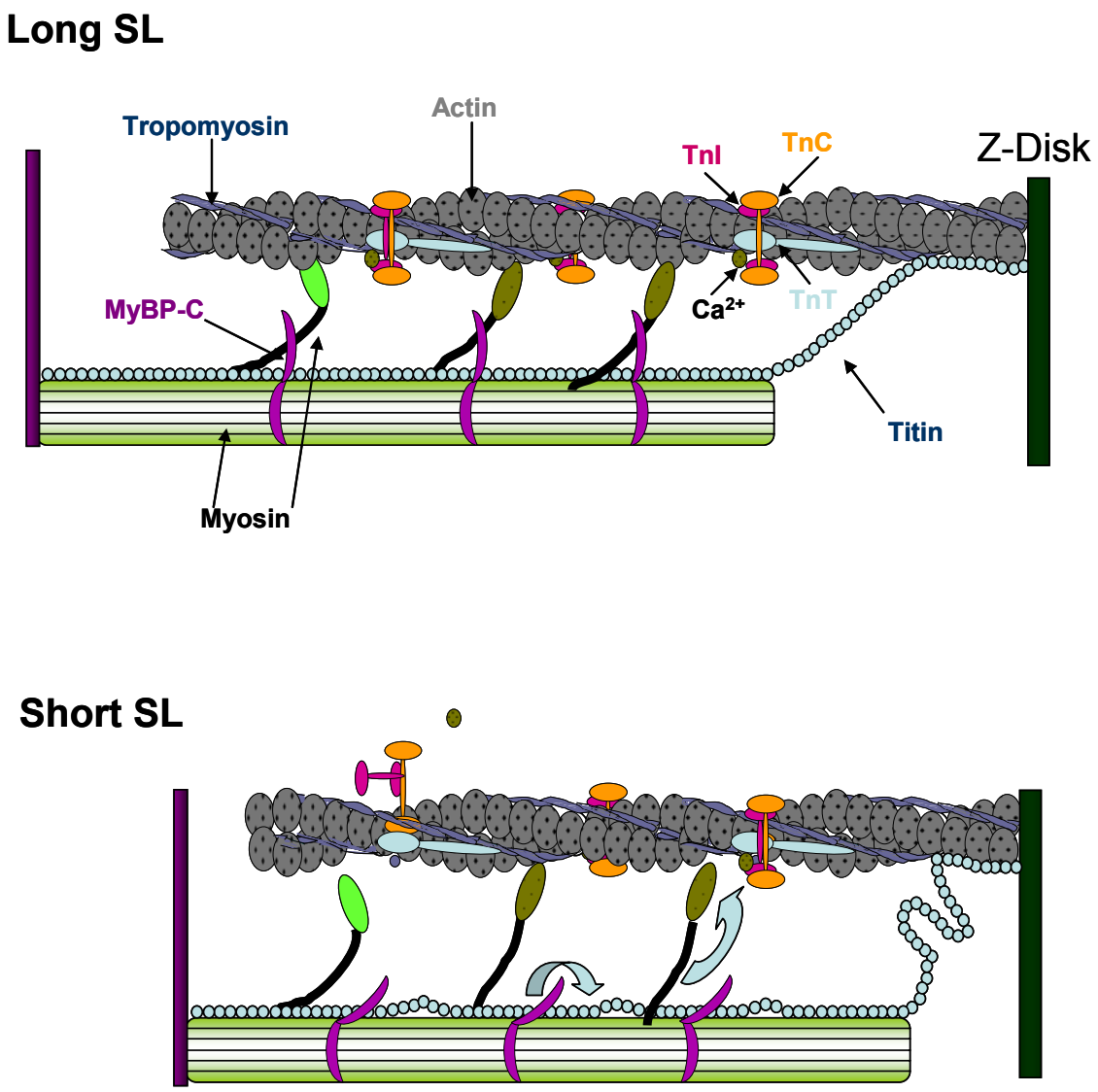

Figure 3.8: Crossbridge model of increased kinetics at short SL.

A. Representation of sarcomeric proteins at long SL. Titin is extended and provides passive tension that may help maintain extension of MyBP-C from the thick filament to provide constraint on the myosin crossbridge. **B.** At short SL, titin is slack and this lack of passive tension may alleviate MyBP-C constraint of the crossbridge, which, in α-MyHC, may lead to greater crossbridge extension from the thick filament backbone and, in both α-MyHC and β-MyHC, increased crossbridge kinetics, similar to that observed with MyBP-C phosphorylation.

resulting in slower shortening and lower power. Furthermore, β-MyHC is more susceptible to changes in lattice spacing than is α-MyHC, possibly due to less length dependent crossbridge radial extension from the thick filament backbone, which makes it less able to maintain thin filament activation during loaded shortening. This leads to a greater difference in power between long and short SL and less of an increase in power when force levels are matched.

Sarcomere length and myosin heavy chain dependence of the force-pCa relationship

The decrease in isometric force at short SL compared to long SL, whereby maximal Ca^{2+} activated isometric force at short SL was ~70% of that at long SL in both α-MyHC and β-MyHC myocytes, is in agreement with previous studies. We [85] and others [107, 152] previously have shown there is no difference in maximal isometric tension between α-MyHC and β-MyHC, as we also observed here. However, previous studies regarding tension-pCa relationship differences between α-MyHC versus β-MyHC produced discordant results. Saponin treated bundles of rabbit myocardium showed no difference in Ca^{2+} sensitivity of force [132], whereas ventricular bundles from hypothyroid rat (β-MyHC) were left-shifted (i.e. more sensitive) compared to bundles from euthyroid rat (α-MyHC) [40]. Studies utilizing single myocyte preparations also have provided mixed results, either demonstrating no change [32] or a right-shift (i.e. less sensitive) in the force-pCa relationship with β-MyHC [107]. We hypothesized that these discrepancies may arise from different levels of PKA-induced phosphorylation of myofibrillar proteins (i.e., MyBP-C and cTnI), which would alter the tension-pCa relationship. We attempted to control this potential variable by maximally phosphorylating myofilaments with the catalytic subunit of PKA, and then measuring the

tension-pCa relationship. Regarding PKA treatment, it was previously reported that PKA phosphorylation of myofibrillar proteins increased the length dependence of Ca^{2+} sensitivity of isometric force [83], while others have noted that PKA phosphorylation of MyBP-C and cTnI does not change sarcomere length dependence of Ca^{2+} sensitivity [174]. In this study, we only measured the tension-pCa relationship following PKA treatment in an attempt to discern differences between α-MyHC and β-MyHC. We found that α-MyHC myocytes were less responsive to Ca^{2+} than β-MyHC myocytes, but that there is no MyHC difference in ΔpCa_{50} in response to sarcomere length changes following PKA treatment. The enhanced Ca^{2+} sensitivity in β-MyHC may be due to its slower duty cycle than α-MyHC that would tend to prolong actin attachment and maintain thin filament activation, resulting in less Ca^{2+} being required to activate the thin filament, as has been previously proposed [10]. On the other hand, phosphorylation by other kinases such as PKC could be responsible for the different Ca^{2+} sensitivities between α-MyHC and β-MyHC myocytes in this study, but we did not explore this due to the wide array of kinases required to maximally phosphorylate all sites.

Sarcomere length and myosin heavy chain dependence on the rate constant of force development

MyHC has been shown to be a key determinant of the rate of tension development , whereby α-MyHC exhibited ~3 times greater rate constant of force development (k_{tr}) than β-MyHC in rat skinned ventricular muscle preparations [152]. Our current findings are in agreement with that study in that α-MyHC myocytes exhibited k_{tr} values that were about twice as fast as β-MyHC myocytes for a given SL or activation level. The SL

dependence of k_{tr} was previously addressed by Adhikari et al. [1], who discovered that k_{tr}'s at 2.3 μm and 2.0 μm were comparable at maximal Ca^{2+} activation and faster at force matched submaximal Ca^{2+} activation in rat skinned cardiac trabeculae. We also saw no difference in k_{tr} at long and short SL in α-MyHC myocytes, but it was higher at short SL at the same Ca^{2+} activation levels as at long SL and when myocyte width was matched. Interestingly, a novel finding of this study is that β-MyHC myocytes exhibited higher k_{tr} values at short SL than at long SL despite lower force levels and was even higher when at the same level of thin filament activation or the same myocyte width. This is somewhat surprising given that β-MyHC myocytes had such a significant decrease in power at short SL, but this decrease was likely due, in large part, to the increase in myocyte width. Here again, similar to what was seen with power, the rate of force development at short SL with matched force was not significantly different from short SL. However, the rate of force development at short SL with matched width was significantly faster than at short SL, again illustrating the susceptibility of β-MyHC to width. Overall, our estimates of the rate constant of force development are in agreement with the idea that crossbridge kinetics are inherently greater at short SL in both α-MyHC and β-MyHC myocytes.

Physiological significance

The Frank-Starling mechanism is a physiological phenomenon that tunes myocardial function on a beat-to-beat basis by altering stroke volume, a primary index of the heart's ability to function as a pump [161]. Ventricular function curves plotted as end-diastolic volume versus stroke volume have been considered a unifying basis for

changes in ventricular function [153], and depression of this relationship is associated with heart failure [12, 72, 120, 157, 172]. Interestingly, failing human myocardium has increased β-MyHC content [109]. It may be possible that β-MyHC is expressed early in the compensatory phase as it is more energetically favorable [50, 71, 91, 152] and associated with a slower heart rate [49]. Teleologically, a slower heart rate allows for more filling time and, thus, a greater potential end-diastolic volume. Based on our results a heart containing β-MyHC may be more responsive to a change in end-diastolic volume, meaning greater reliance on the Frank-Starling relationship as a way to tune ventricular power output (i.e., stroke volume). This is consistent with observations that rat left ventricles that had >70% β-MyHC exhibited steeper ventricular function curves than left ventricles that contained predominantly α-MyHC [31]. Additionally, we have seen that working rat heart preparations that contained primarily α-MyHC had a ~50% increase in left ventricular power output when left atrial filling pressure was increased from 7.5 cm H_2O to 15 cm H_2O, whereas hearts containing primarily β-MyHC exhibited an ~150% increase in left ventricular power (unpublished data).

It is also interesting that α-MyHC myocytes were less sensitive to Ca^{2+} than β-MyHC myocytes. Because α-MyHC myocytes exhibited faster loaded shortening velocity and higher power output, which translates to greater pulse pressure and ejection [86], the decrease in Ca^{2+} sensitivity may be beneficial as it would lead to a more rapid thin filament inactivation and more rapid diastolic relaxation. On the other hand, enhanced Ca^{2+} sensitivity of β-MyHC myocytes may shorten the isovolumic phase of contraction and prolong time for ejection. This, coupled with the observed increase in

rate of force development at short SL in β-MyHC myocytes, may be a mechanism for β-MyHC to maintain adequate stroke volume in the face of decreased EDV. Most interestingly, a main finding of this study is that crossbridge kinetics actually are increased at short SL in both α-MyHC and β-MyHC. This may help maintain ventricular power with decreased end-diastolic volumes and help sustain adequate blood flow to the heart and periphery when venous return is compromised.

Chapter 4. DISCUSSION

4.1 Summary of Results

The heart's pumping performance is determined by factors intrinsic to the myocardium, and can be altered on a beat-to-beat basis through changes in sarcomere length or Ca^{2+} sensitivity, or long-term through changes in myofilament protein isoform expression. The pumping action occurs when individual myocytes undergo loaded shortening in response to activation. My work has primarily focused on the effects of sarcomere length and thick filament protein expression on loaded shortening velocity and power output in single skinned cardiac myocytes. I have determined the effect of ablation of the thick filament protein MyBP-C on force, rate of force development, loaded shortening velocity, and power output in mouse skinned cardiac myocytes. Ablation of MyBP-C resulted in increased loaded shortening velocity and power output during maximal and half-maximal Ca^{2+} activation, and this effect was more pronounced during half-maximal Ca^{2+} activation (Figures 2.2 and 2.3). Furthermore, the rate of force development also was increased with MyBP-C ablation, but only during half-maximal Ca^{2+} activation (Figure 2.4). This underscores the importance of MyBP-C in regulating myocardial function, as the myocardium *in vivo* is thought to mostly encounter half-maximal Ca^{2+} concentrations.

The effects of sarcomere length on force, Ca^{2+} sensitivity of force, rate of force development, loaded shortening velocity and power output were determined in rat skinned cardiac myocytes as well. Moreover, because β-MyHC is upregulated with heart

failure, and heart failure is associated with a reduced Frank-Starling mechanism, sarcomere length dependence was determined in myocytes containing either α-MyHC or β-MyHC to assess potential MyHC dependence of sarcomere length responsiveness. Decreasing sarcomere length from 2.3 μm to 2.0 μm resulted in decreased peak absolute and normalized loaded shortening velocity and power output in both α-MyHC and β-MyHC myocytes, but the effect was more pronounced in β-MyHC myocytes. Changing sarcomere length from 2.3 μm to 2.0 μm, however, had no effect on the rate of force development in α-MyHC myocytes and actually increased the rate of force development in β-MyHC myocytes. Because decreasing sarcomere length results in decreased thin filament activation, the effect of sarcomere length also was measured in myocytes with matched levels of thin filament activation as indexed by force. This resulted in faster loaded shortening velocity at short SL and increased power to values that even exceeded those seen at long SL in α-MyHC myocytes. β-MyHC myocytes experienced increased loaded shortening velocity at high loads, but peak power remained depressed at short SL with matched force. The rate of force development in both α-MyHC and β-MyHC myocytes was faster at short SL with matched force than at long SL. Another consequence of decreasing sarcomere length is an increase in myocyte width and interfilament lattice distance. Thus, the effect of sarcomere length also was measured in myocytes with matched width brought about by application of the osmotic polymer dextran. Loaded shortening velocity, power output, and the rate of force development were increased at short SL with matched myocyte width as compared to long SL in both α-MyHC and β-MyHC. Taken together, these results imply that crossbridge cycling is increased at short SL. Finally, MyHC dependence of Ca^{2+} sensitivity of force was

examined at both long and short SL following treatment with PKA in an attempt to normalize for differences in basal PKA-induced phosphorylation. β-MyHC myocytes were found to be more sensitive to Ca^{2+} than α-MyHC myocytes, but there was no difference in their change in Ca^{2+} sensitivity of force with changes in sarcomere length..

Overall, these results provide a molecular and cellular basis for functional changes that occur with the Frank-Starling relationship, and how that relationship can be altered with myocardial plasticity.

4.2 Effects of MyBP-C on Myocardial Function

The data presented here are consistent with the idea that MyBP-C normally acts to limit crossbridge kinetics by constraining myosin-actin interaction. In the past, it was postulated that it does so by tethering the crossbridges to the thick filament backbone to limit the range of crossbridge movement [15, 68, 69], and that phosphorylation relieved this constraint [39, 46]. More recent evidence suggests that MyBP-C may exert its effects independent of a tether mechanism. Addition of MyBP-C fragments consisting of the N-terminal, S2-binding C1C2 portion of the molecule, which lack binding sites for the rod portion of myosin and are, thus, "untethered", resulted in increased myofilament Ca^{2+} sensitivity in normal myocardium [53]. There also was an increase in Ca^{2+} sensitivity in myocardium lacking MyBP-C with the addition of the C1C2 fragment [53], indicating that the fragment is not simply competing away endogenous MyBP-C, but is instead likely directly affecting myosin crossbridges perhaps by binding the S2 region of myosin and altering its conformation and, thus, its interaction with actin. Furthermore, phosphorylation of this fragment reduced its ability to enhance Ca^{2+} sensitivity [53],

implying its interaction with myosin was attenuated. This strengthens the argument that phosphorylation of MyBP-C results in a reduction in its interaction with myosin crossbridges. Another recent study showed that high concentrations of the MyBP-C fragment C0C2 can activate force production in the absence of Ca^{2+} [63]. The author's attribute this to a direct effect of the C0C2 fragment on myosin crossbridges, because immunohistochemical analysis showed no evidence for C0C2 interaction with proteins in the I-band (thin filament only) or the H-zone (myosin backbone only). Again, this implies that MyBP-C affects myosin independent of a tether mechanism and MyBP-C may directly affect crossbridge interactions with thin filaments. Interestingly, this study also showed that lower concentrations of C0C2 increased myofibrillar Ca^{2+} sensitivity, but only at SL of 1.9 μm and not at SL of 2.3 μm [63]. This provides evidence that MyBP-C may be involved in mediating the sarcomere length dependence of cross-bridge position and is consistent with my model whereby alleviation of titin strain allosterically alters the interaction between MyBP-C and myosin.

A major discrepancy arising from my study is that we saw enhanced contractile function in myocytes lacking MyBP-C, while hearts that either lack MyBP-C or express truncated MyBP-C demonstrate contractile *dys*function *in vivo* [52, 133, 134]. Hearts that contained truncated MyBP-C or lacked MyBP-C presented with similar phenotypes including increased mass, decreased ejection fraction *in vivo*, and left ventricular chamber dilation. Interestingly, the maximal rate of pressure development was no different in MyBP-C truncated or ablated hearts and their respective controls, whereas the rate of pressure decline was much slower in MyBP-C truncated and ablated hearts. This

is very similar to an observation that intact rat ventricular myocytes showed decreased time to half-relaxation when MyBP-C binding to endogenous myosin S2 was competitively reduced by addition of exogenous myosin S2 [15]. This putative slowdown in relaxation in MyBP-C truncated/ablated mice implies that these hearts experience compensated hemodynamic loads due to less time for ventricular filling. Decreased ventricular filling would lead to decreased stroke volume in accordance with the Frank-Starling relationship. An additional factor thought to reduce ejection fraction in MyBP-C truncated/ablated mice seems to arise from a marked abbreviation of systolic ejection. The exact mechanism for this abbreviation is unclear but has been proposed to arise from the notable reduction in the stiffness of myosin crossbridges in MyBP-C ablated/truncated hearts [133, 134]. Here again, MyBP-C seems to provide a stabilizing constraint to myosin that enables it to maintain low compliant, strong crossbridge binding to actin that, in turn, sustains thin filament activation. So, in myocytes lacking MyBP-C, the crossbridges are more compliant and therefore accelerate thin filament *in*activation that normally occurs during ejection [100]. So, for example, during normal ejection as myocytes shorten, the spacing between the thick and thin filament increases, reducing the probability of myosin strongly interacting with actin. In addition, it is well known that the intracellular Ca^{2+} concentration is transient, and therefore declining, throughout systole. Thus, the intracellular environment favors thin filament inactivation as systole proceeds (due to both decreasing levels of activating calcium and decreasing numbers of strongly bound myosin crossbridges). For the situation of myocytes lacking MyBP-C, the more compliant crossbridges would tend to accelerate this process and lead to truncated ejection because the myocytes are unable to sustain the load needed to keep the

aortic valve open in the face of systolic arterial pressures. Interestingly, I propose that these more compliant, less constrained crossbridges (due to the lack of MyBP-C) also can lead to slower relaxation. While these crossbridges are unable to sustain systolic loads, their enhanced range of motion prevents full thin filament inactivation due to their propensity to interact with actin, which prolongs isovolumic relaxation and leaves less time for filling.

An alternative mechanism for systolic dysfunction in MyBP-C truncated/ablated hearts arises from a recent study that showed that MyBP-C ablation accelerated stretch activation [164]. First identified in insect flight muscle by J.W.S. Pringle in 1949, the stretch-activation response takes advantage of a property that generates oscillatory power output in the presence of a persistently elevated calcium concentration [142]. When activated muscle is subjected to a quick stretch, there is a nearly instantaneous increase in force which quickly decays. Then, even though the muscle remains in an isometric state, there is second rise in tension. This delayed second rise in tension is the hallmark of the stretch-activation response, and is governed by a time delay that seems to be related to the resonant frequency of maximal power output in an oscillating system such as beating insect wings or a beating heart [16]. Stretch activation, therefore, may be an important mechanism for regulation of heart function including myocardial power generation and ejection. In fact, mathematical modeling suggests that stretch-activation uses crossbridge activation to help determine the steepness of the Frank-Starling relationship [16]. A consequence of reliance on crossbridge activation, however, would also likely enhance inactivation of crossbridges during muscle shortening. Experimentally, this was observed when ablation of MyBP-C was shown to accelerate stretch activation in mouse skinned

myocardium [163], and as discussed above, also apparently accelerates crossbridge inactivation during ejection [134]. This also is interesting in light of the torsional aspect to cardiac contraction noted in the introduction [16, 23, 165, 177]. Torsional motion is wrought by the orientation of cardiac myofibers which form a left-handed helix on the epicardium from the apex to the base while the endocardial surface spirals in a counter right-handed helix [167]. Epicardial fibers are known to dominate over endocardial fibers during ejection, thus 'weaker' endocardial fibers are effectively being stretched at the onset of systole, which may initiate the stretch-activation response that results in a delayed tension peak near the end of systole when force would otherwise be declining. Accelerated stretch activation due to lack of MyBP-C may result in premature force development in subendocardial regions of the heart that eliminates the delayed tension development that helps maintain ejection, which could account for the observed sudden abbreviation in systolic ejection.

There is another aspect to muscle contraction that shares many similarities with stretch-activation: the overshoot in tension that occurs following a slack-restretch maneuver such as for the measurement of rate of force development. Following a rapid shortening and restretch protocol, tension often temporarily exceeds isometric tension before eventually declining to the original steady-state value, especially when muscle is activated with submaximal Ca^{2+} [17]. We do not normally observe tension overshoot because our typical tension recovery records are cut off prior to overshoot occurring. Using a longer time scale record has revealed tension overshoots in a number of different muscle preparations [17, 18, 104, 145]. Interestingly, tension overshoots typically occur

in skinned cardiac preparations, but are notably absent following MyBP-C extraction and in MyBP-C ablated myocardium (unpublished observations, conversations with K.S. Campbell and K.S. McDonald). Recall that MyBP-C ablated myocardium has a faster rate of force development at submaximal Ca^{2+} activations, and accelerated stretch activation. The lack of overshoot implies that the accelerated stretch-activation helped speed the rate of force development, but the acceleration has diminished by the time overshoot normally occurs. I have proposed a model (Figure 3.8) whereby a conformational change in MyBP-C that occurs between long and short sarcomere length is responsible for the increase in crossbridge kinetics seen at short SL when force is normalized, and that titin may be involved in transduction of passive force, or lack thereof, to MyBP-C to initiate the conformational change. This can be tested experimentally by measuring mechanical properties before and after titin degradation by mild trypsin digestion, which has been shown to preferentially degrade titin without affecting other sarcomeric proteins [35, 37, 44, 57]. Cleavage of titin should speed the rate of force development and eliminate tension overshoot similar to MyBP-C ablation. Indeed, titin cleavage did result in increased rate of force development and elimination of tension overshoot (Figure 4.1), implying that titin affects crossbridge interaction with the thin filament either directly or indirectly through MyBP-C as proposed. The possibility exists that titin may be interacting with and stretching the thin filaments during restretch, which may activate regulatory units and allow more crossbridges to bind, leading to tension overshoot. However, increased availability of regulatory units would tend to increase the rate of force development, which is actually increased when titin is degraded and unavailable to exert activating effects on the thin filament.

Figure 4.1

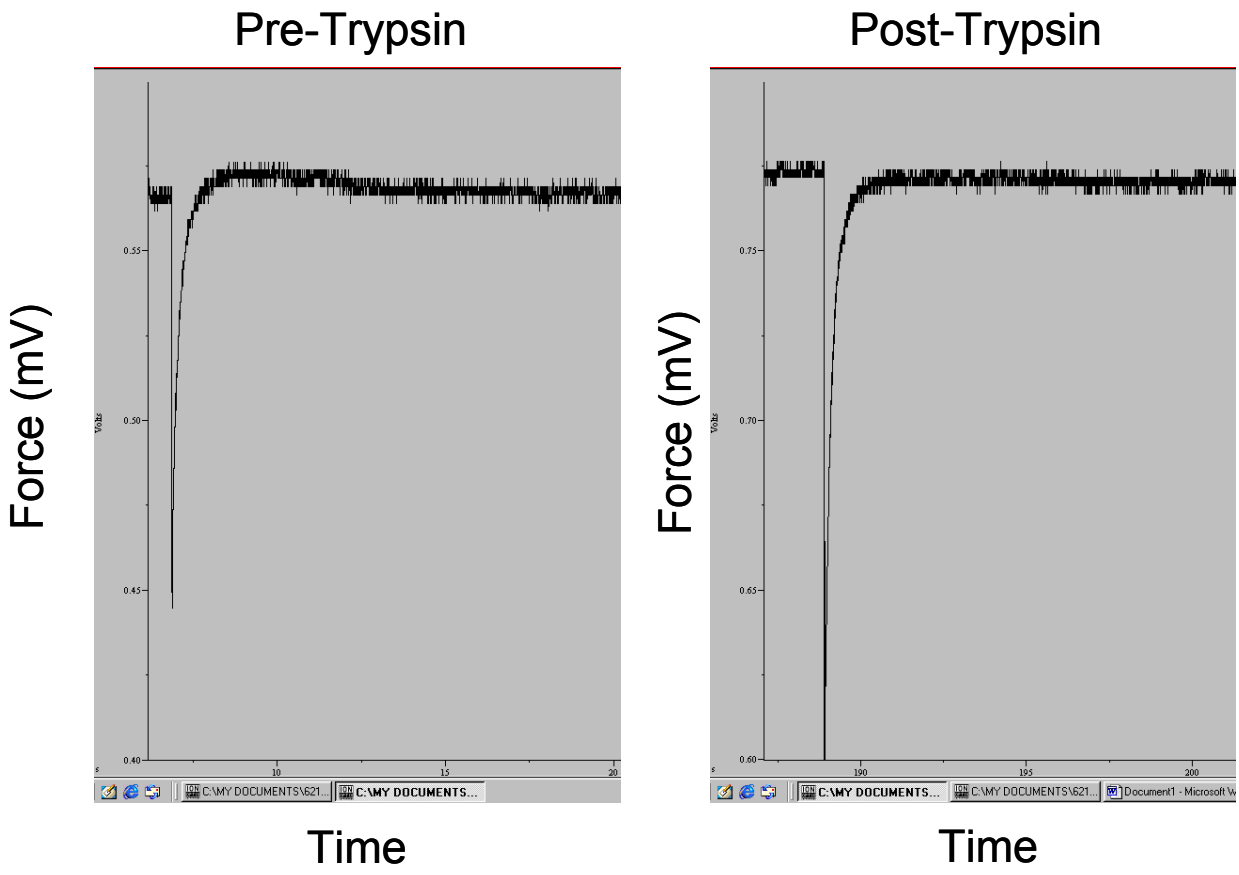

Figure 4.1: Tension overshoot in skinned cardiac myocytes before and after titin degradation.

Normal myocardium at submaximal Ca^{2+} activation shows evidence of transient tension overshoot following rapid shortening to slack length and restretching to original length. Titin degradation following trypsin treatment abolishes the tension overshoot and speeds the rate of force development.

Furthermore, I showed that the rate of force development is faster or unchanged at short sarcomere length as compared to long sarcomere length, when titin is slack and not exerting any passive force that could potentially activate the thin filament. Expanding the recorded time scale should also show that tension overshoot is depressed at short sarcomere length, which we observed as well (data not shown). Cleavage of titin by mild trypsin digestion should also speed loaded shortening velocity and increase power output similar to MyBP-C ablation. Experimental results, though, show that there was no significant change in loaded shortening velocity or power output following titin degradation (data not shown). However, there are a number of potential explanations for this result. First, titin is the number one contributor to passive tension in cardiac myocytes [36, 44, 122], and passive tension has been correlated with active force production [20, 37, 124]. Thus, degradation of passive force would be expected to decrease active force production, which would tend to slow loaded shortening velocity. In this experiment, passive force declined with trypsin treatment, but there was no difference in isometric force. Second, titin, when stretched, may then be able to assist with loaded shortening, as it has been shown to increase unloaded shortening velocity [108], probably by passive recoil. If this were the case, degradation of titin would tend to slow loaded shortening velocity, which, when coupled with a subsequent MyBP-C mediated increase in loaded shortening velocity, may offset and present as no change as observed. Finally, SDS-agarose-PAGE analysis designed specifically for detection of titin showed that we degraded approximately 30-35% of titin content (data not shown). This may be enough to account for changes we have seen in rate of force development

and tension overshoot, but not enough to cause differences in loaded shortening velocity and power. There are 6 titins per thin filament so, assuming a stoichiometric ratio, our trypsin degradation would still leave ~4 titins per thick filament. The interpretation of the results would be clarified with more complete degradation of titin.

It also may be possible that titin is opposing loaded shortening velocity by providing an internal load. In vitro motility assays demonstrated that the PEVK region of titin interacted with actin to slow filament sliding, and it was suggested that similar action in cardiac myocytes may occur. The calcium binding protein S100A1 was shown to relieve the PEVK-actin interaction in a Ca^{2+} dependent manner, leading the authors to speculate that S100A1 could reduce passive resistance during contraction. We tested this hypothesis by addition of exogenous S100A1 to skinned cardiac myocytes. There was no difference in loaded shortening velocity or power output before or after addition of exogenous S100A1 (Figure 4.2). Furthermore, there was no endogenous S100A1 present to confound these results, as shown using western blot with an antibody to S100A1 (data not shown). Taken together, these results suggest that titin is not providing an internal load. Overall, our results regarding tension overshoot before and after trypsin degradation coupled with similar results following MyBP-C extraction or ablation support our model whereby titin-MyBP-C interaction regulates, at least in part, sarcomere length dependence of myocyte function.

Figure 4.2

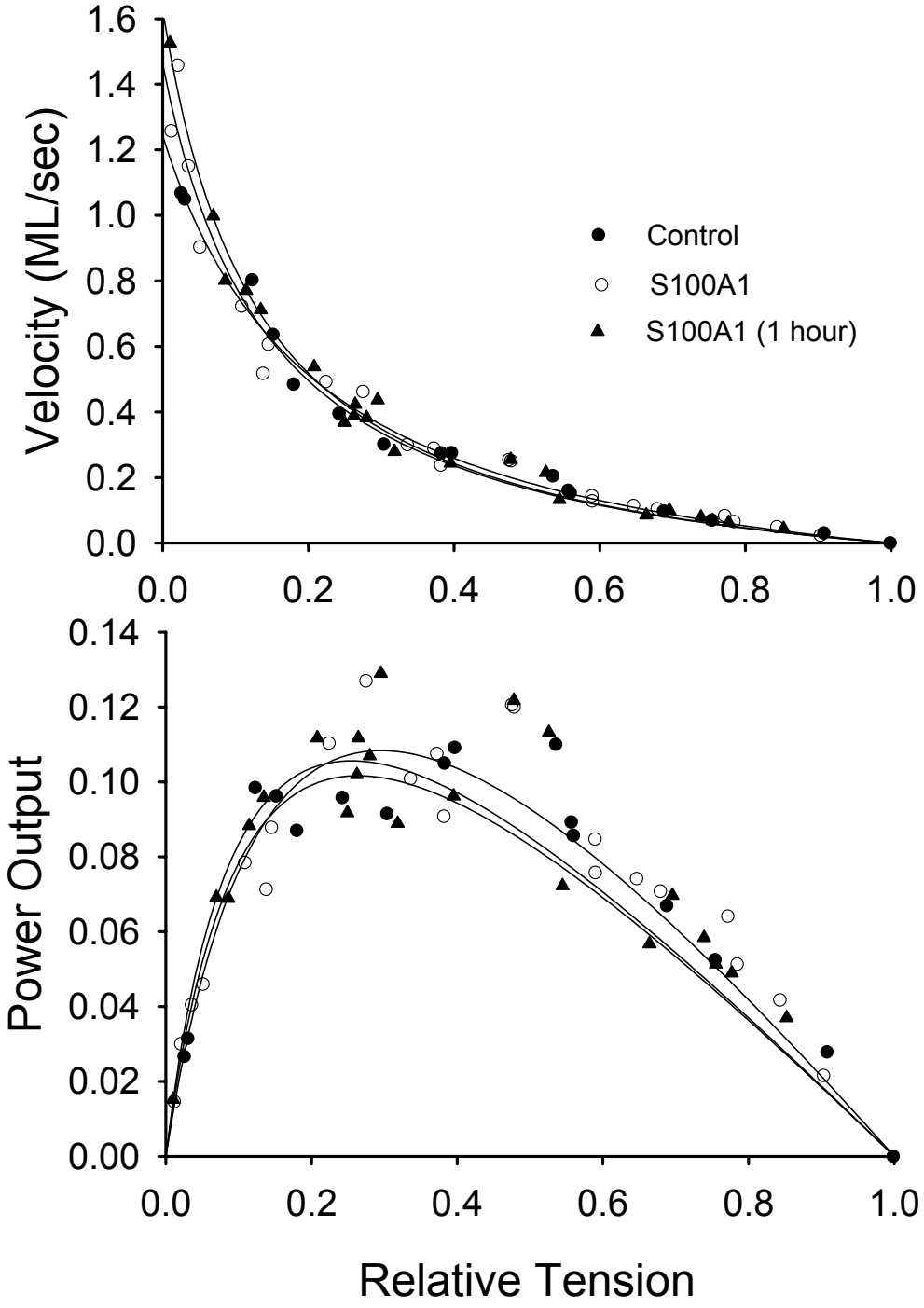

Figure 4.2: Force-velocity and power load curves before and after treatment with S100A1

There was no difference in loaded shortening velocity between control, treatment with S100A1 for 20 minutes, or incubation with S100A1 for 1 hour.

4.3 Role of MyHC in sarcomere length dependence of mechanical properties

The studies in this dissertation demonstrate that crossbridge cycling rates are increased at short SL as compared to long SL, which may be due to an increase in myosin flexibility that results in crossbridge extension from the thick filament. X-ray diffraction is a useful tool that may provide insight into the possibility of crossbridge orientation following changes in sarcomere length. For example, the intensity of M3 meriodonal reflection is thought to arise from axial repeats of myosin heads along the thick filament [144]. An increase in intensity of the M3 reflection suggests that the heads become more perpendicular to the thick filament; i.e., they extend away from the thick filament. It has already been seen that increasing temperature from 0 to 17 in frog skeletal muscle intensified the M3 reflection during isometric contraction, correlating with the temperature dependent increase in force [89]. M3 reflections also were found to change with sarcomere length, but appeared to be due completely to the degree of overlap between thick and thin filaments. This is to be expected for skeletal muscle that was used for these experiments, which has a much shallower length-tension relationship than cardiac muscle. To the best of my knowledge, the effects of sarcomere length changes on the M3 reflections in cardiac muscle has not been examined, but would likely provide insight into the structural mechanism that governs the steep length-tension relationship in cardiac muscle.

Light microscopy is another way of testing whether crossbridges extend farther away from the thick filament backbone at shortened sarcomere length. As noted in the introduction, muscle is strongly birefringent; it polarizes light. Muscle birefringence

arises from the anisotropic band of the sarcomere, which is known to be caused by myosin. Use of interference microscopy can be used to assess changes in birefringence that reflects movement of myosin crossbridges. A greater birefringence value is thought to be due to the myosin S-2 fragment (which interacts with and is bound by MyBP-C) moving closer to the thick filament shaft, while a smaller birefringence value is due to S-2 away from the thick filament backbone [159]. The model for sarcomere length dependent changes in loaded shortening velocity proposed in this dissertation is that myosin is extended away from the thick filament at short sarcomere length, speeding crossbridge cycling. Birefringence, therefore, may be able to detect changes in the thickness of the thick filament in response to changes in sarcomere length that can be correlated with myosin extension.

4.4 Conclusion

The studies in this dissertation show that when thin filament activation levels are matched loaded shortening velocity and power output are actually increased at short SL compared to long SL. Loaded shortening velocity and power output also were shown to increase in myocytes lacking MyBP-C compared to control myocytes. The mechanism(s) for the increased loaded shortening velocity and power output in both these experimental manipulations is proposed to be similar. I have proposed a model in which the sarcomere length dependence of power arises from a conformational change in MyBP-C, whereby the stabilizing constraint of MyBP-C on myosin cross-bridges is alleviated at short sarcomere length because of less stress imposed by titin. Titin has been shown to be primarily responsible for passive tension in cardiac and skeletal muscle and titin may

transmit this passive tension to MyBP-C, eliciting a conformation in MyBP-C that stabilizes its interaction with myosin. At short sarcomere length, passive tension is reduced or eliminated, which would alleviate the conformational stability of MyBP-C on myosin, resulting in more extensible (and also more compliant crossbridges). These crossbridges would tend to accelerate rates of force development and rates of loaded shortening by perhaps faster crossbridge interaction kinetics *per se* and, even more likely, altered recruitment of thin filament regulatory units by cross-bridges. Experiments are needed to directly test this theory; such experiments would include mechanical measurements before and after more complete titin degradation and x-ray and light diffraction measurements to assess crossbridge extensibility and binding in response to changes in sarcomere length and MyBP-C truncation/ablation/extraction.

LITERATURE CITED

1. Adhikari, B.B., et al., *Cardiac length dependence of force and force development kinetics with altered cross-bridge cycling.* Biophysical Journal, 2004. **87**: p. 1784-1794.
2. Allen, D.G. and J.R. Blinks, *Calcium transients in aequorin-injected frog cardiac muscle.* Nature, 1978. **273**: p. 509-513.
3. Allen, D.G., B.R. Jewell, and J.W. Murray, *The contribution of activation processes to the length-tension relation in cardiac muscle.* Nature, 1974. **248**: p. 509-513.
4. Allen, D.G. and J.C. Kentish, *The cellular basis of the length-tension relation in cardiac muscle.* Journal of Molecular and Cellular Cardiology, 1985. **17**: p. 821-840.
5. Allen, D.G. and S. Kurihara, *The effects of muscle length on intracellular calcium transients in mammalian cardiac muscle.* Journal of Physiology, 1982. **327**: p. 79-84.
6. Alpert, J.S., P. Peterson, and J. Godtfredsen, *Atrial fibrillation: natural history, complications and management.* Annual Review of Medicine, 1988. **39**: p. 41-52.
7. Alpert, N.R., et al., *Molecular mechanics of mouse cardiac myosin isoforms.* American Journal of Physiology, 2002. **283**: p. H1446-H1454.
8. Babu, A., E.H. Sonnenblick, and J. Gulati, *Molecular basis for the influence of muscle length on myocardial performance.* Science, 1988. **240**: p. 74-76.
9. Bennett, P., et al., *The ultrastructural location of C-protein, X-protein, and H-protein in rabbit muscle.* Journal of Muscle Research and Cell Motility, 1986. **7**: p. 550-567.
10. Brandt, P.W., et al., *Regulation of tension in skinned muscle fibers.* Journal of Molecular Biology, 1982. **79**: p. 997-1016.
11. Braunwald, E., et al., *Studies on Starling's law of the heart.* Journal of Clinical Investigation, 1960. **39**: p. 1874-1884.
12. Braunwald, E., J. Ross, and E.H. Sonnenblick, *Mechanisms of contraction in the normal and failing heart.* New England Journal of Medicine, 1967. **277**: p. 1012-1022.
13. Bremel, R.D. and A. Weber, *Cooperation within actin filament in vertebrate skeletal muscle.* Nature New Biology, 1972. **238**: p. 97-101.
14. Brenner, B. and E. Eisenberg, *Rate of force generation in muscle: correlation with actomyosin ATPase activity in solution.* Proceedings of the National Academy of Sciences of the USA, 1986. **83**: p. 3542-3546.
15. Calaghan, S.C., et al., *A role for C-protein in the regulation of contraction and intracellular Ca^{2+} in intact rat ventricular myocytes.* Journal of Physiology, 2000. **528.1**: p. 151-156.
16. Campbell, K.B. and M. Chandra, *Functions of stretch activation in heart muscle.* Journal of General Physiology, 2006. **127**: p. 89-94.
17. Campbell, K.S., *Tension recovery in permeabilized rat soleus muscle fibers after rapid shortening and restretch.* Biophysical Journal, 2006. **90**: p. 1288-1294.

18. Campbell, K.S. and R.L. Moss, *History-dependent mechanical properties of permeabilized rat soleus muscle fibers.* Biophysical Journal, 2002. **82**: p. 929-943.
19. Carrier, L., et al., *Organization and sequence of human cardiac myosin binding protein C gene (MYBPC3) and identification of mutations predicted to produce truncated proteins in familial hypertrophic cardiomyopathy.* Circulation Research, 1997. **80**: p. 427-434.
20. Cazorla, O., et al., *Titin-based modulation of calcium sensitivity of active tension in mouse skinned cardiac myocytes.* Circulation Research, 2001. **88**: p. 1028-1035.
21. Cecchi, G., et al., *Detection of radial crossbridge force by lattice-spacing changes in intact single muscle fibers.* Science, 1990. **250**: p. 1409-1411.
22. Chizzonite, R.A., et al., *Comparison of myosin heavy chains in atria and ventricles from hyperthyroid, hypothyroid, and euthyroid rabbits.* Journal of Biological Chemistry, 1984. **259**(24): p. 15564-71.
23. Davis, J.S., et al., *The overall pattern of cardiac contraction depends on a spatial gradient of myosin regulatory light chain phosphorylation.* Cell, 2001. **107**: p. 631-641.
24. De Tombe, P.P. and E.D.J. ter Keurs, *An internal viscous element limits unloaded velocity of sarcomere shortening in rat cardiac trabeculae.* Journal of Physiology, 1992. **454**: p. 619-642.
25. Dillman, W.H., *Diabetes mellitus induces changes in cardiac myosin of the rat.* Diabetes, 1980. **29**: p. 579-582.
26. Edman, K.A.P., *The velocity of unloaded shortening and its relation to sarcomere length and isometric force in vertebrate muscle fibers.* Journal of Physiology, 1979. **291**: p. 143-159.
27. Fabiato, A., *Myoplasmic free calcium concentration reached during the twitch of an intact isolated cardiac cell and during calcium-induced release of calcium from the sarcoplasmic reticulum of a skinned cardiac cell from the adult rat or rabbit ventricle.* Journal of General Physiology, 1981. **78**: p. 457-497.
28. Fabiato, A. and F. Fabiato, *Dependence of the contractile activation of skinned cardiac cells on the sarcomere length.* Nature, 1975. **256**: p. 54-56.
29. Fabiato, A. and F. Fabiato, *Myofilament-generated tension oscillations during partial calcium activation and activation dependence of the sarcomere length-tension relation of skinned cardiac cells.* Journal of General Physiology, 1978. **72**: p. 667-699.
30. Fitzsimmons, D.P., J.R. Patel, and R.L. Moss, *Role of myosin heavy chain composition in kinetics of force development and relaxation in rat myocardium.* Journal of Physiology, 1998. **513**: p. 171-183.
31. Fitzsimons, D.P., D.P. Patel, and R.L. Moss, *Aging-dependent depression in the kinetics of force development in rat skinned myocardium.* Am J Physiol Heart Circ Physiol, 1999. **276**: p. H1511-H1519.
32. Fitzsimons, D.P., J.R. Patel, and R.L. Moss, *Role of myosin heavy chain composition in kinetics of force development and relaxation in rat myocardium.* Journal of Physiology, 1998. **513**: p. 171-183.
33. Freiburg, A. and M. Gautel, *A molecular map of the interactions between titin and myosin binding protein C. Implications for sarcomeric assembly in familial*

hypertrophic cardiomyopathy. European Journal of Biochemistry, 1996. **235**: p. 317-323.
34. Fuchs, F. and D.A. Martyn, *Length-dependent calcium activation in cardiac muscle: some remaining questions.* Journal of Muscle Research and Cell Motility, 2005.
35. Fukuda, N., et al., *Length dependence of tension generation in rat skinned cardiac muscle.* Circulation, 2001. **104**: p. 1639-1645.
36. Fukuda, N., et al., *Titin isoform variance and length dependence of activation in skinned bovine cardiac muscle.* Journal of Physiology, 2003. **533.1**: p. 147-154.
37. Fukuda, N., et al., *Titin-based modulation of active tension and interfilament lattice spacing in skinned rat cardiac muscle.* Pflugers Archive - European Journal of Physiology, 2005. **449**: p. 449-457.
38. Garber, D.W. and J.R. Neely, *Decreased myocardial function and myosin ATPase in hearts from diabetic rats.* American Journal of Physiology, 1983. **244**(4): p. H586-91.
39. Gautel, M., et al., *Phosphorylation switches specific for the cardiac isoform of myosin binding protein C: a modulator of cardiac contraction?* EMBO Journal, 1995. **14**: p. 1952-1960.
40. Gibson, L.M., I.R. Wendt, and D.G. Stephenson, *Contractile activation properties of ventricular myocardium from hypothyroid, euthyroid, and juvenile rats.* Pfluger Archives, 1992. **422**: p. 16-23.
41. Gilbert, R., et al., *The carboxy terminus of myosin binding protein C (MyBP-C, C-protein) specifies incorporation into the A-band of striated muscle.* Journal of Cell Science, 1996. **109**: p. 101-111.
42. Gordon, A.M., E. Homsher, and M. Regnier, *Regulation of contraction in striated muscle.* Physiological Reviews, 2000. **80**: p. 853-924.
43. Gordon, A.M., A.F. Huxley, and F.J. Julian, *The variation in isometric tension with sarcomere length in vertebrate muscle fibers.* Journal of Physiology, 1966. **184**: p. 170-192.
44. Granzier, H.L. and T.C. Irving, *Passive tension in cardiac muscle: Contribution of collagen, titin, microtubules, and intermediate filaments.* Biophysical Journal, 1995. **68**: p. 1027-1044.
45. Grimm, A.F., H. Lin, and B.R. Grimm, *Left ventricular free wall and intraventricular pressure-sarcomere length distributions.* Am J Physiol Heart Circ Physiol, 1980. **239**: p. H101-H107.
46. Gruen, M., H. Prinz, and M. Gautel, *cAPK-phosphorylation controls the interaction of the regulatory domain of cardiac myosin binding C with myosin-S2 in an on-off fashion.* FEBS Letters, 1999. **453**: p. 254-259.
47. Guccione, J.M., et al., *Anterior and posterior left ventricular sarcomere lengths behave similarly during ejection.* American Journal of Physiology, 1997. **272**: p. H469-H477.
48. Guth, K. and J.D. Potter, *Effect of rigor and cycling cross-bridges on the structure of troponin C and on the Ca^{2+} affinity of the Ca^{2+}-specific regulatory sites in skinned rabbit psoas fibers.* Journal of Biological Chemistry, 1987. **262**: p. 13627-13635.

49. Hamilton, N. and C.D. Ianuzzo, *Contractile and calcium regulating capacities of myocardia of different sized mammals scale with resting heart rate.* Molecular and Cellular Biochemistry, 1991. **106**: p. 133-141.
50. Harris, D.E., et al., *Smooth, cardiac, and skeletal muscle myosin force and motion generation assessed by cross-bridge mechanical interactions in vitro.* Journal of Muscle Research and Cell Motility, 1994. **15**: p. 11-19.
51. Harris, S.P., et al., *Hypertrophic cardiomyopathy in cardiac myosin binding protein-C knockout mice.* Circulation Research, 2002. **90**: p. 594-601.
52. Harris, S.P., et al., *Targeted ablation of the mouse cardiac myosin binding protein-C gene.* Biophysical Journal, 2001. **80**: p. 89A.
53. Harris, S.P., et al., *Binding of myosin binding protein-C to myosin subfragment S2 affects contractility independent of a tether mechanism.* Circulation Research, 2004. **95**: p. 930-936.
54. Harrison, S.M., C. Lamont, and D.J. Miller, *Hysteresis and the length dependence of calcium sensitivity in chemically-skinned rat cardiac muscle.* Journal of Physiology, 1988. **401**: p. 115-143.
55. Hartzell, H.C., *Effects of phosphorylation and unphosphorylated C-protein on cardiac actomyosin ATPase.* Journal of Molecular Biology, 1985. **186**: p. 185-195.
56. Harvey, W., *On the motion of the heart and blood in animals.* The Harvard Classics, 2004. **38**(Scientific Papers).
57. Helmes, M., et al., *Titin determines the Frank-Starling relation in early diastole.* Journal of General Physiology, 2003: p. 97-110.
58. Herron, T.J., et al., *Age dependence of isometric crossbridge cycling and α-MyHC isoform expression in human ventricular myocytes.* Biophysical Journal, 2005.
59. Herron, T.J., et al., *Power output varies as a linear function of β-myosin heavy chain in both single rat cardiac myocytes and whole hearts.* Biophysical Journal, 2002. **82**: p. 399a.
60. Herron, T.J., F.S. Korte, and K.S. McDonald, *Loaded shortening and power output in cardiac myocytes are dependent on myosin heavy chain isoform expression.* American Journal of Physiology, 2001. **281**: p. H1217-1222.
61. Herron, T.J., F.S. Korte, and K.S. McDonald, *Power output is increased after phosphorylation of myofibrillar proteins in rat skinned cardiac myocytes.* Circulation Research, 2001. **89**: p. 1184-1190.
62. Herron, T.J. and K.S. McDonald, *Small amounts of α-myosin heavy chain isoform expression significantly increase power output of rat cardiac myocyte fragments.* Circulation Research, 2002. **90**: p. 1150-52.
63. Herron, T.J., et al., *Activation of myocardial contraction by the N-terminal domains of myosin binding protein-C.* Circulation Research, 2006. **98**: p. 1290-1298.
64. Hibberd, M.G. and B.R. Jewell, *Calcium- and length-dependent force production in rat ventricular muscle.* Journal of Physiology, 1982. **329**: p. 527-540.
65. Hill, A.V., *The heat of shortening and the dynamic constants of muscle.* Proc. R. Soc. London Ser. B., 1938. **126**: p. 136-195.

66. Hofmann, P.A. and F. Fuchs, *Effect of length and cross-bridge attachment on Ca^{2+} binding to cardiac troponin C.* American Journal of Physiology, 1987. **253**: p. C90-C96.
67. Hofmann, P.A. and F. Fuchs, *Bound calcium and force development in skinned cardiac muscle bundles: effect of sarcomere length.* Journal of Molecular and Cellular Cardiology, 1988. **20**: p. 667-677.
68. Hofmann, P.A., M.L. Greaser, and R.L. Moss, *C-Protein limits shortening velocity of rabbit skeletal muscle fibres at low levels of Ca^{2+} activation.* Journal of Physiology, 1991. **439**: p. 701-715.
69. Hofmann, P.A., H.C. Hartzell, and R.L. Moss, *Alterations in Ca^{2+} sensitive tension due to partial extraction of C-protein from rat skinned cardiac myocytes and rabbit skeletal muscle.* Journal of General Physiology, 1991. **97**: p. 1141-1163.
70. Hoh, J.F.Y., P.A. McGrath, and P.T. Hale, *Electrophoretic analysis of multiple forms of rat cardiac myosin: effects of hypophysectomy and thyroxine replacement.* Journal of Molecular and Cellular Cardiology, 1977. **10**: p. 1053-1076.
71. Holubarsch, C., et al., *The economy of isometric force development, myosin isozyme pattern and myofibrillar ATPase activity in normal and hypothyroid rat myocardium.* Circulation Research, 1985. **56**: p. 78-86.
72. Holubarsch, C., et al., *Existence of the Frank-Starling mechanism in the failing human heart. Investigations on the organ, tissue, and sarcomere levels.* Circulation, 1996. **94(4)**: p. 683-689.
73. Huxley, H.E. and W. Brown, *The low-angle x-ray diagram of vertebrate striated muscle and its behaviour during contraction and relaxation.* Journal of Molecular Biology, 1967. **30**: p. 383-434.
74. Irving, T.C., et al., *Myofilament lattice spacing as a function of sarcomere length in isolated rat myocardium.* American Journal of Physiology, 2000. **279**: p. H2568-H2573.
75. Iwamoto, I., *Thin filament cooperativity as a major determinant of shortening velocity in skeletal muscle fibers.* Biophysical Journal, 1998. **74**: p. 1452-1464.
76. Jacob, R., B. Dierberger, and G. Kissling, *Functional significance of the Frank-Starling mechanism under physiological and pathophysiological conditions.* European Heart Journal, 1992. **13**(Supplement E): p. 7-14.
77. Janssen, P.M.L. and P.P. De Tombe, *Protein kinase A does not alter unloaded velocity of sarcomere shortening in skinned rat cardiac trabeculae.* American Journal of Physiology (Heart Circ. Physiol.), 1997. **42**: p. H2415-H2422.
78. Kanaya, N., et al., *Propofol increases phosphorylation of troponin I and myosin light chain 2 via protein kinase C activation in cardiomyocytes.* Anesthesiology, 2003. **98**: p. 1363-71.
79. Kentish, J.C., et al., *Comparison between the sarcomere length-force relations of intact and skinned trabeculae from rat right ventricle.* Circulation Research, 1986. **58**: p. 755-768.
80. Kitzman, D.W., et al., *Exercise intolerance in patients with heart failure and preserved left ventricular systolic function: failure of the Frank-Starling*

mechanism. Journal of the American College of Cardiology, 1991. **17**: p. 1065-1072.
81. Komamura, K., et al., *Exhaustion of Frank-Starling mechanism in conscious dogs with heart failure.* American Journal of Physiology, 1993. **265**: p. H1119-H1131.
82. Konhilas, J.P., T.C. Irving, and P.P. de Tombe, *Myofilament calcium sensitivity in skinned rat cardiac trabeculae.* Circulation Research, 2002. **90**: p. 59-65.
83. Konhilas, J.P., et al., *Troponin I in the murine myocardium: influence on length-dependent activation and interfilament spacing.* Journal of Physiology, 2003. **547**: p. 951-961.
84. Koretz, J.F., *Effects of C-Protein on synthetic myosin filament structure.* Biophysical Journal, 1979. **27**: p. 443-446.
85. Korte, F.S., et al., *Power output is linearly related to MyHC content in rat skinned myocytes and isolated working hearts.* Am J Physiol Heart Circ Physiol, 2005. **289**(2): p. H801-812.
86. Korte, F.S., et al., *Loaded Shortening, Power Output, and Rate of Force Redevelopment Are Increased With Knockout of Cardiac Myosin Binding Protein-C.* Circ Res, 2003. **93**(8): p. 752-758.
87. Kunst, G., et al., *Myosin binding protein C, a phosphorylation-dependent force regulator in muscle that controls the attachment of myosin heads by its interaction with myosin S2.* Circulation Research, 2000. **86**: p. 51-58.
88. Lakatta, E.G. and B.R. Jewell, *Length-dependent activation.* Circulation Research, 1977. **40**: p. 252-257.
89. Linari, M., et al., *The structural basis of the increase in isometric force production with temperature in frog skeletal muscle.* Journal of Physiology, 2005. **567**: p. 456-469.
90. Litten, R.Z.r., et al., *Altered myosin isozyme patterns from pressure-overloaded and thyrotoxic hypertrophied rabbit hearts.* Circulation Research, 1982. **50**(6): p. 856-64.
91. Loiselle, D.S., I.R. Wendt, and J.F.Y. Hoh, *Energetic consequences of thyroid-modulated shifts in ventricular isomyosin distribution in the rat.* Journal of Muscle Research and Cell Motility, 1982. **3**: p. 5-23.
92. Lompre, A.M., B. Nadal-Ginard, and V. Mahdavi, *Expression of cardiac alpha- and beta-myosin heavy chain genes is developmentally and hormonally regulated.* Journal of Biological Chemistry, 1984. **259**: p. 6437-6446.
93. Lowes, B., et al., *Changes in gene expression in intact human heart: downregulation of alpha-myosin heavy chain in hypertrophied failing ventricular myocardium.* Journal of Clinical Investigation, 1997. **100**: p. 2315-2324.
94. Malhotra, A., et al., *Expression and regulation of mutant forms of cardiac TnI in a reconstituted actomyosin syste: role of kinase dependent phosphorylation.* Molecular and Cellular Biochemistry, 1997. **170**: p. 99-107.
95. Mann, D.L., et al., *Cellular versus myocardial basis for the contractile dysfunction of hypertrophied myocardium.* Circulation Research, 1991. **1991**: p. 402-415.
96. Margossian, S.K., *Reversible dissociation of dog cardiac myosin regulatory light chain 2 and its influence on ATP hydrolysis.* Journal of Biological Chemistry, 1985. **260**: p. 13747-13754.

97. Martyn, D.A., J.F. Rondinone, and L.L. Huntsman, *Myocardial segment velocity at a low load: time, length, and calcium dependence.* American Journal of Physiology (Heart & Circulatory Physiology), 1983. **13**: p. H708-H714.
98. Matsubara, I. and B.M. Millman, *X-ray diffraction studies on skinned single fibers of frog skeletal muscle.* Journal of Molecular Biology, 1972. **72**: p. 657-699.
99. McDonald, K.S., *Ca^{2+} dependence of loaded shortening in rat skinned cardiac myocytes and skeletal muscle fibers.* Journal of Physiology, 2000. **525**: p. 169-181.
100. McDonald, K.S., *Thin filament inactivation during isotonic shortening in skinned striated muscle preparations.* Biophysical Journal, 2000.
101. McDonald, K.S., et al., *Length dependence of Ca^{2+} sensitivity of tension in mouse cardiac myocytes expressing skeletal troponin C.* Journal of Physiology, 1995. **483**: p. 131-139.
102. McDonald, K.S. and R.L. Moss, *Osmotic compression of single cardiac myocytes reverses the reduction in Ca^{2+} sensitivity of tension observed at short sarcomere length.* Circulation Research, 1995. **77**: p. 199-205.
103. McDonald, K.S. and R.L. Moss, *Strongly binding myosin cross-bridges regulate loaded shortening and power output in cardiac myocytes.* Circulation Research, 2000. **87**: p. 768-773.
104. McDonald, K.S., M.R. Wolff, and R.L. Moss, *Sarcomere length dependence of the rate of tension redevelopment and submaximal tension in rat and rabbit skinned skeletal muscle fibers.* Journal of Physiology, 1997. **501**: p. 607-621.
105. McDonald, K.S., M.R. Wolff, and R.L. Moss, *Force-velocity and power-load curves in rat skinned cardiac myocytes.* Journal of Physiology, 1998: p. 519-531.
106. McNally, E.M., et al., *Full-length rat alpha and beta cardiac myosin heavy chain sequences.* Journal of Molecular Biology, 1989. **210**: p. 665-671.
107. Metzger, J.M., et al., *Effects of myosin heavy chain isoform switching on Ca^{2+}-activated tension development in single adult cardiac myocytes.* Circulation Research, 1999. **84**: p. 1310-1317.
108. Minajeva, A., et al., *Titin-based contribution to shortening velocity of rabbit skeletal myofibrils.* Journal of Physiology, 2002. **540.1**: p. 177-188.
109. Miyata, S., et al., *Myosin heavy chain isoform expression in the failing and nonfailing human heart.* Circulation Research, 2000. **86**: p. 386-390.
110. Moolman-Smook, J., et al., *Identification of novel interactions between domains of myosin binding protein-C that are modulated by hypertrophic cardiomyopathy missense mutations.* Circulation Research, 2002. **91**: p. 704-711.
111. Moos, C., *Fluorescein microscope study of the binding of added C-protein to skeletal muscle myofibrils.* Journal of Cellular Biology, 1981. **90**: p. 25-31.
112. Moos, C. and I.N.M. Feng, *Effect of C-protein on actomyosin ATPase.* Biochemica Biophysica ACTA, 1980. **632**: p. 141-149.
113. Moos, C., et al., *The binding of skeletal muscle C-protein to F-actin, and its relation to the interaction of actin with myosin subfragment-1.* Journal of Molecular Biology, 1978. **124**: p. 571-586.
114. Moos, C., et al., *Interaction of C-protein with myosin, myosin rod and light meromyosin.* Journal of Molecular Biology, 1975. **97**: p. 1-9.

115. Morkin, E., I.L. Flink, and S. Goldman, *Biochemical and physiologic effects of thyroid hormone on cardiac performance.* Progress in Cardiovascular Diseases, 1983. **25**(5): p. 435-64.
116. Moss, R.L., *Sarcomere length-tension relations of frog skinned muscle fibres during calcium activation at short lengths.* Journal of Physiology, 1979. **292**: p. 177-202.
117. Moss, R.L., *Effects of shortening velocity of rabbit skeletal muscle due to variations in the level of thin-filament activation.* Journal of Physiology, 1986. **377**: p. 487-505.
118. Moss, R.L., *Ca^{2+} regulation of mechanical properties of striated muscle: mechanistic studies using extraction and replacement of regulatory proteins.* Circulation Research, 1992. **70**: p. 865-884.
119. Moss, R.L., L.O. Nwoye, and M.L. Greaser, *Substitution of cardiac troponin C into rabbit muscle does not alter the length dependence of Ca^{2+} sensitivity of tension.* Journal of Physiology, 1991. **440**: p. 273-289.
120. Najad, N.S., et al., *Assessment of myocardial contractility from ventricular pressure recordings.* Cardiovascular Research, 1971. **5**: p. 15-23.
121. Nakao, K., et al., *Myosin heavy chain gene expression in human heart failure.* Journal of Clinical Investigation, 1997. **100**: p. 2362-2370.
122. Neagoe, C., et al., *Gigantic variety: expression patterns of titin isoforms in striated muscles and consequences for myofibrillar passive stiffness.* Journal of Muscle Research and Cell Motility, 2003. **24**: p. 175-189.
123. Nejad, N.S., et al., *Assessment of myocardial contractility from ventricular pressure recordings.* Cardiovascular Research, 1971. **5**: p. 15-23.
124. Niederlander, N., et al., *Regulation of the actin-myosin interaction by titin.* European Journal of Biochemistry, 2004. **271**: p. 4572-4581.
125. Niimura, H., et al., *Mutations in the gene for cardiac myosin-binding protein C and late-onset familial hypertrophic cardiomyopathy.* New England Journal of Medicine, 1998. **338**: p. 1248-1257.
126. Noland, J.R., et al., *Cardiac troponin I mutants. Phosphorylation by protein kinases C and A and regulation of Ca^{2+}-stimulated MgATPase of reconstituted actomyosin S-1.* Journal of Biological Chemistry, 1995. **43**: p. 25445-25454.
127. Noland, J.R. and T.A. Kuo, *Protein kinase C phosphorylation of cardiac troponin I or troponin T inhibits Ca^{2+}-stimulated actomyosin MgATPase activity.* Journal of Biological Chemistry, 1991. **266**: p. 4974-4978.
128. Noland, J.R. and T.A. Kuo, *Protein kinase C phosphorylation of cardiac troponin T decreased Ca^{2+}-dependent actomyosin MgATPase and troponin T binding to tropomyosin F-actin complex.* Biochemical Journal, 1993. **288**: p. 2705-2711.
129. Offer, G., C. Moos, and R. Starr, *A new protein of the thick filaments of vertebrate skeletal myofibrils.* Journal of Molecular Biology, 1973. **74**: p. 653-676.
130. Okagaki, T., et al., *The major myosin binding domain of skeletal muscle MyBP-C (C-protein) resides in the COOH-terminal, immunoglobin C2 repeat.* Journal of Cell Biology, 1993. **123**: p. 619-626.
131. Pagani, E.D. and F.J. Julian, *Rabbit papillary muscle myosin isozymes and the velocity of muscle shortening.* Circulation Research, 1984. **54**: p. 586-594.

132. Pagani, E.D., R. Shemin, and F.J. Julian, *Tension-pCa relations of saponin-skinned rabbit and human heart muscle.* Journal of Molecular and Cellular Cardiology, 1986. **18**: p. 55-66.
133. Palmer, B.M., et al., *Role of cardiac myosin binding protein C in sustaining left ventricular stiffening.* Circulation Research, 2004. **94**: p. 1249-1255.
134. Palmer, B.M., et al., *Reduced cross-bridge dependent stiffness of skinned myocardium from mice lacking cardiac myosin binding protein-C.* Molecular and Cellular Biochemistry, 2004. **263**: p. 73-80.
135. Patel, J.R., et al., *PKA accelerates rate of force development in murine skinned myocardium expressing alpha- or beta-tropomyosin.* American Journal of Physiology, 2001. **280(6)**: p. H2732-9.
136. Patterson, S.W., H. Piper, and E.H. Starling, *The regulation of the heart beat.* Journal of Physiology, 1914. **48**: p. 465-513.
137. Pearson, J.T., et al., *In situ measurements of crossbridge dynamics and lattice spacing in rat hearts by X-ray diffraction: sensitivity to regional ischemia.* Circulation, 2004. **109**: p. 2976-2979.
138. Pettigrew, J.B., *Design in nature*. 1908, London: Longmans, Green, and Co. 506-518.
139. Pi, Y., et al., *Protein kinase C and A sites on troponin I regulate myofilament Ca2+ sensitivity and ATPase activity in the mouse myocardium.* Journal of Physiology, 2003. **552.3**: p. 845-857.
140. Pollack, G.H. and L.L. Huntsman, *Sarcomere length-active force relations in living mammalian cardiac muscle.* American Journal of Physiology, 1974. **227**: p. 383-389.
141. Pope, B., J.F.Y. Hoh, and A. Weeds, *The ATPase activities of rat cardiac myosin isoenzymes.* FEBS Letters, 1980. **118**: p. 205-208.
142. Pringle, J.W.S., *The excitation and contraction of the flight muscles of insects.* Journal of Physiology, 1949. **108**: p. 226-232.
143. Rayment, I., et al., *Three-dimensional structure of myosin subfragment-1: a molecular motor.* Science, 1993. **261**: p. 50-58.
144. Reconditi, M., et al., *The conformation of myosin head domains in rigor muscle determined by X-ray interference.* Biophysical Journal, 2003. **85**: p. 1098-1110.
145. Regnier, M., D.A. Martyn, and B.P. Chase, *Calcium regulation of tension redevelopment kinetics with 2-deoxy-ATP or low [ATP] in rabbit skeletal muscle.* Biophysical Journal, 1998. **74**: p. 2005-2015.
146. Regnier, M., et al., *Thin filament near-neighbor regulatory unit interactions affect rabbit skeletal muscle steady-state force-Ca^{2+} relations.* Journal of Physiology, 2002. **540**: p. 485-497.
147. Robertson, S.P., et al., *The effect of troponin I phosphorylation on the Ca^{2+}-binding properties of the Ca^{2+}-regulatory site of bovine cardiac troponin.* Journal of Biological Chemistry, 1982. **257**: p. 260-263.
148. Rome, E., *Light and X-ray diffraction studies of the filament lattice of glycerol-extracted rabbit psoas muscle.* Journal of Molecular Biology, 1967. **27**: p. 591-602.
149. Rome, L.C., et al., *Why animals have different muscle types.* Nature, 1988. **335**: p. 824-827.

150. Ross, J., et al., *Diastolic geometry and sarcomere lengths in the chronically dilated canine left ventricle.* Circulation Research, 1971. **28**: p. 49-61.
151. Rundell, V.L., et al., *Depressed cardiac tension cost in experimental diabetes is due to altered myosin heavy chain isoform expression.* American Journal of Physiology, 2004. **287**: p. H408-H413.
152. Rundell, V.L.M., et al., *Impact of {beta}-myosin heavy chain isoform expression on cross-bridge cycling kinetics.* Am J Physiol Heart Circ Physiol, 2005. **288**(2): p. H896-903.
153. Sarnoff, S.J., *Myocardial contractility as described by ventricular function curves; observations on Starling's law of the heart.* Physiological Reviews, 1955. **35**: p. 107-122.
154. Schiaffino, S., et al., *Myosin changes in hypertrophied human atrial and ventricular myocardium. A correlated immunofluorescence and quantitative immunochemical study on serial crysections.* European Heart Journal, 1984. **75**: p. 95-102.
155. Schultheiss, T., et al., *Differential distribution of subsets of myofibrillar proteins in cardiac nonstriated and striated myofibrils.* Journal of Cell Biology, 1990. **110**: p. 1159-1172.
156. Schwartz, K., et al., *Myosin isozymic distribution correlates with speed of myocardial contraction.* Journal of Molecular and Cellular Cardiology, 1981. **13**: p. 1071-1075.
157. Schwinger, R.H., et al., *The failing human heart is unable to use the Frank-Starling mechanism.* Circulation Research, 1994. **74**: p. 959-969.
158. Shiner, J.S. and R.J. Solaro, *The Hill coeffecient for the calcium activation of striated muscle contraction.* Biophysical Journal, 1984. **46**: p. 541-543.
159. Skrebnitskaia, L.K., et al., *Monitoring the orientation of myosin bridges on two-dimensional maps of birefringence in a single muscle fiber.* Biofizika, 2002. **47**: p. 686-690.
160. Sonnenblick, E.H., *Force-velocity relations in mammalian heart muscle.* American Journal of Physiology, 1962. **202**: p. 931-939.
161. Starr, I., L.H. Collins, and F.C. Wood, *Basal work and output of the heart in clinical conditions.* Journal of Clinical Investigation, 1933. **12**: p. 13.
162. Starr, R. and G. Offer, *The interaction of C-protein with heavy meromyosin and subfragment-2.* Biochemical Journal, 1978. **171**: p. 813-816.
163. Stelzer, J.E., S.B. Dunning, and R.L. Moss, *Ablation of myosin-binding protein-C accelerates stretch activation in murine skinned myocardium.* Circulation Research, 2006. **98**: p. Early online publication.
164. Stelzer, J.E., D.P. Fitzsimons, and R.L. Moss, *Ablation of myosin-binding protein-C accelerates force development in mouse myocardium.* Biophysical Journal, 2006. **90**: p. 4119-4127.
165. Stelzer, J.E., et al., *Activation dependence of stretch activation in mouse skinned myocardium: implications for ventricular function.* Journal of General Physiology, 2006. **127**: p. 95-107.
166. Strang, K.T., et al., *B-adrenergic receptor stimulation increases unloaded shortening velocity of skinned single ventricular myocytes from rats.* Circulation Research, 1994. **74**: p. 542-549.

167. Streeter, D.D., et al., *Fiber orientation in the canine left ventricle during diastole and systole.* Circulation Research, 1969. **24**: p. 339-347.
168. Sugiura, S., et al., *Comparison of unitary displacements and forces between 2 cardiac myosin isoforms by the optical trap technique: molecular basis for cardiac adaptation.* Circulation Research, 1998. **82**: p. 1029-1034.
169. Sumandea, M., et al., *Identification of a functionally critical protein kinase C phosphorylation residue of cardiac troponin T.* Journal of Biological Chemistry, 2003. **278**: p. 35135-35144.
170. Sumandea, M.P., et al., *Identification of a functionally critical protein kinase C phosphorylation residue of cardiac troponin T.* Journal of Biological Chemistry, 2003. **278**: p. 35135-44.
171. Tardiff, J.C., *Sarcomeric proteins and familial hypertrophic cardiomyopathy: linking mutations in structural proteins to complex cardiovascular phenotypes.* Heart Failure Reviews, 2005. **10**: p. 237-248.
172. ter Keurs, H.E.D.J., *Heart failure and Starling's law of the heart.* Canadian Journal of Cardiogy, 1996. **12**: p. 1047-1057.
173. ter Keurs, H.E.D.J., et al., *Tension development and sarcomere length in rat cardiac trabeculae: evidence of length-dependent activation.* Circulation Research, 1980. **46**: p. 703-714.
174. van der Velden, J., et al., *Effect of protein kinase A on calcium sensitivity of force and its sarcomere length dependence in human cardiomyocytes.* Cardiovascular Research, 2000. **46**: p. 487-495.
175. van der Velden, J., et al., *Increased Ca2+ sensitivity of the contractile apparatus in end-stage human heart failure results from altered phosphorylation of contractile proteins.* Cardiovascular Research, 2003. **57**: p. 37-47.
176. VanBuren, P., et al., *Cardiac V_1 and V_3 myosins differ in their hydrolytic and mechanical activities in vitro.* Circulation Research, 1995. **77**: p. 439-444.
177. Vemuri, R., et al., *The stretch-activation response may be critical to the proper functioning of the mammalian heart.* Proceedings of the National Academy of Sciences USA, 1999. **96**: p. 1048-1053.
178. Venema, R. and J. Kuo, *Protein kinase C-mediated phosphorylation of troponin I and C-protein in isolated myocardial cells is associated with inhibition of myofibrillar actomyosin MgATPase.* J. Biol. Chem., 1993. **268**(4): p. 2705-2711.
179. Wattanapermpool, J., X. Guo, and R.J. Solaro, *The unique amino-terminal peptide of cardiac troponin I regulates myofibrillar activity only when it is phosphorylated.* Journal of Molecular and Cellular Cardiology, 1995. **27**: p. 1383-1391.
180. Weisberg, A. and S. Winegrad, *Alteration of myosin cross-bridges by phosphorylation of myosin-binding protein C in cardiac muscle.* Proceedings of the National Academy of Sciences USA, 1996. **93**: p. 8999-9003.
181. Weisberg, A. and S. Winegrad, *Relation between crossbridge structure and actomyosin ATPase activity in rat heart.* Circulation Research, 1998. **83**: p. 60-72.
182. Wick, M., *Filament assembly properties of the sarcomeric myosin heavy chain.* Research and Reviews: Meat, 2001. **Special Circular 172**: p. Online publication.
183. Winegrad, S., *Cardiac myosin binding protein C.* Circulation Research, 1999. **84**: p. 1117-1126.

184. Winegrad, S. and A. Weisberg, *Isozyme specific modification of myosin ATPase by cAMP in rat heart.* Circulation Research, 1987. **60**: p. 384-392.
185. Witt, C.C., et al., *Hypercontractile properties of cardiac muscle fibers in a knock-in mouse model of cardiac myosin binding protein-C.* Journal of Biological Chemistry, 2001. **276**: p. 5353-5369.
186. Woledge, R.C., N.A. Curtin, and E. Homsher, Energetic aspects of muscle contraction., 1985. **Academic Press, London**: p. pp.47-71.
187. Yagi, N., et al., *Sarcomere-length dependence of lattice volume and radial mass transfer of myosin cross-bridges in rat papillary muscle.* Pflugers Archive, 2004. **448**: p. 153-160.
188. Yang, Q., et al., *A mouse model of myosin binding protein C human familial hypertrophic cardiomyopathy.* Journal of Clinical Investigation, 1998. **102**(7): p. 1292-1300.
189. Yang, Q., et al., *In vivo modeling of myosin binding protein C familial hypertrophic cardiomyopathy.* Circulation Research, 1999. **85**: p. 841-847.
190. Zimmer, H., *Who discovered the Frank-Starling mechanism?* News in Physiological Sciences, 2002. **17**: p. 181-184.

VITA

Frederick Steven Korte was born March 16th, 1975 in Boonville, MO. He attended public school in Boonville, MO and graduated from Boonville High School in May, 1993. He received a B.S. degree in Biochemistry from the University of Missouri-Columbia in December, 1997. He married the former Ms. Amanda Elizabeth Gilbert on November 7th, 1998 while working for Dr. Kerry McDonald in the Department of Physiology at the University of Missouri. He joined the department as a graduate student in August, 2001 and graduated with a Ph.D. in Physiology in July, 2006. He will continue research as a postdoctoral fellow in the Department of Bioengineering at the University of Washington in Seattle, WA under the supervision of Dr. Michael Regnier.